INVESTIGATION THE EFFECT OF EDM PROCESS PARAMETERS ON MACHINING PERFORMANCE OF DIN 1.2767 TOOL STEEL

2022
PhD THESIS
MANUFACTURING ENGINEERING

Abubaker Yousef FATATIT

Thesis Advisor
Assoc.Prof.Dr. Ali KALYON

INVESTIGATION THE EFFECT OF EDM PROCESS PARAMETERS ON MACHINING PERFORMANCE OF DIN1.2767 TOOL STEEL

Abubaker Yousef FATATIT

T.C.
Karabuk University
Institute of Graduate Programs
Department of Manufacturing Engineering
Prepared as
PhD Thesis

Assoc.Prof.Dr. Ali KALYON

KARABUK

June 2022

I certify that in my opinion the thesis submitted by Abubaker Yousef FATATIT titled "INVESTIGATION THE EFFECT OF EDM PROCESS PARAMETERS ON MACHINING PERFORMANCE OF DIN1.2767 TOOL STEEL" is fully adequate in scope and in quality as a thesis for the degree of PhD.

Assoc.Prof.Dr. Ali KALYON .....
Thesis Advisor, Department of Manufacturing Engineering

This thesis is accepted by the examining committee with a unanimous vote in the Department of Manufacturing Engineering as a PhD thesis. June 24, 2022

Examining Committee Members (Institutions)		Signature
Chairman	: Prof.Dr. İsmail KARACAN (KBÜ)	.....
Member	: Assoc.Prof.Dr. Ali KALYON (YÜ)	.....
Member	: Assoc.Prof.Dr. Mustafa AYYILDIZ (DÜ)	.....
Member	: Assist.Prof.Dr. Harun ÇUĞ (KBÜ)	.....
Member	: Assist.Prof.Dr. Muhammed ELİTAŞ (BŞÜ)	.....

The degree of PhD by the thesis submitted is approved by the Administrative Board of the Institute of Graduate Programs, Karabuk University.

Prof. Dr. Hasan SOLMAZ .....
Director of the Institute of Graduate Programs

"I declare that all the information within this thesis has been gathered and presented in accordance with academic regulations and ethical principles and I have according to the requirements of these regulations and principles cited all those which do not originate in this work as well."

Abubaker Yousef FATATIT

ABSTRACT

PHD Thesis

INVESTIGATION THE EFFECT OF EDM PROCESS PARAMETERS ON MACHINING PERFORMANCE OF DIN1.2767 TOOL STEEL

Abubaker Yousef FATATIT

Karabük University
Institute of Graduate Programs
The Department of Manufacturing Engineering

Thesis Advisor:
Assoc.Prof.Dr. Ali KALYON

June 2022, 126 pages

Accompanying the technological development and the advancement in the industry, the demand for materials with superior properties such as high strength, hardness and toughness is increasing. This made it difficult or impossible to cut these materials by conventional methods. Electric discharge machining (EDM) is one of the most important unconventional machining methods that have the ability to cut electrically conductive materials regardless of their mechanical properties. DIN1.2767 tool steel has wide application in the industry due to its good mechanical properties such as high toughness, good through-hardenability, high impact strength and pressure resistance.

This study aims to investigate the effect of process parameters on EDM performance of DIN 1.2767 tool steel. The process parameters and their levels were electrode materials (Cu-Cr-Zr, Cu, CNB, NSS and B2), discharge current (Ip) (6, 12 and 25 A),

pulse on-time (T_{on}) (50, 200 and 800 μs) and pulse off-time (T_{off}) (50, 200 and 800 μs).

Surface crack density (SCD) and white layer thickness (WLT) were investigated by Scanning Electron Microscopy (SEM). Data analysis and the contribution of the process parameters were statistically evaluated using Analysis of Variance (ANOVA). The experimental results identified the set of process parameters that achieve the optimal EDM performance measures, the effect of each parameter on the performance measures, and the parameter interactions for the performance measures. However, Ip was the most dominant parameter affecting Material Removal Rate (MRR), followed by T_{off}. The highest material removal rate can be achieved by setting parameters on NSS electrode, Ip (25A), T_{on} (200μs) and T_{off} (50 μs). Ip has the highest effect on Tool Wear Ratio (TWR) followed by T_{on} and the minimal TWR was at Cu electrode Ip (6A), T_{on} (800 μs) and T_{off} (200μs). T_{on} was the most dominant parameter affecting Surface Roughness (SR), followed by Ip. The optimal surface finish was obtained at setting parameters B2 electrode, Ip (6A), T_{on} (800μs) and T_{off} (800μs). For the Overcut (OC), electrode material was the most significant parameter followed by Ip and the minimal OC was at NSS electrode, Ip (12A), T_{on} (50 μs) and T_{off} (800μs). T_{on} was the most significant parameter affecting WLT, followed by Ip and the minimal WLT was determined at using CNB electrode, Ip (25A), T_{on} (50 μs) and T_{off} (200μs) and the most dominant factor for SCD was T_{on} followed by electrode material and the best surface free of cracks attained at utilizing CNB electrode, Ip (25A), T_{on} (50 μs) and T_{off} (50μs).

Key Words : EDM, DIN 1.2767 tool steel, MRR, TWR, R_a, OC, WLT, SCD.
Science Code : 91438

ÖZET

EEİ PARAMETRELERİNİN DIN1.2767 TAKIM ÇELİKLERİNİN İŞLEME PERFORMANSINA ETKİSİNİN İNCELENMESİ

Abubaker Yousef FATATIT

Karabük Üniversitesi
Lisansüstü Eğitim Enstitüsü
İmalat Mühendisliği Anabilim Dalı

Tez Danışmanı:
Doç. Dr. Ali KALYON
Haziran 2022, 126 sayfa

Teknolojik gelişme ve sektördeki ilerleme ile birlikte yüksek dayanım, sertlik ve tokluk gibi üstün özelliklere sahip malzemelere olan talep artmaktadır. Bu durum, bu malzemelerin geleneksel yöntemlerle işlenmesini zorlaştırmakta veya imkansız hale getirmektedir. Elektrik Erozyon ile İşleme (EEİ), elektriksel iletkenliğe sahip malzemeleri mekanik özelliklerinden bağımsız olarak kesme yeteneğine sahip en önemli geleneksel olmayan işleme yöntemlerinden biridir. DIN1.2767 takım çeliği, yüksek tokluk, yüksek sertlik, yüksek darbe dayanımı ve basınç direnci gibi mekanik özellikleri nedeniyle endüstride geniş bir uygulama alanına sahiptir.

Bu çalışma, işleme parametrelerinin DIN 1.2767 takım çeliğinin EEİ işleme üzerindeki etkisini araştırmayı amaçlamaktadır.. İşleme parametreleri ve seviyeleri olarak, elektrot malzemeleri (Cu-Cr-Zr, Cu, CNB, NSS ve B2), boşalım akımı (Ip) (6, 12 ve 25 A), vurum süresi (T_{on})(50, 200, 800 µs) ve bekleme süresi (T_{off})(50, 200 ve 800 µs) belirlenmiştir. Yüzey Çatlak Yoğunluğu (YÇY) ve Beyaz Katman Kalınlığı (BKK), Taramalı Elektron Mikroskobu (TEM) kullanılarak incelenmiştir. Veri analizi ve işleme parametrelerinin katkısı Varyans Analizi (ANOVA) kullanılarak istatistiksel

olarak değerlendirilmiştir. Deneysel sonuçlar kullanılarak ideal EEİ performans değerlerine ulaşan işleme parametre seti, her parametrenin performans ölçüleri üzerindeki etkisi ve performans ölçüleri için parametre etkileşimleri tanımlanmıştır. İş parçası İşleme Hızını (İİH) etkileyen en etkili parametre Ip'dir ve bunu sırasıyla Toff izlemektedir. En yüksek işparçası işleme hızı, NSS elektrotu, Ip (25A), T_{on} (200µs) ve T_{off} (50 µs) değerlerinde elde edilmiştir. Ip, elektrot aşınma hızı üzerinde en yüksek etkiye sahiptir ve bunu sırasıyla T_{on} izlemiştir ve en düşük elektrot aşınma hızı Cu elektrot Ip (6A), T_{on} (800 µs) ve T_{off} 'ta (200µs) değerlerinde elde edilmiştir. Ton, yüzey pürüzlülüğünü etkileyen en etkili parametredir ve bunu sırasıyla Ip izlemektedir. İdeal yüzey pürüzlülüğü B2 elektrotu ile Ip (6A), T_{on} (800µs) ve T_{off} (800µs) parametreleri değerlerinde elde edilmiştir. Yanal açıklık için elektrot malzemesi en önemli parametredir, bunu sırasıyla Ip izlemiştir ve minimum Yanal Açıklık NSS elektrotunda, Ip (12A), T_{on} (50 µs) ve T_{off} 'ta (800µs) değerinde elde edilmiştir. Beyaz katman kalınlığını etkileyen en önemli parametre T_{on}, ardından sırasıyla Ip'dir ve minimum Beyaz Katman Kalınlığı CNB elektrotu ile Ip (25A), T_{on} (50 µs) ve T_{off} (200µs) ile elde edilmiştir. Yüzey çatlak yoğunluğu için en etkili faktör Ton ve ardından elektrot tipidir. CNB elektrot ile Ip (25A), T_{on} (50 µs) ve T_{off} (50µs) değerleri kullanılarak en düşük yüzey çatlak yoğunluğu elde edilmiştir.

Anahtar Kelimeler : EDM, DIN 1.2767 takım çeliği, işparçası işleme hızı, elektrot aşınma hızı, Ra, yanal açıklık, beyaz katman kalınlığı, yüzey çatlak yoğunluğu.

Bilim Kodu : 91438

ACKNOWLEDGMENT

First of all, my gratitude and thanks to ALLAH, the Most Gracious and the Most Merciful, who gives me strength and makes me successful.

I wish to express my sincere gratitude to my advisor Assoc. Prof. Dr Ali KALYON for suggesting the research point, for his timely guidance, support and encouragement during all thesis stages. In addition, I would like to express my thanks to Prof. Dr. İsmail KARACAN, Assist. Prof. Dr. Harun ÇUĞ for the valuable discussions throughout the stages of this work. I also appreciate the help and support provide by the staff of laboratories and workshops of faculty of Technology. Finally, I am forever indebted to my mother and my family for their constant love and encouragement throughout my life.

CONTENTS

Page

APPROVAL ii
ABSTRACT iv
ÖZET vi
ACKNOWLEDGMENT viii
CONTENTS ix
LIST OF FIGURES xii
LIST OF TABLES xv
SYMBOLS AND ABBREVITIONS INDEX xvii

PART 1 1
INTRODUCTION 1

PART 2 3
LITERATURE REVIEW 3
2.1 PREVIOUS WORK ON EFFECT OF PROCESS PARAMETERS ON EDM PERFORMANCE 3
2.2 SUMMARY AND GAB IN KNOWLEDGE 22

PART 3 24
ELECTRIC DISCHARGE MACHINING 24
3.1. INTRODUCTION 24
3.2 TYPES OF EDM 25
3.3 BASIC PRINCIPLES OF EDM 27
3.4 EDM PROCESS PARAMETERS 29
3.5 EDM RESPONSE MEASURES 32
3.6 DIELECTRIC FLUID 33
3.7 EDM ELECTRODES 34

Page

3.8 ELECTRIC DISCHARGE MACHINED SURFACES 36
3.8.1 Surface Topography 37
3.8.2 Surface Layers 38
3.9 APPLICATION OF EDM 40
3.10 ENVIRONMENTAL IMPAVT OF EDM 40

PART 4 42
EXPERIMENTAL WORK AND DESIGN 42
4.1 INTRODUCTION 42
4.2 DESIGN OF EXPERIMENTS 42
4.5.1 Taguchi Method 45
4.2.2 Analysis of Variance (ANOVA) 46
4.3 EXPERIMENTAL SETUP 47
4.3.1 Power Supply 48
4.3.2 Control Unit 48
4.3.3 Servo Control System 48
4.3.4 The Dielectric Fluid Delivery System 48
4.3.5 Work Table 48
4.4 The Workpiece 49
4.5 Tool Electrode 50
4.6 CONDUCTING THE EXPERIMENTS 51
4.7 MEASURMENTS AND CALCULATIONS 52

PART 5 57
RESULTS AND DISCUSSION 57
5.1 EXPERIMENTAL RESULTS 57
5.2 ANALYSIS AND DISCUSSION OF RESULTS 59
5.2.1 Effect of Process Parameters on MRR 59
5.2.2 Effect of Process Parameters on TWR 65
5.2.3 Effect of Process Parameters on Ra 69
5.2.4 Effect of Process Parameters on OC 74
5.2.5 Effect of Process Parameters on WLT 81

Page

5.2.6 Effect of Process Parameters on SCD 87
5.3 SUMMARY 93
PART 6 98
CONCLUSION AND RECOMMENDATIONS ……...98
6.1 CONCLUSION 98
6.2 RECOMMENDATIONS 100
REFERENCES..... 101

APPENDIX A. 110
LARGER VIEWS OF MSTs 110
APPENDIX B 113
MATERIALS AND EQUIMENTS 113
APPENDIX C 121
SURFACE ROUGHNESS MEASURMENTS 121
RESUME 129

LIST OF FIGURES

Page

Figure 3. 1 Schematic Illustration of EDM Process [79] 26
Figure 3. 2 The Phases of a Single Electrical Discharge[82] 29
Figure 3. 3 EDM Electrode Wears[4]. 35
Figure 3. 4 SEM Micrograph, Craters in EDMed Surface 37
Figure 3. 5 SEM Micrograph, Micro Crack, Globule and Pockmarks in EDMed surface. 38
Figure 3. 6 SEM Micrograph, White Layer. 39
Figure 4. 1 Design of Experiments Phases. 45
Figure 4. 2 EDM Machine. 47
Figure 4. 3 Measuring Surface Roughness. 54
Figure 4. 4 Measuring the Overcut. ..... .55
Figure 5. 1Comparison of Electrodes Performance for MRR. 61
Figure 5. 2 Main Effects Plot for MRR. 62
Figure 5. 3 Interaction Effect Plot for MRR. 64
Figure 5. 4 Comparison of Electrodes Performance for TWR. 66
Figure 5. 5 The Main Plot of Process Parameters on TWR. 67
Figure 5. 6 Interaction Effect Plot of the Process Parameters on TWR. 69
Figure 5. 7 Comparison of Electrodes Performance for Ra. 71
Figure 5. 8 Main Effects Plot of the Process Parameters on Ra. 72
Figure 5. 9 Interaction Effect Plot of the Process Parameters on Ra. 74
Figure 5. 10 Comparison of Electrodes Performance for OC. 76
Figure 5. 11Microscopic Image of Machined Hole, Minimum OC at Process Parameters E2A2B1C2. 76
Figure 5. 12 Microscopic Image of Machined Hole, Minimum OC at Process Parameters E1A2B1C2 76
Figure 5. 13 Microscopic Image of Machined Hole, Minimum OC at Process Parameters E4A2B1C2. 77

Page

Figure 5. 14 Microscopic Image of Machined Hole, Minimum OC at Process parameters E3A2B1C2. 77
Figure 5. 15 Microscopic Image of Machined Hole, Minimum OC at Process Parameters E5A2B1C2. 77
Figure 5. 16 Main Effects Plot of the Process Parameters on OC. 78
Figure 5. 17 Interaction Effect Plot of the Process Parameters on OC. 81
Figure 5. 18 Comparison of Electrodes Performance for WLT. 82
Figure 5. 19 SEM Micrograph, Min. WLT, EDM Parameters; E1A2B1C2 83
Figure 5. 20 SEM Micrograph, Max. WLT, EDM Parameters; E3A3B3C1 83
Figure 5. 21 SEM Micrograph, Min. WLT, EDM Parameters; E3A1B1C1 83
Figure 5. 22 SEM Micrograph, Min. WLT, EDM Parameters; E2A2B1C2 83
Figure 5. 23 SEM Micrograph, Min. WLT, EDM Parameters; E5A2B1C2 83
Figure 5. 24 SEM Micrograph, Min. WLT, EDM Parameters; E4A2B1C2 83
Figure 5. 25 Main Effects Plot of the Process Parameters on WLT. 84
Figure 5. 26 SEM Micrograph, EDM Parameters; E3A1B1C2. 85
Figure 5. 27 Interaction Effect Plot of the Process Parameters on WLT. 87
Figure 5. 28 Comparison of Electrodes Performance for SCD. 88
Figure 5. 29 SEM Micrograph, High SCD, EDM Parameters; E4A1B2C2 89
Figure 5. 30 SEM Micrograph, no Cracks, EDM Parameters; E4A3B1C3 89
Figure 5. 31Main Effects Plot of the Process Parameters on SCD. 90
Figure 5. 32 SEM Micrograph, EDM Parameters; E3A3B1C1. 91
Figure 5. 33 Interaction Effect Plot of the Process Parameters on SCD. 93
Figure 5. 34 The Contribution Effect of the Process Parameters. 95
Figure Appendix B. 1 Workpieces before Experiments. 114
Figure Appendix B. 2 The Electrodes. 114
Figure Appendix B. 3 Microscopic Images of a CuCrZr electrode ((a) 20X, (b) 100X). 115
Figure Appendix B. 4 Microscopic Images of a Cu Electrode ((a) 20X, (b) 100X). 115
Figure Appendix B. 5 Microscopic Images of a CNB Electrode ((a) 20X, (b) 100X). 115

Page

Figure Appendix B. 6 Microscopic Images of a NSS Electrode ((a) 20X, (b) 100X). 116
Figure Appndix B. 7 Microscopic Images of a B2 Electrode ((a) 20X, (b) 100X). 116
Figure Appendix B. 8 Polishing Machine..... 117
Figure Appendix B. 9 Electronic Scale..... 117
Figure Appendix B. 10 Samples and an Electrode after Experiment. 118
Figure Appendix B. 11An electrode after Experiment. 118
Figure Appendix B. 12 Water-based Monocrystalline. 119
Figure Appendix B. 13 Water-based Diamond Lubricant. 119
Figure Appendix B. 14 Scanning Electron Microscopy. 120
Figure Appendix B. 15 Samples Prepared for SEM Images. 120

LIST OF TABLES

Page

Table 4. 1. Chemical Composition (wt %) of DIN 1.2767. 49
Table 4. 2. Physical Properties of DIN 1.2767. 49
Table 4. 3 Chemical Composition (wt %) of Copper Cu-Cr-Zr Electrode 50
Table 4. 4 Chemical Composition (wt %) of Copper CNB (CuCoNiBe) Electrode. 50
Table 4. 5 Chemical Composition of Nss (CuNi2SiCr) Electrode. 51
Table 4. 6 Chemical Composition of B2 (CuBe2). 51
Table 4. 7 Physical Properties of the Electrodes 51
Table 4. 8 Process parameters and their Levels. 52
Table 5. 1 Experimental Results. 58
Table 5. 2 Comparison of Electrodes Performance for MRR. 60
Table 5. 3 Response for S/N Ratio of MRR. 62
Table 5. 4 Analysis of Variance for SN Ratios of MRR. 63
Table 5. 5 Comparison of Electrodes Performance for TWR. 65
Table 5. 6 Response for S/N Ratio of TWR. 67
Table 5. 7 Analysis of Variance for SN Ratios of TWR. 68
Table 5. 8 Comparison of Electrodes Performance for Ra. 70
Table 5. 9 Response for S/N Ratio of Ra. 72
Table 5. 10 Analysis of Variance for SN ratios of Ra. 73
Table 5. 11 Comparison of Electrodes Performance for OC. 75
Table 5. 12 Response for S/N Ratio of OC. 79
Table 5. 13 Analysis of Variance for SN ratios of OC. 80
Table 5. 14 Comparison of Electrodes Performance for WLT. 82
Table 5. 15 Response for S/N Ratio of WLT. 85
Table 5. 16 Analysis of Variance for SN Ratios of WLT. 86
Table 5. 17 Comparison of Electrodes Performance for SCD. 88
Table 5. 18 Response for S/N Ratio of SCD. 91
Table 5. 19 Analysis of Variance for SN Ratios of SCD. 91
Table 5. 20 The Effect of Parameters on the Responses. 94

Page

Table 5. 21 Contribution of Process Parameters and Interactions on the Responses. 94
Table 5. 22 the Rank of the Effect of Electrode Material on the Responses. 96
Table 5. 23 The Optimal Levels of Process Parameters for Responses..... 96
Table Appendix A. 1 Design of Experiments. 111
Table Appendix C. 1 Measurements of Workpieces Surface Roughness Using Cu-Cr-Zr Electrode. 122
Table Appendix C. 2 Measurements of Workpieces Surface Roughness Using Cu Electrode. 122
Table Appendix C. 3 Measurements of Workpieces Surface Roughness Using CNB Electrode. 123
Table Appendix C. 4 Measurements of Workpieces Surface Roughness Using NSS Electrode. 124
Table Appendix C. 5 Measurements of Workpieces Surface Roughness Using B2 Electrode. 124

SYMBOLS AND ABBREVITIONS INDEX

SYMBOLS

α : Confidence Coefficient

σ : Standard Deviation

% : Percentage

ABBREVITIONS

A : Ampere

Adj MS : Adjust Mean of Squares (Variance)

Adj SS :Adjust Sum of Squares

ANOVA : Analysis of Variance

B2 : (CuBe2) Electrode

CNB : (CuCoNiBe) Electrode

DF : Degrees of Freedom

DOE : Design of Experiments

E : Electrode

EDM : Electrical Discharge Machining

EWR : Electrode Wear Ratio / Tool Wear Ratio

GB : Gap Between Electrodes

HAZ : Heat Effected Zone

Ip : Peak Current/ Discharge Current

J : Joule

MRR : Material Removal Rate

μs : Micro Second

NSS : (CuNi2SiCr) Electrode

OA : Orthogonal Array

OC : Radial Overcut

Ra : Average of Roughness

RSM : Response Surface Methodology

SCD : Surface Crack Density

SEM : Scanning Electron Microscopy

Seq SS : Sequential Sum of Squares

SR : Surface Roughness

T_{off} : Pulse Off-time/ Pause Time

T_{on} : Pulse On-time/ Pulse duration

TWR : Tool Wear Ratio / Electrode Wear Ratio

V : Volt / Gap Voltage

WLT : White Layer Thickness

PART 1

INTRODUCTION

Industrial development witnessed the challenge of new engineering materials characterized by superior properties such as high hardness, high strength and high toughness, in addition to the growing need for accuracy and precision in manufacturing, manufacturing unusual and/or intricate shapes and 3D shapes that make them impossible or difficult to machine by conventional methods (i.e., turning, drilling, grinding, milling). Non-conventional machining processes can easily machine hard and brittle materials, complex geometries and delicate or fragile components (that cannot withstand conventional cutting forces) with tight tolerance, extreme surface finish and free of burrs. Electric discharge machining (EDM) is one of the non-conventional machining processes that can machine any conductive material regardless of its mechanical properties. EDM based on the conversion of electric energy into extremely high temperature (plasma channel) in localized region impinge on the work material surface caused melting or evaporating [1-3]. One well-established application of EDM is in machining die cavities and moulds used for die casting, extrusion, compacting, plastic molding, wiredrawing, cold-heading and forging. Another important application of EDM is in the metal forming field to produce punch, stamping dies, or trim. Also, EDM is used to produce small holes, orifices and slots [4].

Thousands of types of metals, alloys, ceramics and other materials are used in industry. Each material has its own characteristic properties, price, machining cost and ability of machining. The performance and efficiency of the EDM depend on many factors, including the type of working material, the electrode material is used and the characteristics of the product required. In addition to that knowing the influence of machining process parameters on the work material properties is an important issue in manufacturing. The scientific researches and experiments provide availability of

information about machining factors and their impact on the outputs which have a significant role in reducing effort, time, cost, and achieving the satisfied results (required quality). This has made the development of EDM a wide area of research and is still in progress.

DIN 1.2767 tool steel has crucial applications in industry such as cutting and bending tools, drawing jaws, plastic molds, gears requiring shock resistance, heavy-duty shafts and axles.

In EDM, not all parameters have the same effect on the performance. Some may have a significant effect on output performance, while others may have a moderate effect or none at all. As a result, the goal of a well-designed experiment is to figure out which set of parameters in a process has the highest influence on performance and then to determine the ideal levels for these parameters in order to achieve satisfactory output performance.

In this study, the experimental investigations are conducted on DIN 1.2767 tool steel using CuCrZr, Cu, CNB, NSS and B2 electrodes and statistical analysis was used to obtain the effect of process parameters on EDM performance of DIN 1.2767 tool steel.

PART 2

LITERATURE REVIEW

Electric discharge machining is one of the significant machining processes in manufacturing that provide a high ability to cut difficult- to- cut materials, cutting intricate shapes in addition to its precision and accuracy. The first use of EDM in the industry was after world war II, since that time, as a result of researchers' and scientists' efforts a notable development and performance improvement have occurred in EDM which contribute to its worldwide use and versatility.

Researches have handled the effect of process parameter on EDM performance, process controlling and employing mathematical models and statistical techniques to provide information on machining factors, their effect on the responses and achieving the optimum machining condition which contributes to and facilitate the manufacturing process that significantly reduces effort, time, cost, and achieving satisfying results (required quality). This has made manufacturing by EDM a large research field and is still in progress [1]. Nevertheless, the way for full potential is very long because of material variety and a large number of factors are affecting EDM.

2.1 PREVIOUS WORK ON EFFECT OF PROCESS PARAMETERS ON EDM PERFORMANCE

Some of the literature reviews related to the subject are summarized as follows:
Ramabalan mentioned that substantial researches have been conducted for improving EDM performance measures such as MRR, TWR and surface roughness (Ra). The most widely used material are steel materials, EN series, Ti-6AL-4V, SiC, B4C, WC-Co, Al2O3+Ti S45C, and Inconel 718. The main electric input parameters that have been used are T_{on}, T_{off}, Ip and V and non-electric parameters including dielectric medium, flashing pressure and electrode rotation. There are many optimization

techniques and results analysis tools used such as Taguchi, Response Surface Methodology, Gray Relationships Analysis, ANOVA, Multiple Regression Analysis [5].

Ho and Newman reviewed previous researches relating to EDM development, fundamentals, and application. They reported that the efforts carried out to improve performance characteristic measures, optimize the process parameters, observe and control the discharge process, and simplify the electrode design and fabrication. Also, they mentioned that most of the studies that are about EDM focus on improving MRR, TWR, and SR, and they pointed out the future trends of EDM researches [1].

Venkatesh, Naveen, Maurya, & Shanthi Priya studied the EDM machining performance of EN 31, EN 8, and HCHCr, and they used three electrodes, copper, brass and chromium copper. They mentioned that the optimal MRR and TWR were at chromium copper electrode followed by copper then brass. The brass electrode achieved minimal surface roughness, but TWR was high and MRR was low. Besides, performance measures were influenced by workpiece material [6].

Gostimirovic, Kovac, Sekulic, & Skoric conducted EDM experiments on ASTM A681, using a copper electrode and petroleum dielectric. The results proved that the increase of any Ip or T_{on} or both will increase the material removal rate (MRR) and surface roughness (SR). However, Ip has a significant effect more than T_{on}. The increase of Ip and T_{on} increases the white layer thickness (WLT), while T_{on} has more effect on WLT [7].

Kumar and Kumar have carried out experiments to investigate and optimize the influence of four machining parameters. The machining parameters are Ip (4, 6and 8 A), T_{on} (40, 80 and 120 μs), T_{off} (30, 40 and 50μs) and V (40, 50 and 60V). The results show that the most process parameters effect on MRR are Ip, T_{on}, T_{off}, and V respectively. The optimal machining parametric combination for MRR are Ip (8 A), T_{on} (80 μs), V (40 v), and T_{off} (50 μs), for Mild steelwork material and copper electrode [8].

Dhakry, Bangar, & Bhadauria performed EDM experiments on tungsten carbide using copper electrodes, Taguchi techniques and ANOVA were used for experiments design and data analysis. The significant effect of machining parameters on MRR are Ip, Duty cycle, T_{on} and gap voltage respectively [9].

Patil & Jadhav have discussed the influence of EDM input machining factors on the performance measures and concluded that the Ip has the highest influence on MRR, while T_{on} and V have a considerable influence on MRR. TWR is mainly affected by Ip and T_{on}, but the effect of V and Duty cycle are neglected. SR increases with the increase of Ip and T_{off}, whereas the T_{on} at higher values improves surface finishes. Ip has the greatest impact on overcut (OC). The duty cycle and T_{on} have a considerable impact on OC. The influence of gap voltage (V) on OC is insignificant [10].

Pradhan has studied the influence of EDM process parameters on the surface integrity of AISI D2 tool steel and using a copper electrode. SRM was used for optimizing and ANOVA for results verification. The results illustrate that the Ip is the most significant parameter for all response measures (SCD, WLT and SR). As a result of increasing Ip, WLT is increased and SCD is decreased. Ip, T_{on} and Tau have a significant influence on SR and WLT, whereas V is insignificantly affecting WLT. Ip, T_{on} and V have a significant influence on SCD, however no influence of Tau on SCD. The optimal operational conditions for minimum SCD, WLT and SR were Ip (3A), T_{on} (50 μs), Tau (0.8) and V (40V). Furthermore, interaction Ip* T_{on} is also significantly affecting SR [11].

Khan, Ali, & Haque have studied the effect of electrode shape and discharge current on MRR, SR, EWR, and WR of mild steel EDM machined by a copper electrode. The discharge current settings (2.5, 3.5 and 6.5A). The electrode shapes were square, round, triangular, and diamond of equal cross-sectional area. The best results (high MRR, minimum EWR, minimum EW, and minimum surface roughness) were achieved in this order; round electrodes followed by square, triangular and diamond-shaped electrodes. The effect of the shape configuration of the electrode on surface finishing was insignificant. Also, this study revealed that the EDM is able to produce intricate shapes and sharp corners and achieve high accuracy. However, forming sharp

corners requires many different electrode shapes. Additionally, MRR, TWR and SR increased with the increase of Ip [12].

Jaharah, Liang, Wahid, Ab Rahman, & Che Hassan have conducted EDM experiments on AISI H13 tool steel using a cylindrical copper electrode to investigate MRR, EWR, and SR. The process parameters were Ip (1, 2 and 4 A), T_{on} (3, 6 and 12 µs) and T_{off} (1, 2 and 4µs). However, the minimum surface roughness was at Ip (1 A), T_{on} (3 µs), and T_{off} (1µs). High Ip and T_{on} are the main factors of high surface roughness value. The highest MRR was at Ip (4A), T_{on} (3µs), and T_{off} (1µs). In addition, MRR increases due to the increase of Ip. The Ip has the highest influence on the MRR and SR. At high Ip, high T_{on}, and low T_{off}, the EWR was negligible [13].

Chandramouli & Eswaraiah have conducted EDM experiments on 17-4 PH steel, the copper-tungsten electrode was used, L27 based on the Taguchi method was applied to plan experiments and parameters optimisation. The input parameters are Ip (9,12,15A), T_{on} (50, 100, 200 µs), T_{off} (20, 50, 100 µs), and lift time (10,20, 50 µs). However, Ip and T_{on} have been shown to have a significant effect on both MRR and Ra, while T_{off} has a lower effect than Ip and T_{on}. T_{on} has the highest contribution effect on MRR and Ra, followed by Ip, and the contribution of T_{off} and lift time were negligible. The optimal parametric combination of MRR and Ra are (Ip 15A, T_{on} 50µs, T_{off} 100µs, lift time 10µs) and (Ip 9A, T_{on} 200µs, T_{off} 20µs, and lift time 10µs) respectively. Also, for MRR, there is no interaction effect between process parameters, while for surface roughness, there is a slight interaction effect between process parameters [14].

Bose & Mahapatra studied the machining of AISI H13 using die-sinking EDM with input parameters Ip (7,9 and 11A), T_{on} (16,20 and 24µs), T_{off} (12,16 and 20µs), and spark gap (SG) (0.16, 0.18 and 0.2 mm), a copper electrode was used and statistical techniques were applied for designing the experiments, analysis results and optimization of EDM performance measures. The study shows that the most affected parameter on MRR is Ip. MRR increases with the increase of Ip. T_{on} has a higher influence on SR and it decreases with respect to the increase of T_{on}. SG affected on OC greater than Ip and T_{on}. Due to the increase of SG, the OC decreases until SG =

0.18 mm then OC starts to increase. Also, it is noticed from the S/N ratio that the MRR attains its maximum value with the parametric combination of T_{on} (16 µs), T_{off} (12 µs), Ip (11 A), SG (0.16 mm). Lower Ra was attained at T_{on} (24 µs), T_{off} (16 µs), Ip (7 A), SG (0.20 mm). Similarly, lower OC is achieved at T_{on} (16 µs), T_{off} (16 µs), Ip (7 A), SG (0.18 mm) [15].

Mishra & Routara have used the Taguchi approach and multi Objective Grey Relational Grade for planning experiments and optimizing output responses (MRR and TWR) and ANOVA for obtaining significant effect and contribution of the process parameters on the responses. EDM experiments were performed on EN-24 alloy steel using a cylindrical copper electrode. The input parameters are Ip (10,15 and 20A), T_{on} (20,60 and 100 µs), T_{off} (10, and 20µs), and Flushing pressures (Fp) (0.25 0.50 0.75 Kg/cm²). However, the achieved findings are; the maximum MRR was at Ip 15A, T_{on} 60µs, T_{off} 20µs and Fp o.75 Kg/cm². The significance of the input parameters of MRR are T_{on}, Ip, Fp, and T_{off} respectively. The minimum TWR was at Ip 10A, T_{on} 100µs, T_{off} 10µs and Fpo.25 Kg/cm². The significance of the input parameters of EWR are Ip, T_{on}, T_{off} and Fp respectively. The optimal input parameters settings for optimization multi responses (MRR and TWR) are Ip 15A, T_{on} 100µs, T_{off} 30µs and Fp o.25 Kg/cm². Besides, it was noticed that Taguchi's parameter design is a robust, simple, systematic, and more efficient technique for optimization of the machining process parameters [16].

Nikalje et al have carried out EDM experiments on MDN 300 steel using a copper electrode to obtain the effect of process parameters on EDM responses. The process parameters are Ip (10, 15, 20A), T_{on} (25, 45, 65µs) and T_{off} (24. 36, 48µs). Taguchi technique L9 orthogonal arrays were applied for planning the experiments and optimising the response measures. It was found that Ip has a greater influence than T_{on} for MRR and TWR, but T_{on} was more significant than Ip for wear ratio (RWR) and SR. T_{off} has a low impact on all performance measures. Lower Ip and shorter T_{on} produce less surface damage. Also, SEM image's revealed that lower Ip and shorter T_{on} gives smoother surface characteristics with fewer craters, globules of debris, and micro-cracks than that of higher Ip and higher T_{on} [17].

Sanjeev Sharma, Rajdeep Singh, & Sandeep Jindal have studied the influence of some input parameters such as Ip, T_{on} and T_{off} on performance characteristics in EDM of EN31 die steel. The experiments were planned by using Taguchi methodology. The working range of the input parameters are Ip (10,15 and 20A), T_{on} (30, 60 and 90µs), and T_{off} (15, 30 and 45µs). The results reveal that the performance measures (MRR, TWR, and SR) are highly affected by Ip followed by T_{on}, and the effect of T_{off} is low. The optimum combination of process parameters for MRR Ip (20A), T_{on} (90 µs) and T_{off} (45 µs), for TWR Ip (10A), T_{on} (30 µs) and T_{off} (45 µs) and for SR Ip (10A), T_{on} (60 µs) and T_{off} (45 µs). Furthermore, at high Ip and T_{on} arcing may occur [18].

Kiyak & Çakir have examined the effect of EDM process parameters on surface roughness. Tool steel (AISI P20) was EDM machined by a copper electrode. EDM parameters were Ip (8, 16 and 24 A), T_{on} (2, 3, 4, 6, 12, 24, 48 and 100 µs) and T_{off} (2 and 3µs). It was concluded that SR and TWR were influenced by Ip and T_{on}, higher values of these parameters increased SR. Lower Ip, lower T_{on} and relatively higher T_{off} produced a better surface finish [19].

Shabgard, Faraji, Khosrozadeh, Amini, & Seyedzavvar conducted an experimental study on the EDM of γ-TiAl using a copper electrode and they reported that the MRR is directly proportional to Ip. The results reveal that even at the lowest level of discharged energy, the EDM process parameters affect the surface integrity of γ-TiAl and causes the formation of surface cracks. The increase in the discharge energy leads to the formation of longer wider cracks. Also, an increase in the discharge current results in an increase in MRR and TWR, but with constant T_{on} and with further increase in Ip, MRR does not increase, but it decreases in some settings with a mild slope [20].

Sihore & Somkuwar has performed EDM experiments on SS316H using a copper electrode and EDM oil as a dielectric fluid, statistical techniques (Taguchi and ANOVA) were used for optimization. It was found that for Material removal rate the main significant parameter is Ip followed by T_{on}. MRR increased as Ip increased and maximum MRR was at high values of Ip and T_{on}. The minimum SR was at low values of both Ip and T_{on}. For SR the most significant process parameter T_{on} followed by T_{off} [21].

Straka & Hašová used a copper electrode to conduct EDM experiments on EN X210Cr12. It has been established that as Ip and T_{on} are increased, the MRR increases dramatically. It was also demonstrated that increasing the T_{on} has an effect only within a specific range and that the MRR reduces over this range at constant Ip. TWR increases significantly as Ip increases, but a rise in T_{on} at constant Ip causes TWR to decrease [22].

Yadava, Dixit, & Verma investigated the effect of input machining parameters on the performance of AISI D3 steel for EDM utilizing brass electrodes, designing experiments and optimizing input machining parameters using the Taguchi technique. Ip (5,8 and 11 A), T_{on} (6,9 and 12 µs), T_{off} (2,5 and 8 µs), and FP (1,2 and 3 kg/cm²) are the input machining parameters. It was found that the highest MRR was achieved at the experimental level of Ip (8Amp), T_{on} (6µs), T_{off} (8µs), and Fluid Pressure (1 kg/cm²), whereas the minimum TWR was achieved at the experimental level of Ip (1Amp), T_{on} (6µs), T_{off} (8µs) and Fluid Pressure (1 kg/cm²). In addition, (Ip) has the greatest influence on MRR, whilst other parameters have a minor impact. Peak current (Ip) and pulse on time (T_{on}) are the key factors that influence electrode wear rate; fluid pressure has little effect [23].

Hadad, Bui, & Nguyen have carried out EDM experiments on AISI 1050 hardened steel with a copper electrode and reported that the electrode initial surface roughness has a significant influence on MRR and TER and slightly influences on the SR of work material after EDM machining. As initial electrode surface roughness increases, the rate of material removal will be slow and TWR increases [24].

Raman, Sathiya, Saisujith, & Mani studied the effect of machining parameters in EDM of AISI D2 tool steel with copper electrodes and kerosene as a dielectric fluid, where the copper electrodes diameter (D) (9.5, 12 and 20 mm) and discharge current (Ip) were measured (3.5 and 6.5A). The best MRR and EWR were found when the electrode diameter was 20mm and the discharge current was (6.5 A) in a parametric combination. In order to achieve a high MRR and a low EWR, either a low Ip with a small tool diameter or a high Ip with a large tool diameter is required [25].

Hamid & Lajis have studied the impact of high values of process parameters on AISI D2 hardened steel EDM machined in kerosene with a copper tungsten tool electrode. The process parameters Ip (20,32 and 40A), T_{on} (400,500 and 600 µs) and the duty factor was 80%. The experimental results revealed that the highest MRR was at Ip (40A) and T_{on} (400µs), the lowest TWR was at Ip (20A) and T_{on} (400µs), the lowest SR was at Ip (20A) and T_{on} (600µs). The optimum machining performance for these three responses was achieved by the combination of Ip and T_{on} at (40A) and (600µs) respectively [26].

Koteswararao, Siva Kishore Babu, Ravi, Kumar, & Chandra Shekar have investigated the influence of EDM machining parameters (Ip, T_{on}, and electrode diameter) on EN31 alloy steel utilizing a copper electrode. L18 orthogonal array based on Taguchi design experiments were conducted. The results showed that the Ip is the most influential parameter on both MRR and TWR, then T_{on} and, lastly, the electrode diameter. MRR increased with the peak current (Ip). As the pulse on-time prolonged, the MRR reductions monotonically. Ip and T_{on} are the most influencing parameter for MRR and as well as the interaction between Ip and T_{on} is significant. The most essential parameter in OC is Ip, followed by D, with no effect of pulse on-time [27].

Hwa Teng Lee, Hsu, & Tai investigated the effect of EDM machining input parameters on surface integrity of AISI 1045 using Cu- W electrode. The machining input parameters are Ip (1,4, 8and 12 A), T_{on} (9, 12,18 and 23 µs), T_{off} (9,12,18 and 23µs), duty factor 0.5 and the open voltage (200V). It was figured out that the values of MRR, SR, OC, WLT and induced residual stress be likely to increase at higher values of Ip and T_{on}. However, for prolonged pulse on-time, it was found that the MRR, SR, and SCD all decrease. Additionally, the results show that clear cracks are always apparent in thicker white layers. A smaller Ip (i.e. 1A) tends to raise SCD, whereas a longer T_{on} (i.e. 23 µs) enlarges the surface crack's opening degree, lowering SCD. Moreover, a significant crack opening is linked to a smaller SCD [28].

Paul & Jose compared the results of EDMed machining of Cupper with two distinct tool materials (Cupper and Stainless steel). Stainless steel has a lower TWR and a higher MRR. The MRR and EWR differ depending on the workpiece and electrode

materials. Furthermore, they demonstrated that as V increases, MRR increases as well, up to a point, after which MRR decreases. Arcing may occur at high V values. T_{off} should not be too short to allow debris to be removed from the gap between the electrodes [29].

Amorim & Weingaertner carried out EDM experiments on AISI P20 tool steel with graphite and copper electrodes. The findings show that the maximum MRR were attained using graphite electrodes with negative polarity. Graphite and copper tools gave similar results of MRR for positive polarity. The optimum surface finish was achieved by copper electrodes with negative polarity [2].

Vishwakarma, Yadav, Kumar, & Krishhna have reviewed many papers related to EDM and the utilization of different dielectrics, additives to the dielectrics, and Al, Cu, Brass and CuW electrodes. They stated that copper electrodes and Kerosene (dielectric) have major use in EDM, whereas using other type of dielectric fluid like water, EDM oil, water with additives such as Servotherm, powder additives dielectric for example titanium powder, graphite powder, Al powder etc. improves EDM performance. The copper electrode produces lower SR, whereas the graphite electrode with additives mix Kerosene produces higher MRR in EDM [30].

Mahajan, Krishna, Singh, & Ghadai have reviewed researches about the performance of copper, brass and Copper- tungsten electrodes in EDM and mentioned that TWR is proportional to peak current and voltage. TWR is inversely proportional to melting temperature and thermal conductivity. MRR increases with respect to the increase in peak current regardless of electrode material. MRR, TWR, SR, OC and dimensional accuracy are influenced by electrode material. Also, copper tungsten electrode material produces the highest MRR and the lowest TWR in comparison to brass and copper electrode [31].

Muttamara compared the performance of graphite (Poco EDM-3) and copper infiltrated-graphite (Poco EDM-C3) electrodes in EDM of Ti6Al4V. The electrode material has an impact on MRR and TWR. In comparison to PocoEDM-C3, the PocoEDM-3 electrode has a higher MRR and a lower TWR. The PocoEDM-C3

electrode produces a better surface finish than Poco EDM-3 electrode. The micro-hardness of the recast layer is 3-4 times higher than the substrate [32].

Singh, Maheshwari, & Pandey experimentally investigated the influences of machining parameters such as discharge current on MRR, TWR, SR and OC in electric discharge machining of En-31 tool steel using four electrodes (copper, copper–tungsten, brass and aluminium). The results show that the performance measures of EDM increase with the increase in discharge current and the best machining rates are attained with copper and aluminium electrodes[33].

Puthumana, Govindan presented an analytical study to estimate the influence of micro-EDM process parameters on TWR. Alpha-beta titanium superalloy was machined by a brass electrode. The input factors are Ip (0.5, 1, 1.5, 2 and 2.5 A), T_{on} (1,4,8,2 and 16μs), gap voltage (30, 35, 40, 45 and 50V) and dielectric flushing pressure (0.15, 0.2, 0.25, 0.3 and 0.35 kg/cm2). The results show that EWR is inversely proportional to T_{on}, and the minimal EWR was observed at the T_{on} range between 8 and 12μs. TWR increases with an increase in IP in the micro-EDM process up to 1.5 A. A maximum increase was attained between Ip of 1 and 1.5 A. Also, it is observed that EWR increases with an increase in flushing pressure from 0.2 to 0.25 kg/cm2 and then decreases [34].

Keskin, Halkaci, & Kizil performed experiments to study the effect of EDM process parameters on SR and a mathematical model was derived to determine surface roughness by applying multiple regression when using steel work material and copper electrodes. It was revealed that when the pulse on-time increases, the surface roughness increases. This is essential because of increased discharge energy being released at this time and the diameter of the discharge channel increasing [35].

Habib has carried out experiments on tool steel AISI 2714, using copper and graphite electrodes and kerosene as a dielectric. Taguchi technique was applied for designing experiments and optimizing EDM performance (MRR, SR and OC). ANOVA was employed for verifying the results and obtaining the contribution effect of input parameters on the performance measures. The results show that when the copper

electrode is used, T_{on} has the highest influence on machining performance followed by Ip, T_{off}, and V respectively. But when using graphite electrodes, the influence of process parameters can be ranked as follows; T_{on}, T_{off}, Ip, and V. That is the significance of the influence of process parameters depends on electrode material [36].

Teepu and Sultan have experimentally investigated the influence of the process parameters on EN 353 steel with a tubular copper electrode. The experiments were designed and the process parameters optimized by employing SRM, and the results were analyzed by applying ANOVA. The input parameters are Ip (2,25 and 45A), T_{on} (100,340 and 580 µs) and T_{off} (4,16 and 25µs). Minimum surface roughness was achieved at process parameters T_{on}, T_{off} and Ip at (147.01 µs), (26.69 µs) and (9.03A) respectively. Besides, a better surface finish can be attained by setting Ip and T_{on} at low levels [37].

Krishna Mohana Rao & Hanumantha Rao investigated the influence of work material, discharge current, voltage on surface roughness and surface hardness. EDM tests were carried out on four different types of work materials (Ti6Al4V, HE15, 15CDV6, and M-250), and it was discovered that the workpiece material has the greatest impact on performance measurements [38].

Salonitis, Stournaras, Stavropoulos, & Chryssolouris constructed a thermal-based model to predict MRR and SR, and then verified the results by comparing them to the results of conducted experiments. They found that increasing Ip, V, or T_{on} produces a higher MRR and SR. T_{off} reduction, on the other hand, increases material removal rate and slightly improves surface finish. Besides, there is an interaction effect of Ip and T_{off} on SR. The deviation between the model's predictions results and experimental was acceptable [39].

Fikri, Romlie, & Aminnudin have experimentally evaluated the effect of process parameters on EDM performance (MRR and Ra) of AISI P20M Steel. They verified their results statistically. Graphite, copper and brass were used as electrodes. It was concluded that the types of electrode material, the value of discharge current, and material removal rate affect the surface roughness. Surface roughness is influenced by

physical parameters of the electrode, such as thermal conductivity, melting temperature, and electrical resistivity. In addition, it was discovered that the graphite electrode had the greatest influence on Ra, followed by brass, and finally copper. These findings are based on the fact that graphite electrodes have the highest electrical conductivity, followed by brass, then copper electrodes. Furthermore, the results confirmed that higher Ip leads to higher Ra [40].

Ahmad & Lajis have conducted experiments on Inconel 718 with a copper electrode. The EDM process parameters were at high values; Ip (20, 30, 40A), T_{on} (200, 300, 400 μs), and V (120 V). It was concluded that when EDMing Inconel with a Copper electrode, the discharge current has the greatest influence on producing high MRR, whereas pulse on-time has an insignificant effect. The longer the pulse on-time, the lower the tool wear rate, but the higher the discharge current used, the worse the TWR. In order to produce a satisfactory surface finish, the lowest discharge current and pulse on-time are recommended for surface roughness. Also, according to the results of the experiment, machining at a discharge current of (40A) and a pulse on-time of (200 μs) produces the highest MRR, while machining at a discharge current of 20A and a pulse on-time of (400μs) achieves the lowest TWR. At the lowest discharge current of (20A) and a pulse on-time of (200 μs), the lowest SR was achieved [41].

Kumar conducted EDM experiments on OHNS Die Steel by using three different electrodes (copper-chromium, brass, and copper), kerosene as the dielectric fluid and discharge current ranging from 6 to 12A (Ip = 6,7.5,9,10.5 and 12A). Their results showed that the copper-chromium electrode produced higher MRR, better surface finish, lower TWR compared to other electrodes [42].

Nallusamy has performed an experimental investigation of MRR and TWR on OHNS using EDM with copper and brass electrodes. The results revealed that MRR and TWR increase with the increase of Ip for both electrodes. The copper electrode gives higher MRR than the brass electrode, and the copper electrode is appropriate for both rough and finishes machining, whereas the brass electrode is appropriate only for rough machining [43].

Bhattacharyya, Gangopadhyay, & Sarkar have applied SRM to develop mathematical models for SR, SCD and WLT. The workpiece material and electrode were Die Steel (M2-hardened and annealed) and copper respectively. They reported that a better surface finish was achieved when the magnitudes of T_{on} and Ip were at the minimum (20µs and 2A). For minimum WLT the Ip and T_{on} should be at a range of 2-5A and 163-510µs respectively. To minimize CSD the Ip and T_{on} could be in the range 18–22A and 20–100µs respectively. The minimum SR can be achieved by using lower values of T_{off} and Ip. The experimentations and the mathematical models show that the lowest values of SR, SCD can be obtained when the parametric combination (Ip and T_{on}) values are (3.5A) and 20µs [44].

Ghanem, Braham, & Sidhom used a graphite electrode to conduct EDM experiments on hardenable and non-hardenable steels and found that the workpiece material has a significant role in metallurgical transformation, surface residual stress, and surface hardening. Near-surface hardness is roughly three times that of the substrate. Ip has the greatest influence on SR, while workpiece material has a little influence. Hardenability and Ip both enhance SCD. The chemical composition of the near-surface is affected by the dielectric fluid and electrode material [45].

Boujelbene, Bayraktar, & Wissem have researched the effect of EDM parameters on surface integrity. The specimen materials are X200Cr15 and 50CrV4 steel. When using a copper electrode, the discharge current (3 - 30A) and pulse discharge energy (5.76 – 560.8 J). it is concluded that the increase of discharge energy leads to increase SR and WLT. Lower Ip and short T_{on} should be used for a thin heat affected zone (HAZ) and minimal hardened surface but that reduces the MRR. High discharge energy causes electric arcs which damage the electrode surfaces and workpiece surface and it can cause micro-cracks. Cracks are created as a result of the stress induced by the EDM. CSD increases with the increase of discharge energy [46].

Çaydaş & Hasçalik in their experimental study on Ti-6Al-4V alloy EDM machined, they applied SRM and ANOVA for model developing and checking the adequacy of the model. They revealed that the Ip was the most significant factor that influences

both WLT and TWR, while T_{off} has no crucial influence on both responses. There is an interaction of Ip and T_{off} that is highly significant for TWR and WLT [47].

Cusanelli et al have studied the microstructure of the white layer of Böhler W300 ferritic steel EDM machined with a copper electrode. It is reported that the white layer consists of various microstructures: columnar and dendritic structures with different thicknesses. The white layer hardness is larger than the substrate workpiece as a result of the high carbon content in the white layer. Interface white layer/HAZ, and HAZ have different microstructures as a result of different cooling rates [48].

Younis et al. investigated two different grade carbon electrodes on DIN 1.2080 and DIN 1.2379 tool steels. However, the higher Ip and short T_{on} exhibited higher SCD; moreover, high T_{on} and low Ip caused high residual stresses. The type of electrode has a significant effect on SR and TWR [49].

L. C. Lee, Lim, & Wong proved that the dielectric fluid has a significant role in determining the chemical composition of the recast layer. As a result of materials having better thermal conductivity, the WLT will be thinner and less SCD [50].

Wang, Chow, Yang, & Lu have researched the eliminating of the white layer using etching and mechanical grinding for Inconel 718 by means of electrical discharge machining (EDM). The experiments were designed and optimized by applying the Taguchi method. The process parameters, polarity (+, -), Ip (20,30,40A), T_{on} (200,400,800µs), T_{off} (100,300,600µs) and V (50,75,100V). The results showed that the most significant is the polarity, as contribution ratio 51.014%, will dramatically affect WLT followed by T_{on} (27.672%) next T_{off} (14.306%) then Ip (5.099%) and Gap voltage has a small impact with 1.906% for the contribution ratio. The findings of the ANOVA clearly reveal that there are no interaction effects of process factors for simultaneously enhancing WLT. The optimal combination is represented as A1B3C2D2E2 [51].

Ekmekci has studied white layer composition and cracks formation on plastic mould and roll Steel EDM machined using a copper electrode. The study shows that the

properties of workpiece parent material and white layer chemical composition are significant factors for cracks formation, their distribution and penetration depth. Cracks' penetration depth is proportional to the pulse energy. Surface cracks, which start at the surface, move down perpendicularly toward the parent material and end at the interferential layer. The amount of these cracks largely depends on the mechanical properties and thermal properties of the parent material. Also, the thickness of the white layer increases with the increase of both peak current and pulse on-time [52].

Guu has investigated the impact of EDM discharge energy on the surface quality of AISI D2 tool steel. The process factors are Ip (0.5,1 and 1.5A), T_{on} (3.2 and 6.4µs) and T_{off} (20 µs). The findings revealed that, to avid surface degradation, achieving minimum surface roughness and low depth of micro-cracks, Ip and T_{on} must be at low values [53].

Straka & Hašová have investigated sub-surface layers of mildly-alloyed chrome-molybdenum-vanadium tool steel EN X32CrMoV12-28 (W.-Nr. 1.2365) EDM machined with SF-Cu electrode in non-ionized water. Process parameters setting range for rough machining Ip (40-60A), T_{on} (150-300µs), T_{off} (75-120µs) and V(70-90V), semi-finishing Ip (10-40A), T_{on} (50-150µs), T_{off} (35-75µs) and V(70-95V) and for finishing Ip (2-10A), T_{on} (5-50µs), T_{off} (5-35µs) and V(70-95V). It was reported that the HAZ consists of the Black layer (BL), White layer (WL) and Transition layer (TL) which are distinguished by having a specific microstructure, and properties. Each layer's thickness and properties are based on a set of process parameters [22].

H. T. Lee & Tai have researched the impact of EDM process parameters and the formation of surface cracks. The work materials were D2 and H13 tool steel. The experiments were designed by using a full factorial design. The results revealed that the surface roughness and WLT increase as Ip and T_{on} increase. While the effect of T_{on} is more significant for WLT. The SCD is affected by WLT, that is the thicker the WLT, the more SCD. Machining with parametric combination Ip in the range of (12–16A) and T_{on} of (6–9µs), the cracks in the surface can be avoided. Also, it revealed that because H13 has a higher thermal conductivity than D2, the likelihood of crack formation in H13 is lower than in D2 [54].

L. C. Lee, Lim, Narayanan, & Venkatesh attempted to determine the surface damage on tool steels (AISI A2, D2, O1, and D6) due to EDM machining. The surface damage (WLT/ recast layer) is based on peak current, pulse energy, rapid solidification and thermal properties of melted material. The magnitude of the Ip has little influence on the WLT. Also, it is obtained that SCD is inversely proportional to WLT and depends on the thermal properties of the tool steel concerned [55].

Kruth, Stevens, Froyen, & Lauwers studied the role of dielectric fluid in EDM on the white layer. The white layer hardness, microstructure and chemical composition are affected by the type of the dielectric fluid. The carbon continent and the hardness, both of them in the white layer are higher than in the base metal. Carbon in the white layer is transferred from the dielectric fluid. The rapid cooling of molten material caused the forming of a dendritic structure in the white layer [56].

Shailesh Dewangan, Gangopadhyay, & Biswas have conducted EDM experiments. The work material in these experiments was AISI P20 tool steel and the tool material was copper. Grey-fuzzy logic-based hybrid technique was used to optimize SCD, WLT, and SR. It is revealed that the most significant parameter that affects the SCD, WLT and SR are T_{on} followed by Ip, for multiple response characteristics of surface integrity (SCD, WLT, and SR) [57].

Ekmekci has studied the influence of dielectric fluid and electrode material on white layer structure. The work material was Plastic mould steel DIN 1.2738 stress-free, the electrodes were copper and graphite and the dielectric fluids were kerosene and de-ionized Water. It is noted that the electrode material and dielectric fluid type affected on sublayer structure; in addition, when using kerosene as dielectric, the surface of the work material is saturated with carbon irrespective of the type of the electrode. Also, figured out that the surface residual stresses on machined surfaces grow as the white layer's non-homogeneities increase. Such stresses may exceed the material's fracture strength, resulting in a random distribution of micro-cracks on the machined surface [58].

Yerui, Zongfeng, Yongfeng, & Zongfeng conducted experiments on TiC/Ni using EDM. The experimental results revealed that as the Ip increased, the discharge energy increased, which results in an increase in the MRR. MRR increases with the increase of T_{on}, but when T_{on} was longer than 30 μs MRR decreased slowly. This was a result of the expansion of the plasma channel and the effect of debris on it [59].

Dastagiri & Hemantha Kumar reported that the higher the Ip, the more discharging energy. Then, the metal temperature rises in a very localized region, thus more MRR can be achieved. T_{on} increases, MRR increases and then decreases [60].

Kalyon applied Taguchi method and GRA for optimization of EDM of Caldie cold work tool steel, considering process parameters such as Ip, T_{on} and electrode materials (graphite and copper). The results revealed that with increasing Ip and T_{on}, the MRR and Ra increased. The optimal parametric combination for MRR is a copper electrode, 25 A and 200 μs and the optimal parameter setting for maximum MRR and minimum Ra obtained by grey relational analysis is graphite electrode, 6A and 50μs [61].

Habib has performed experiments by using copper as a tool electrode on an EDM with selected input parameters on conductive metal matrix composite Al/SiC. Results of the study showed that the higher Ip offered higher MRR. An increase in T_{on} caused an increase in MRR until it reached 200 μs and then MRR began to decrease. TWR was found to be directly proportional to Ip and T_{on} [62].

Gopalakannan, Senthilvelan, & Ranganathan have investigated EDM machining performance and optimized the process parameters of AL7075-B4C MMC using response surface methodology. The process parameters were Ip, T_{on}, T_{off} and gap voltage. It was concluded that the two main significant process parameters that affect the MRR were Ip and T_{on}. The MRR increased with the increase in T_{on} and then decreased with longer T_{on}. Also, TWR decreased with the increase of T_{on}. Ip and T_{on} have a statistically significant effect on TWR [63].

Arunkumar, Rawoof, & Vivek have explored the influence of electrode material on the performance characteristics of electrical discharge machining of EN31 (air-

hardened steel). It was observed that the copper electrode provides less TWR, higher MRR, less taper value and variation in the average Ra compared with aluminium and En-24 electrodes [64].

Haron, Deros, Ginting, & Fauziah have investigated the effect of discharge current and electrode diameter on MRR and TWR when machining AISI 1045 tool steel. Low discharge current was found to be appropriate for small diameter electrodes, while high discharge current was found to be appropriate for large diameter electrodes [65].

Haron, Ghani, Burhanuddin, Seong, & Swee have experimentally investigated the effect of the process parameters on MRR and TWR of XW42 tool steel using graphite and copper electrodes. The results revealed that the increase in the Ip and electrode diameter reduced TWR as well as MRR [66].

A. Mahajan, Sidhu, & Devgan have studied the effect of EDM performance parameters on the MRR and Ra of Co-Cr alloy employing the Taguchi L18 orthogonal array. Two dielectric fluids (deionised water and EDM oil) and three electrodes (graphite, tungsten and tungsten-copper) were used. It was found that the most significant parameter affecting Ra is T_{on}, followed by Ip and electrode material, and for MRR, the dielectric had the highest influence than Ip and electrode material. T_{off} was exhibited as an insignificant parameter for both responses [67].

Panda, Mishra, Biswal, & Nanda have investigated the EDM of S304 grade stainless steel using the copper electrode. Experimental results showed that the Ip, T_{on} and dielectric flashing pressure significantly affected the MRR and TWR, while Ip and T_{on} affected the surface roughness [68] .

M. Kumar, Kumar, Kr, & Sahoo have optimized MRR and SR in EDM of EN31 tool steel. It was revealed that with an increase in Ip and T_{on}, MRR and SR increase. Scanning electron microscopy (SEM) was used to study surface morphology and it is observed after machining, the machined surface is rougher and contains plenty of globules and debris particles on the surface [69].

Kumar and Bighensh carried out experimental research to investigate aspects of EDM on Inconel 718 super-alloy using a Copper electrode. It has been revealed that MRR, WLT and SCD are directly proportional to T_{on} [70].

Roy & Kumar have studied process parameters affecting material removal parameters on EDM of EN 19 and EN41 material with copper tool electrode, Taguchi method was applied for designing the experiments and to predict the best parametric combination of optimal response and Analysis of variance was used to determine the importance of the process parameters that affecting the responses. It was found that the Discharge current had a larger impact on the MRR followed by T_{off} then V and the last was T_{on} [71].

P. Kumar, Dewangan, & Pandey have studied the effects of EDM process parameters on overcut and surface integrity of the machined surface. Optimization of performance measures has been performed using the RSM method. P91 steel acts as a workpiece while copper is selected as the electrode tool. The process parameters Ip (2,5,8A), T_{on} (50,100,150μs) and Tau (0.7, 0.8, .09). The results indicated that for all the performance measures, Peak Current is the most significant parameter followed by Pulse-On Time and then the Duty-Cycle. Optimal parametric combination for OC, Ip (2A), T_{on} (50 μs) and Tau (0.7), for SCD, Ip (5A), T_{on} (50 μs) and Tau (0.8) and for SR, Ip (2A), T_{on} (50 μs) and Tau (0.9) [72].

S Dewangan, Biswas, & Gangopadhyay have studied the effect of various tool electrode materials like brass, copper and graphite and different process parameters such as peak current, pulse-on time, duty cycle, and polarity on EDMed surface integrity. The work material is AISI P20 tool steel. The results showed that maximum WLT, SCD, and SR were attained for the graphite tool. The brass electrode performed best then the copper electrode when different aspects of surface integrity were analyzed. discharge current was obtained to be the most significant process parameter affecting machined surface integrity [73].

2.2 SUMMARY AND GAB IN KNOWLEDGE

The current study attempted to review several scientific theoretical and practical researches to address the most relevant topics of this thesis. Which focuses on studying and investigating the effect of process parameters such as electrode material, Discharge Current (Ip), Pulse on-time (Ton) and Pulse off-time (Toff) on the performances of electric discharge machining such as MRR, TWR, SR, OC, WLT and SCD. These studies have led to the following conclusions:

- In general, the most effective electrical process parameters on EDM performance are Ip, T_{on}, T_{off}, and V respectively. Also, electrode material and workpiece material have important effect on EDM performance.
- The effective range of the electrical process parameters on performance measures varies according to both work material and electrode materials. And each type of electrode material or work material required particular study to determine its performance in EDM.
- The trend of the effect of some parameters may be changed at a particular value.
- The effect of the combined process parameters (interaction) on the performance of EDM has a complex relationship, and the use of statistical methods and mathematical equations helps in achieving satisfactory results.

Various studies have been conducted on EDM utilizing workpiece materials such as tool steels, composites, and alloys, however, it has been noticed that no considerable work has been performed to investigate the effect of process parameters using copper and copper alloys electrodes on the EDM performance measures of cold work tool steel DIN 1.2767.

This study aims to determine the effect of the process parameters (Ip, T_{on}, T_{off} and electrode material) on the EDM performance measures (MRR, TWR, SR, OC, WLT and SCD) of DIN 1.2767 tool steels. The study also attains the best set of process parameters that achieve the optimal performance. As a result, providing information

about EDM for DIN1.2767 Tool Steel, improving the EDM machinability and enhancing the application of EDM in manufacturing.

PART 3

ELECTRIC DISCHARGE MACHINING

3.1. INTRODUCTION

In conventional machining processes (i.e., drilling, milling, turning, shaping, broaching, sawing) a sharp cutting tool is used to remove the excess material and to achieve the desired geometry. The sharp cutting tool has one or more edges harder than workpiece material. In non-conventional machining, the excess material is removed by various energy forms for example thermal, mechanical, chemical and electrochemical energy or hybrid. The requirement of machining new materials which have superior properties (e.g., high hardness, high strength, high toughness), unusual and/or intricate part geometries and avoiding surface damage that accompanies the stresses produced by conventional machining. These requirements led to the development of non-conventional machining. Electric discharge machining (EDM) is one of the non-conventional machining processes that result in the conversion of electric energy into very high thermal energy. This energy is created as the spark between electrode and workpiece in a tiny area which causes the workpiece to melt or vaporize. The EDM began to be used during the 1940s after two Russian scientists (Boris and Natalya Lazarenko) discovered that the erosion of electric contacts was more precisely controlled if the electrodes were submerged in a dielectric fluid. They succeeded to control and maintaining the gap between the electrode and the workpiece and reducing the electric discharge [74]. EDM has the ability to machine any conductive materials with high accuracy, good removal rates, and good surface finish, regardless of the material mechanical properties such as hardness, brittleness, wear resistance or toughness, making it widely used in many fields involving medical, aerospace, automotive, electronics and other industries.

The beginning of the use of EDM was limited to removing broken tools such as taps and drills from expensive workpieces. Then it developed and started simple use in the workshops to make holes and simple milling, where the electrode movement was only vertical. Recently, with the growth of the industry, the increased demand for manufacturing machines, the great development in software and control systems and the use of computer numerical control (CNC) machines in the fields of manufacturing, CNC EDM has also become one of the modern machines equipped with workpiece and tool changer and can drive up to six axes simultaneously in addition to unattended and automated operational processes that keep work going during holidays also make EDM which made EDM machining one of the main and important machining processes that are indispensable in the field of manufacturing [75].

In recent years, the development and improvement of the EDM manufacturing process have become noteworthy, many EDM types have been presented to the production sector; for instance, sinking EDM, dry EDM machining, EDM with powder additives, ultrasonic-assisted EDM, Micro EDM and wire EDM. Each of these machining processes has a distinct performance [76]. In addition, applying the mathematical and statistical technique in predicting and optimizing EDM performances measures have contributed the growth of EDM application [77], also, researchers have succeeded to machine nonconductive ceramic by applying assisting electrode [78], which have a role in enhancing the use of EDM in manufacturing.

3.2 TYPES OF EDM

Manufacturing uses different tools and machines for different purposes to perform different tasks such as cutting, drilling, making cavities, surface finishing, micromachining and other processes required by production. EDM machining has several types, each type performs distinctive works. These types include:

- Sinking EDM: Sinking EDM also known as Ram EDM or Die Sinking EDM. A typical system of Sinking EDM is illustrated in Figure 3.1. The electrode and the work material are connected to a pulse generator, and they are immersed in a dielectric medium, the discharge occurs at the closest points

between the electrodes. The dielectric fluid is filtered from contaminations and debris to sustain its insulation. The electrode (tool) movement towards the work material is controlled by a servo mechanism to maintain the erosion in both electrodes and keep the inter-electrode gap constant. Sinking EDM application in manufacturing parts and tool fabrication, especially that consist cavities, intricate contours, holes and deep holes which they are difficult to machine (hard or brittle materials) by conventional methods.

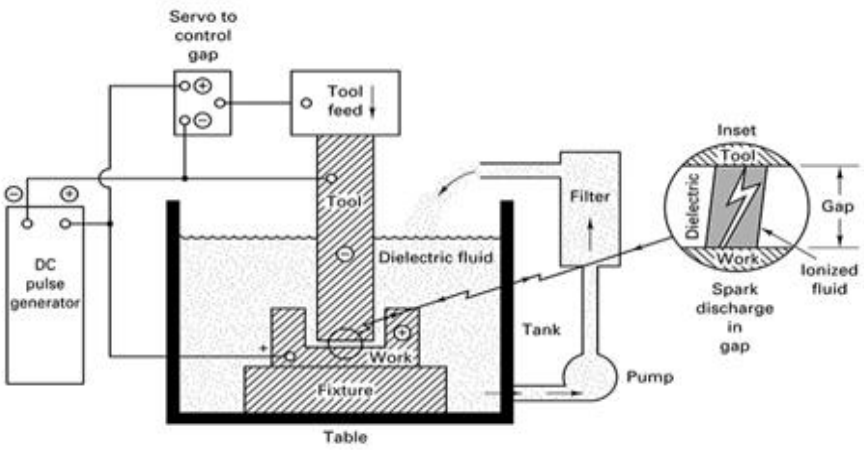

Figure 3. 1 Schematic illustration of EDM process [79]

- Electric discharge grinding (EDG): EDG is similar to EDM; nevertheless, the electrode in EDG is a rotating electric conductive wheel. The electrode (wheel) rotates with speed which makes EDG achieves better results when machining brittle and hard materials compared to EDM. As a result of the wheel rotating, the molten material and debris are ejected from the inter-electrode gap, and the performance of EDG is enhanced. The EDG can be categorized into two types, the first type is the rotating wheel without abrasive and the second type is the wheel made from abrasive bonded with conductive material [80].

- Wire EDM: wire EDM, also called electrical discharge wire cutting (EDWC). It is one of the EDM forms; but, the electrode is a thin electric conductive wire. The discharge (spark) occurs at the nearest points between the wire and the workpiece. The wire continuously travels to avoid wire wearing and breakage

problems. The wire is made from different electrically conductive materials including copper, brass, tungsten, and molybdenum. The wire diameter ranges from 0.076 mm to 0.30 mm, to facilitate the cut of narrow kerfs and sharp corners. Wire EDM is widely used for producing punches, dies, stripper plates, and intricate outline shapes [75].

- Micro EDM: It is a variant of Sinking EDM and WEDM. The process parameters in Micro EDM such as Pulse-on-Time, Pulse-Off-Time, Open Circuit Voltage, Peak Current, Inter Electrode Gap, and Tool size are too small. As a result of that, Micro EDM has the ability to machine and produce dimensions in a few microns and stress-free [81].

3.3 BASIC PRINCIPLES OF EDM

Since the discovery of electricity, it has been observed that when two electrically conductive wires (electrodes) are connected to an electric power supply, and approach or even come into contact, electric arc occurs between them, causing melting and erosion at the points of convergence in very small areas of one or both electrodes. Although this phenomenon is the basic principle of EDM and it has been observed for a long time, its advantages have not been taken until the 1940s [82]. Since then, applications for this type of manufacturing have begun to appear and the development and performance improvement has been apparent; as a result, the use of the EDM is increased.

As well as the research and discoveries of other types of this method of machining, in addition to some modifications in the components of machining tools and controlling the process parameters, which has had a widespread impact on the development and improvement of this technology.

The EDM machine tool, as in Figure 3.1 consists of an electrode connected to a pulsed power supply, the workpiece must be a conductive material and normally the anode. The process is performed in the presence of dielectric fluid which is an insulator up to a specified potential. The dielectric fluid is purified from impurities and pumped into

the tank. The gap distance between electrodes is controlled and maintained by the servo- mechanism.

The erosion mechanism in EDM is a complicated phenomenon that involves a number of physical processes. The material-removing by one spark of EDM is briefly explained in Figure 3.2 Consider the tool is a positive electrode and the workpiece is the negative electrode. At startup, the voltage difference between the electrode and the workpiece rises gradually until the voltage difference reaches a high value needed for dielectric fluid breakdown. The electrode moves in the direction of the workpiece without contact (held at a small inter-electrode gap). At the nearest two points between the electrodes, electrons emitted from the tool toward the workpiece impinge the dielectric fluid molecules. Then, the molecules are broken down into electrons and positive ions; consequently, the fluid molecules become ionized. When the breakdown occurred, the voltage drops and the current rises abruptly and rapidly.

As a result of the ionization of the dielectric and the formation of the path of discharge (plasma channel), the current can pass causing an extremely high temperature rise between 8000° C -12000° C, so a small portion of the workpiece surface is abruptly melted or vaporized, and a small pool of molten metal is formed. During this charge across the inter-electrode gap, the plasma channel is rapidly expanding and the molten metal pool is growing. The time of the current flow (discharges) is called On-time.
Off-time starts at the current and voltage switching off. Then, the plasma channel is broken down under the pressure of surrounding dielectric fluid; consequently, a molten metal pool is partly ejected by the dielectric, which creates a tiny crater on the surface of the workpiece. During the Off-time period, the dielectric expels contaminations and cools this area. The dielectric fluid restores its properties (insulation) and it will be ready for the next spark. Un-expelled molten metal resolidified to form a recast layer. All these actions, which occurred during on-time and Off-time, describe what happened in individual spark, they occur in micro-seconds and are repeated thousands of times per second. As a result, the distance between the workpiece surface at the previous spark is bigger, the next spark occurs at the workpiece surface and the tool surface are the closest point.

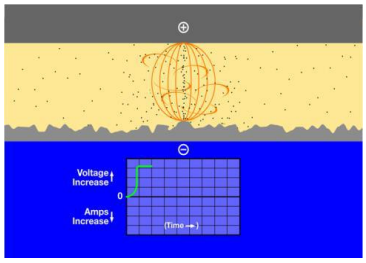

Fig. 3.2a High potential voltage (open gap voltage). The electromagnetic field is created at the closest points between the electrodes, and no current

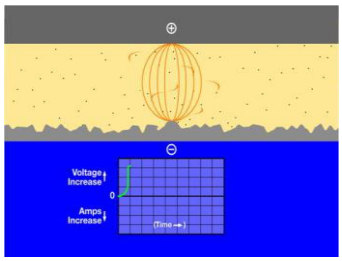

Fig. 3.2b The electromagnetic field rises, the polarizing of the dielectric is begun, its resistivity declined. Open-gap voltage levels off

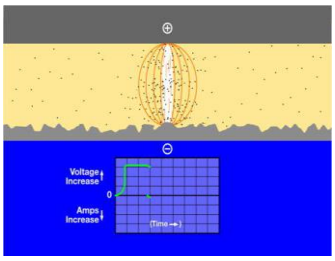

Fig. 3.2c "On-time" begins. Dielectric fluid resistance is overcome and the discharge occurs. The voltage will decrease and the current raises.

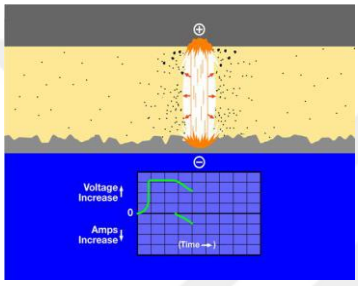

Fig. 3.2d The plasma channel is created, high temperature vaporizes the workpiece and the dielectric in its path, so gasses is produced and rapidly expanded to from gas bubble

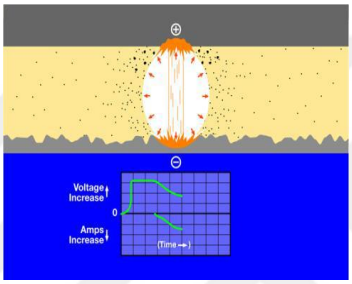

Fig. 3.2e Both voltage and current begin to stabilize, and the gas bubble continues to expand. Creating molten metal begins. Dielectric fluid contamination rises.

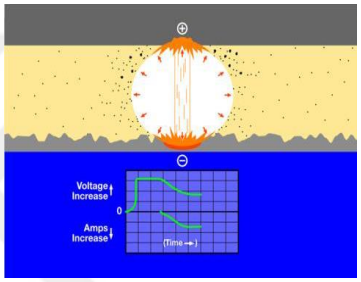

Fig. 3.2f Voltage and current have levelled off the dielectric has become severely contaminated, the power must be interrupted to avoid "dc arcing" or wire-break.

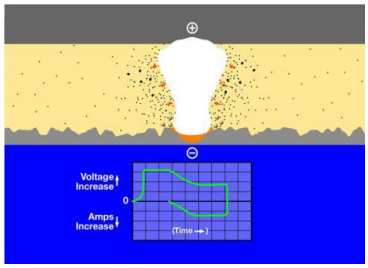

Fig. 3.2g When voltage and current switched off (off-time period of EDM begins). The gas bubble collapses and implodes upon removal of the heat source.

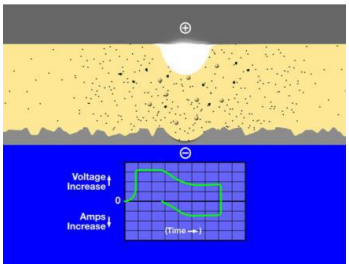

Fig. 3.2h Gases and contaminated dielectric will scatter, and flush perfectly, which reduce dielectric restoration time and increase.

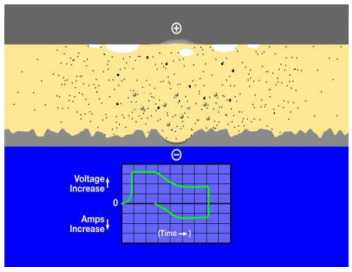

Fig. 3.2i The contaminants and damaged dielectric are ejected, revealing EDM erosion on the workpiece electrode. Dielectric begins reionization, readying for next cycle.

Figure 3. 2 The phases of a single electrical discharge [82].

3.4 EDM PROCESS PARAMETERS

Many parameters affect EDM performance measures correlated with each other by complex relations. They have variant influence and depends on EDM type too. In Sinking EDM, the EDM process parameters are classified into electric process parameters and nonelectric parameters. Electric process parameters include peak current, pulse on time, pulse off time, duty factor, gap voltage, intensity, and pulse frequency. Nonelectric process parameters such as electrode material, electrode shape, rotation of the electrode, workpiece material, dielectric fluid type, and flushing system [10]. These process parameters are explained below:

- Electric process parameters: The most Electric parameters which are affecting the EDM performance are:

a) Peak current (Ip): Also known as Pulse current or Discharge current. The maximum current value that the EDM pulse generator can produce for a very short time. It is the most significant parameter because of its relation to the spark energy applied to the workpiece, hence it has a crucial effect on the performance characteristics of EDM.

b) Pulse on-time (T_{on}): Also called pulse duration, it expresses the time length of the spark in microseconds. Actual machining occurs only during pulse on time. Pulse on time is an important process parameter that has a significant impact on most EDM performance measures. Longer Pulse on time, the energy will be higher and therefore the machining rate is faster.

c) Pulse off-time (T_{off}): It is commonly referred to Pulse interval or Pause time (time between two sparks). At this time neither discharge voltage is applied between electrodes nor discharge current flows between them. Pulse off-time must be long enough to allow the deionization of the dielectric fluid (recovery of the dielectric) and flushing debris away from the gap spark. If the pulse off-time is too short (insufficient), erratic cycling and retraction of the advancing servo will occur, slowing down the process more than a less efficient but stable pulse off-time would. However, the longer Pulse off-time, the longer the job will take.

d) Duty cycle: It refers to the efficiency of EDM frequency. It is the ratio of pulse on-time and the sum of pulse on-time and pulse off-time.

$$\text{Duty cycle} = \frac{\text{Ton}}{\text{Ton+Toff}} \text{x}100 \quad (3.1)$$

e) Discharge voltage (V): also called Open gap voltage, it is the highest potential voltage before the ignition and no current flow between electrodes. It depends on the inter-electrode gap and the strength of the dielectric medium. It is one of the factors that affect the discharge energy, which has a crucial influence on most EDM responses.

f) Pulse frequency: The number of pulse on-time and Pulse off-time created at inter-electrode gap during one second. High frequencies provide higher sparks.

g) Polarity: it refers to which positive or negative charge the tool or the workpiece is received. In EDM, polarity refers to the polarity of the electrode. Polarity has a crucial role in electrode performance especially Electrode Wear Rate (EWR). The negative electrode produces a higher rate of metal removal, whereas the positive electrode produces less EWR and longer machining time. The selecting electrode polarity is based on both type of electrode material and workpiece material. In machining of some materials, it is possible to use only one type of polarity [4].

- Non-Electric process parameters: many Non Electric process parameters drive the EDM process and have an important role in the EDM performance measures. These parameters include:

a) Electrode material: The significant properties of an electrode that has high electric conductivity and high melting temperature. The selection of particular tool electrode material is based on five significant factors: Material Removal Rate (MRR), Tool Wear, Surface Roughness (SR), fabrication electrode cost and row material cost [82].

b) Electrode shape: During EDM the electrode is subjected to wear, the most of wearing at electrode corners, therefore the machining process requires many electrodes of the same or different shape and sizes. In addition to the variety of performance of different electrode shapes and sizes.

c) Workpiece material: In EDM, there is a gap between the tool and the workpiece and no contact between them and the mechanical properties such as hardness,

strength and toughness are not function in this process. But the melting temperature and latent heat have the most significant role on MRR.

d) EDM dielectric fluid: It is a material that does not conduct electricity, but as the voltage increases and the distance between the electrodes approaches, the ionization of the dielectric occurs and a current pass through the inter-electrode gap and a plasma arc are formed. The performance of the EDM process depends largely on the type of dielectric fluid used [30].

e) Flushing: The main function of flushing is to eject out contaminated dielectric fluid and debris from the inter-electrode gap and provide fresh and filtered dielectric. Consequently, the MRR is increased and surface quality improved [83].

f) Inter-electrode gap: also known as spark gap, it refers to the distance between the tool and the workpiece during machining. This gap is controlled or maintained via a servo system.

g) Rotation of electrode: due to the electrode rotational movement, a centrifugal force is generated ejects out more debris faster from the inter-electrode gap, and the MRR is higher than normal EDM.

3.5 EDM RESPONSE MEASURES

The performance of the EDM process is assessed by achieving high MRR, low EWR, low OC, and satisfactory surface finish. In addition to that, some other outputs have had less importance such as WLT, HAZ, SCD, and residual stress.

- Material removal rate (MRR): It expresses the size of metal is removed per unit time. High MRR produces high SR, poor surface integrity and low fatigue properties.
- Tool Wear Rate (TWR): also known as electrode wear rate EWR. It measures the erosion in the electrode (tool) per machining time.
- Wear rate (WR): It compares the tool wear to the amount of material is removed from the workpiece [82].

  $$WR = TWR/MRR$$

- Overcut (OC): It refers to the gap (distance) between the electrode (tool) and the workpiece which is produced as a result of discharge occurrence at the sides and the frontal area of the electrode.

- Surface Roughness (SR): In the EDM the individual machining spark creates individual craters on the workpiece surface. The size and the distribution of these craters affect surface roughness [4].
- White Layer Thickness (WLT): also called recast layer. It is a very thin layer formed during pulse off-time when a portion of melted material is solidified and formed on the workpiece surface. The white layer can affect the surface integrity and /or structure of the EDM surface. It has a different microstructure and chemical composition compared to the parent material. [82].
- Heat Affected Zone (HAZ): It is the layer immediately beneath the white layer that has been affected by thermal energy from EDM. This layer is poor fatigue strength, poor surface integrity and high surface roughness [82].
- Surface Crack Density (SCD): It measures the total length of micro-cracks on EDM surface machined per unit area. During the EDM process, the workpiece surface is subjected to high temperature and quenching, which causes a differential of high contraction-induced stress. The surface cracks are formed when the induced stress exceeds the workpiece's ultimate tensile strength.
- Residual Stress (RS): In EDM, the subsurface undergoes non-homogeneity heating which induces thermal stresses. When the stress exceeded the work material yield stress, it will persist as residual stress.

3.6 DIELECTRIC FLUID

Dielectric fluid is the medium in which the electric spark takes place. It is an insulator material, insulating between the electrodes until the voltage is high enough and a certain inter-electrode gap, then it becomes ionized and the current flows across electrodes and create a path for the discharge. In addition, the dielectric flushes debris out from the inter-electrode gap and cools the electrode and the workpiece surface. Dielectric fluids used in EDM may be liquid or gas for instance distilled or ionized water, hydrocarbon oils and kerosene [79]. The main requirements of the dielectric fluids are high flashing point, low pour point, high oxidation stability, adequate

viscosity, low level of acid number, minimum odor, good electric discharge efficiency and low cost. The dielectric fluid also affects the microstructure and chemical composition of the white layer, for example, the surface hardness is affected by the amount of carbon content transferred from the solution and deposited on the surface of the metal [56].

The dielectric flow method (flushing mode) is a crucial factor that affects the efficiency of the electric discharge machining performance. In EDM the flushing pressure, flow, and mode (type) must be chosen accurately to guarantee flushing performance, especially for machining complex geometries. However, some problems may be encountered when applying the flushing of interrupted cuts, steep tapers, aircraft "honeycomb" and small holes or tubular parts. Inadequate flushing increases electrode wear ratio, machining time and can result in arcing. Dielectric flushing can be classified into four types: (1) normal flow, the fluid is pumped with pressure through a hole in the cutting tool and flows between the workpiece and the cutting tool. It is one of the most widely used methods, but it produces a tapered opening in the workpiece; (2) reverse flow, which is the reverse of normal flow in which fluid is sucked through the hole of the cutting tool and filtered and clean fluid flow between the tool and the workpiece. This method is characterized by that the tapered are lesser than with normal flow method. It is a suitable method in the case of deep cavity cutting when making moulds; (3) jet flow, also called lateral flow, a jet or spray of dielectric fluid directed to the machining area. Machining time using jet flow is longer compared to normal flow and reverse flow; and (4) immersion flushing, simple immersion of the discharge gap is sufficient for many shallow cuts or holes of thin sections. Providing relative motion between the tool and the workpiece can help with cooling and machining debris removal during immersion cutting. Vibration, also known as cycle interruption, is the periodic reciprocation of the tool relative to the workpiece that causes the dielectric fluid to be pumped [84].

3.7 EDM ELECTRODES

Any electrode material must meet the following criteria: it must be electrically conductive, have a high melting point, high specific heat, high density and have a good

tool-to-workpiece wear ratio [79]. The type of electrode material affects the performance of the electrode in terms of its physical properties, shape and size. Aluminium, zinc-tin, brass, steel, copper, tungsten alloys and graphite are all used for electrodes (tools) to suite various conditions. Furthermore, to the material previously stated, a number of other metals, mixtures and various combinations of metal alloys, bonded metallic and bonded nonmetallic, in addition to the bonded metallic and nonmetallic mixture. Each material has its own unique properties and may perform better than others with certain work material [82]. The selection of an electrode material depends mainly upon the specific machining application and upon the best material that will be machined [6].

The EDM process results in high heat in the electric spark region, which wears both electrodes. Figure 3.3 shows the types of wear that occur on the electrode and their effect on the final shape of the workpiece. In order to remedy this defect, the selection of the electrode material and the appropriate process parameters requires, in addition, when designing the electrode, taking into consideration the wear that may occur to it [4].

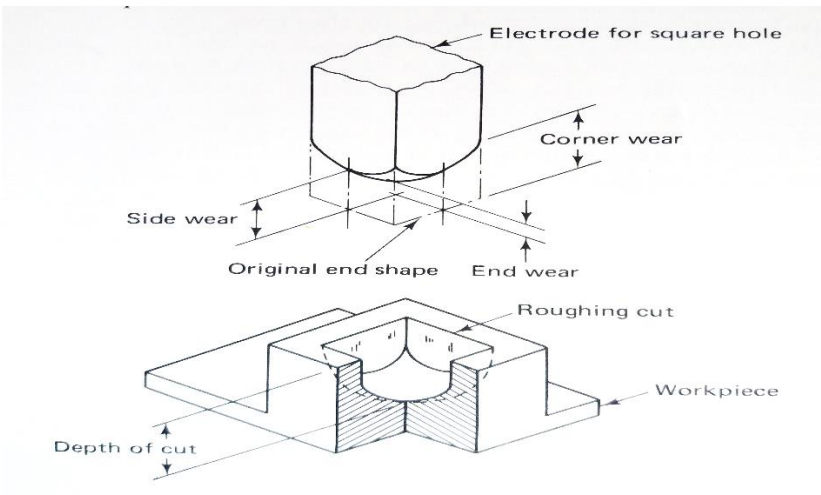

Figure 3. 3 EDM electrode wears [4].

3.8 ELECTRIC DISCHARGE MACHINED SURFACES

Different manufacturing processes affect the surface properties of the workpiece, as they may change its physical, mechanical, thermal and/or chemical properties, which in turn may significantly affect the way the component operates in service. Demands for longer component life and greater strength are often based on changes in surface properties rather than mass properties.

Field and Kahles invented the term surface integrity in 1964 to describe the nature of the surface condition created by the manufacturing process. Surface integrity refers to a component's or specimen's damaged or improved surface quality, which affects its performance in service [79]. There are two components to surface integrity: topography and surface-layer characteristics. If we consider the process to have five major components (machine tool, tool, workpiece, environment, and machining factors (parameters)), we can see that all of these elements can affect surface qualities, resulting in the following:

- The machining process involves high temperatures.
- Work material distortion due to plastic deformation (residual stress).
- Geometry of the surface (cracks, distortion, roughness, waviness).
- Chemical reactions, especially those between the tool and the work material.

It has been nearly 80 years since the discovery and use of electric discharge machining. This technology has proven its effectiveness and its ability to machine electrically conductive materials with high hardness and high strength regardless of their mechanical or physical properties. In addition to the possibility of producing non-circular holes and micro-holes and machining brittle materials, which had a role in increasing their use in manufacturing. However, due to the nature of this process and the resulting high temperature exceeding 8000 degrees Celsius and rapid cooling, as well as the wearing that occurs on the electrode and the change in the roughness of its surface, and the resulting change in the mechanical properties and microscopic composition of the metal surface and below the surface, as well as the wearing that occurs on the electrode and the change in the roughness of its surface, and the resulting

change in the mechanical properties and microscopic composition of the metal surface and below the surface as well, and thus affect the quality and lifetime of the manufactured part.

3.8.1 Surface Topography

Topography is included surface roughness, waviness, flaws and errors of form. A typical roughness profile makes up of the peaks and valleys that are measured independently from waviness. Flaws contribute to surface texture, but they should be considered apart from it. In EDM, a large number of sparks occur in a very short time creating a melted pool that partially ejected in a form of liquid globules and not ejected molten metal is re-solidified and leaves a tiny hemispherical crater which produces and forms the surface textures and affects surface integrity [75,79,82]. Figures 3.4 and 3.5 illustrate the geometric irregularity, globules, pockmarks and craters that form surface roughness and micro-cracks of a surface machined by an electric discharge machine. The volume of melted material is based on the discharge energy. As a result of the discharge energy increases, the surface roughness and the recast layer increase [46].

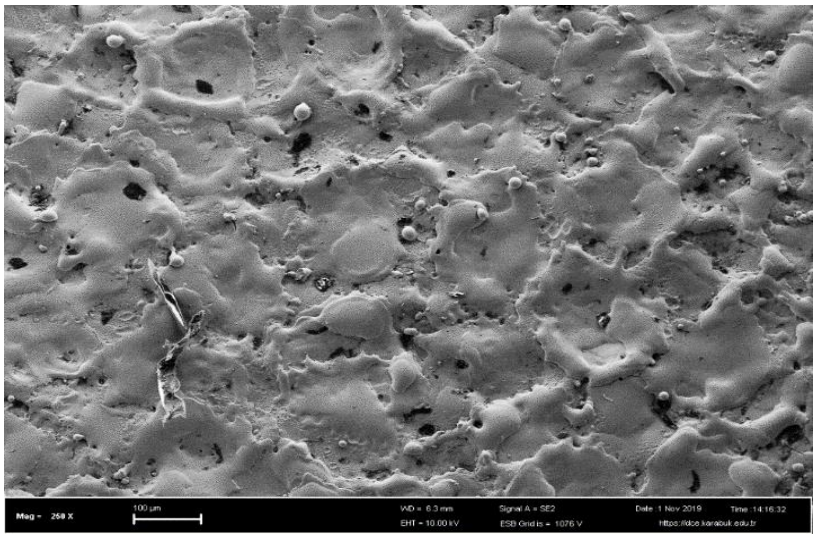

Figure 3. 4 SEM Micrograph, craters in EDMed surface.

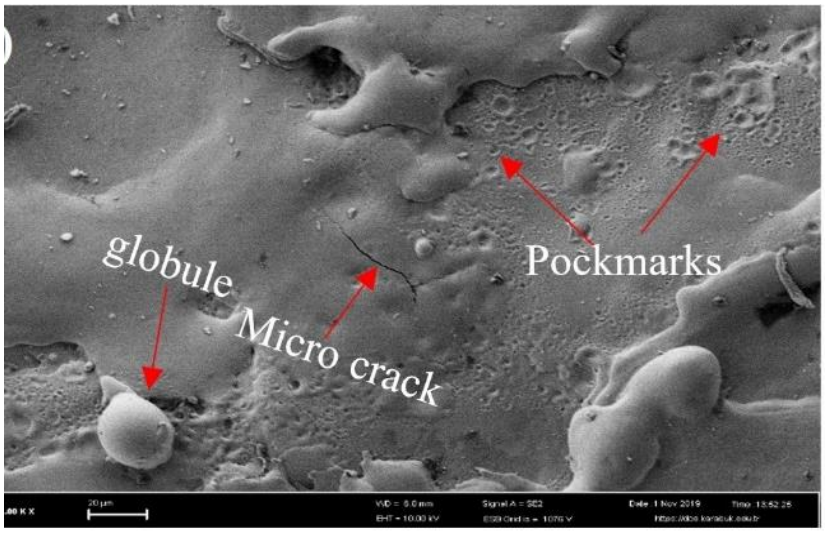

Figure 3. 5 SEM Micrograph, micro crack, globule and pockmarks in EDMed surface.

3.8.2 Surface layers

In electric discharge machining, the workpiece surface is exposed to very high temperature and rapid cooling, causing local melting, evaporating and re-solidifying on the workpiece surface, and this process is repeated continuously during the machining process. Part of the melted metal is expelled and part of it re-solidifies, forming the white layer. Due to the high temperature and rapid cooling, the surface of the workpiece consists of several layers. The first layer from the top is called the white layer or recast layer, followed by heat affected zone, then the transformed layer. The thickness and the properties of each layer depend on the duration, temperature, and rapid cooling to which it was exposed [84].

The white layer is varying in thickness from 4 µm to 130µm and contains micro-cracks, globules and pockmarks as shown in Figure 3.5 and Figure 3.6 and it is viewed under an optical microscope bright and featureless. The micro-cracks start on the white layer and progress in the Heat affected Zone. Also, the white layer has a different microstructure and chemical composition compared to the parent material. The white layer is a highly stressed zone, brittle and very hard that can cause cracking and impart stress risers which can cause premature failure of the workpiece. Furthermore, carbon atoms or any atoms freed from the electrode or the dielectric can be assimilated into the exposed surface of the workpiece material. It is an undesirable layer, and it can be

minimized by controlling the machining variables and/or removed after EDM machining by electrical chemical machining, lapping, grinding or other finishing processes [4,82].

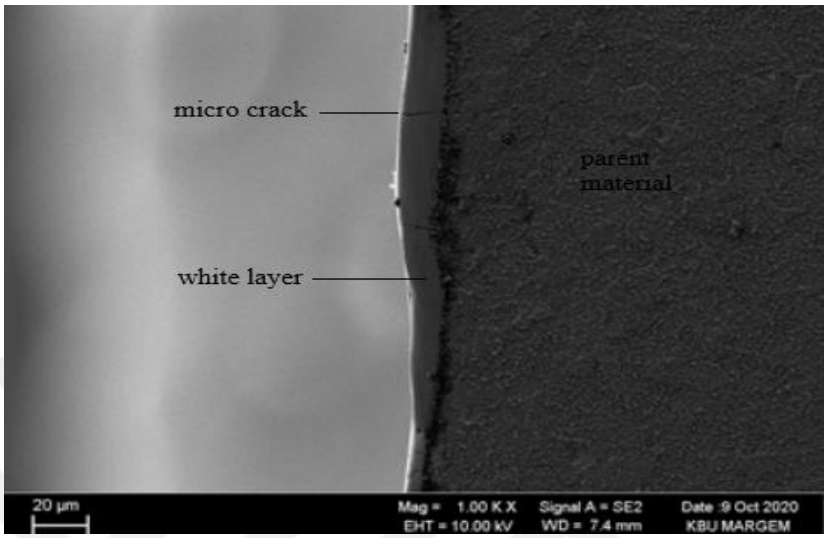

Figure 3. 6 SEM Micrograph, white layer.

The layer directly below the white layer is called the Heat Affected Zone (HAZ) or Hardened Layer, and the thickness of this layer is affected by EDM process parameters and the workpiece material. In heat affected layers, complex phase transformations occur, especially in ferrous alloys where the microstructures are known to be sensitive to heat treatment conditions. The microstructure of this layer differs from that of other layers due to the difference in its exposure to heat and cooling. It also varies from one material to another [55]. Selecting the appropriate cutting condition combination to reduce the thickness of these layers helps to reduce deformations and imperfections in the metal, improving the product's quality and allowing it to be used safely [46].

The third layer is the transformed layer and it is between the heat affected zone and the parent material This layer is exposed to lower temperatures than the white layer and the HAZ, so the microstructure and mechanical properties of this layer differ from them. In addition, the hardness of this layer is lower than that of the other layers, including the parent material [84].

3.9 APPLICATION OF EDM

With the development of industry and the increase in the demand for manufacturing techniques that can cut or shape metals accurately. Electric discharge machining provides many advantages that make it a major tool and has many applications in manufacturing. EDM has the ability to cut hard, brittle materials, delicate material, complex shapes, blind cavities or holes, narrow slots and burr-free. A common and important application of EDM is in machining are die cavities and moulds used for die casting, extrusion, compacting, plastic moulding, wiredrawing, cold-heading and forging. Another important application of EDM is in the metal forming field to produce punch, stamping dies, or trim. In addition, EDM has become a well-established machining process for producing prototypes and short-run parts. Also, as a manufacturing process, EDM is particularly used for micromachining to produce accurate small holes, orifices and slots [4].

3.10 ENVIRONMENTAL IMPACT OF EDM

When operating with electric sparks, electrical energy is converted into heat energy, and the temperature reaches 8000 degrees Celsius in the spark gap, causing melting and evaporation of both electrodes, as well as evaporation of the dielectric fluid. eroding materials resulting from this process mix with the dielectric and produce fumes and pollute the air in the work environment. All EDMs release emissions and waste of harmful substances and affect the environment and health of operators. Among the dangers resulting from the EDM fire hazard, explosive compositions, aerosols, gaseous by products, electromagnetic radiation, heavy metal in slurry, degreasing effects and sharp-edged particles [84].

These hazards vary according to the machining process and the inputs parameters. For the dielectric fluid, the hydrocarbon-based dielectric has the worst effect on the environment and the operator’s health. Using vegetable oil, water, dry, and near-dry can be considered a good alternative and right step to a sustainable environment. Reducing aerosols concentration is possible by controlling dielectric level, discharge current, and pulse on-time. Also employee awareness of the dangers of the EDM and

how to deal with inputs and outputs and all components of the machining process. Furthermore, safety measures must be considered which mitigate and avoid releasing unfriendly environment contaminants during machining.

PART 4

EXPERIMENTAL WORK AND DESIGN

4.1 INTRODUCTION

This part deals with the Taguchi technique that was used in the design of experiments and data analysis. It also shows the machine used in conducting the experiments. The experiments were carried out in three stages: preparing the electrodes and samples, conducting the experiments, and then preparing the samples for tests and measurements.

4.2 DESIGN OF EXPERIMENTS

Many industrial businesses conduct experiments today to improve our awareness and knowledge of various industrial processes. Experiments in industrial companies are frequently carried out in the form of a series of trials or tests with quantifiable results. Understanding the process behaviour, the degree of variability and its effect on processes is critical for continuous improvement in product/process quality. In an engineering environment, experiments are often carried out to understand the data from the process, obtaining the influences of process parameters or factors (input) on the output performance characteristic and validating the predicted results attained from the experiment.

In industrial processes, it is frequently of major interest to explore the relationships between the significant input process parameters (or factors) and the output performance characteristics (or quality characteristics).

Statistical techniques are important and effective tools in planning, conducting, analyzing and interpreting data from engineering experiments. When several variables influence a certain characteristic of a product, the best strategy is then to design an

experiment so that valid, reliable and sound conclusions can be achieved effectively, efficiently and economically.

When designing experiments, parameter values are usually changed to observe their effect on the output functional performance. The effect of these parameters varies, some of them have a high effect, some have a medium effect, and some have a weak or no effect. As a result, the goal of a well-designed experiment is to figure out which set of parameters in a process has the greatest impact on performance and then to obtain the optimal levels for these parameters in order to achieve satisfactory output functional performance in products [85] .

Design of Experiments (DOE) was advanced in the early 1920s by Sir Ronald Fisher. His initial experiments were performed in Rothamsted Agricultural Field Research Station in London, England. He used DOE which could differentiate between the influence of fertilizer and the influence of other factors. Since then, as it was the beginning of the application of design experiments in the biological and agricultural fields. Then it has witnessed a wide and successful spread in many European and American manufacturers. Over time, the design of experiments has evolved and expanded to become extensively used to include numerous applications such as improving process capability and process yield and stability, increasing profits and return on investment, reducing process variability and hence improving product performance consistency, reducing production costs. Helping engineers to solve chronic problems successfully, reducing design and development time, increasing understanding of the relationship between main process input (factors) and output (responses) and other applications in scientific and industrial fields [86].

In carrying out a design of experiments, the input process parameters or machine variables (or factors) are changed intentionally with the purpose of obtaining corresponding changes in the output process. The information obtained is used to improve the performance of the process and the variability of the process. The factors that affect the process are divided into factors that the experimenter can control fairly easily (controllable factors) and factors that are difficult or expensive to control (uncontrollable factors). Uncontrollable factors such as power surges, fluctuations in

ambient temperature, fluctuation in humidity, operator errors, raw material variations, etc. Uncontrolled factors are sources of noise that can be minimized by using the effective design of experiment. The success of design of the experiment is based on good planning, a suitable choice of design, statistical analysis of data and teamwork skills.

The methodology of design of experiments includes planning phase, design phase, conducting the experiments phase and data analyses phase. Figure 4.1 shows the requirements and steps for implementing each phase.

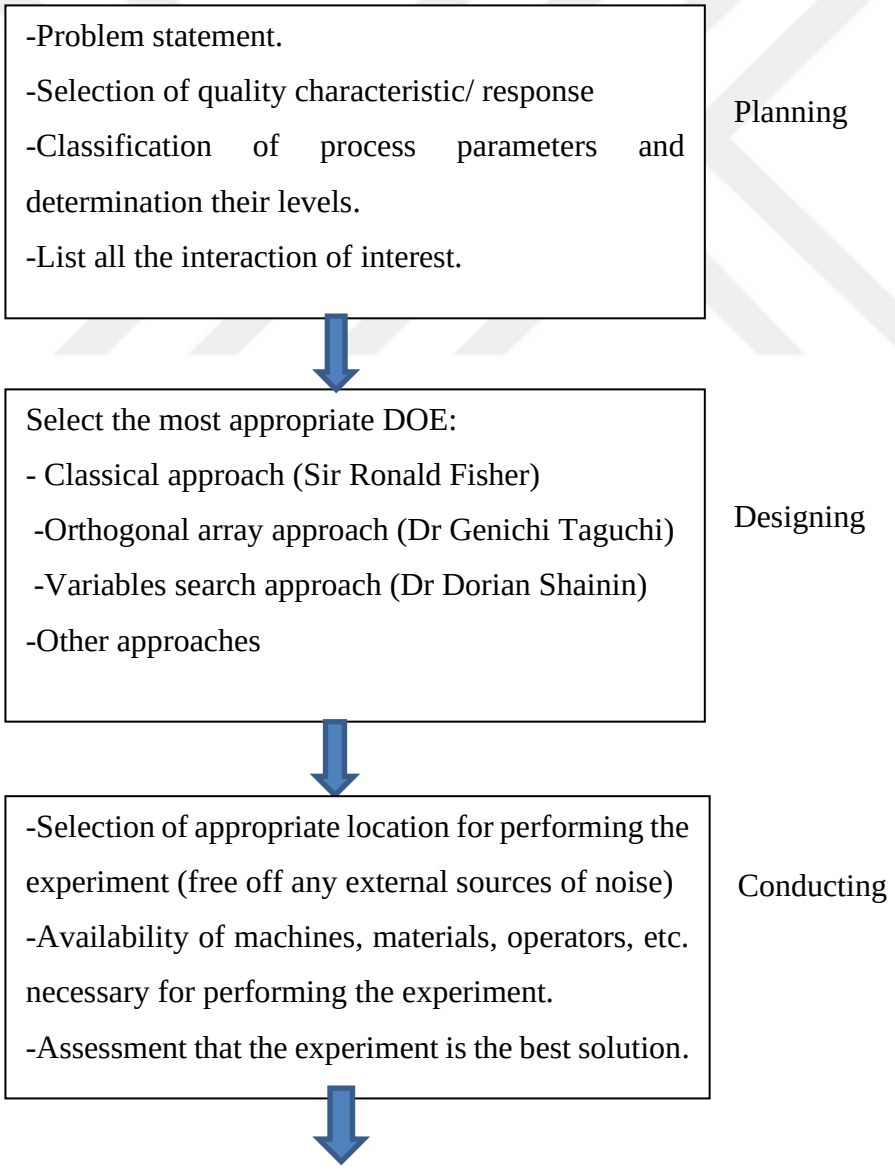

Analyze the data collected from the experiments using: -Analysis of variance (ANOVA). -Confidence interval estimation. -Residual analysis. -Normal probability plot. -Graphical analysis.	Analyzing

Figure 4. 1 Design of experiments phases.

4.5.1 Taguchi Method

Japan in the 1960s witnessed the development of new processes, improved product performance, improved process efficiencies and a solution to complex processes. This is due to the use of Taguchi's method in designing experiments, which provided it with considerable competitive advantage to achieve the best quality of its processes and products. Also, some manufacturing companies in the United States of America has started using the Taguchi method to design experiments into the quality design of processes and products [87]. The design of experiments enables the experimenter to select a process or product that achieves more consistently in the operating environment.

Dr Genichi Taguchi proposed an approach in the early 1980s that involved classifying the parameters (variables or factors) in a product or process as whichever controllable or uncontrollable (noise) and then determining the parametric settings for controllable parameters that minimize the variability and/or sensitivity to noise transmitted to the response from the uncontrollable parameters. During experimentation, the experimenter manipulates uncontrollable factors to force variability to happen and then find the optimal set of control factor that makes the product or process robust, or resistant to variation from the uncontrollable factors. Also, Dr Genich Taguchi advocated the use of Orthogonal Arrays (OAs) for DOE. OA offers the desired information with the minimum possible number of experiments (when fractionated

designed are used) and yet yield reproducible results with satisfactory precision. It is usually used to study main influences and applied in screening experiments. In the OA each factor can be assessed independently of all the other factors, consequently, the influence of one factor does not affect the estimation of another factor. In the 1950s Dr Genich Taguchi developed Robust design. It is said to a process or product is robust if its performance is not affected by uncontrollable factors. Robust design is a method of designing processes and products so that their performance is insensitive to noise. It is an attempt to identify process factor or product parameters levels in order to optimize product functional qualities while minimizing noise sensitivity.

Taguchi has introduced a combined measure of identifying factors that affect mean response and factors that affect the variability of the response. Suppose m is the mean influence and σ^2 represent variance. In Taguchi Robust design these two measures are combined into a single measure characterized by m^2/σ^2 [88].

4.2.2 Analysis of Variance (ANOVA)

Sir Ronald A. Fisher, a British biologist, was the first to propose statistical foundations for experiment design and analysis of variance (ANOVA). In an experiment, ANOVA is a way of partitioning total variation into accountable sources of variation. It's a statistical technique for interpreting data from experiments and making conclusions regarding the parameters under investigation. ANOVA is widely applied to test the statistical significance of the effects through F-Test [88].
ANOVA is defined by the equation 4.1.

Total sum of squares = sum of squares caused by factors + sum of squares caused by error (4.1)

A summary of the analysis of variance is presented in a table containing sum of squares, mean square, F statistic and P-value.

In this study ANOVA is applied to the results of the experiments to identify the significant levels of the process parameters and their contributions affecting the EDM responses.

4.3 EXPERIMENTAL SETUP

The experiments were conducted on the FURKAN M25A sinker electrical discharge machine. The maximum peak current is 25 Amps and the maximum pulse on-time and pulse off-time are 1600 μs. The sinking EDM machine tool consists of the power supply, control unit, tool holder, worktable, servo control system and dielectric fluid delivery system. Figure 4.2 shows an overview of the sinking EDM machine tool components.

Figure 4. 2 EDM machine.

4.3.1 Power Supply

In EDM the electrical energy is in the form of short duration impulses supplied to the inter-electrode gap. Power Supply is responsible for producing pulsed discharges for EDM

4.3.2 Control Unit

The control unit controls the all process parameters of the machining for instance discharge current, pulse on-time, pulse off-time, polarity, flushing mode.

4.3.3 Servo Control System

The inter-electrode gap in EDM has to be continuously monitored and maintained to avoid the occurrences of arcing or short circuits. A servo control system pulls back the tool electrode from time to time and feeds the tool to control the inter-electrode gap to grantee spark generation and to prevent the occurrences of arcing or short circuits.

4.3.4 The Dielectric Fluid Delivery System

The dielectric fluid supply system consists of a reservoir, pump, valves, filters, pipes, pressure gauges and nozzle. The fluid is constantly filtered and recirculated, and the flow rate can be controlled with valves. This machine is equipped with lateral flushing (Jet flushing) which is suitable for a shallow through, or blind hole. The effective resistance of the dielectric fluid is affected by the presence of debris. As a result, filters and dielectric fluid must be replaced frequently.

4.3.5 Work Table

X-Y table fitted to two micrometers and accommodating the working table. If the workpiece is small, it is better to fix it to avoid movement.

4.4 The Workpiece

The work material was DIN 1.2767 tool steel. This type of steel has crucial applications in industry such as cutting and bending tools, drawing jaws, plastic moulds, gears requiring shock resistance, heavy-duty shafts, and axles. Its chemical composition and physical properties are listed in Tables 4.1 and 4.2. The size of each workpiece is 50 mm × 25 mm × 12 mm, as can be seen in Figure Appendix B. 1. The work materials' surface was machined by milling and grinding machines before conducting the EDM experiments.

Table 4. 1. Chemical composition (wt %) of DIN 1.2767.

C	**Si**	**Mn**	**Cr**	**Mo**	**Ni**	**Fe**
0,45	0,25	0,35	1,35	0,25	4,05	Balance

Table 4. 2. Physical properties of DIN 1.2767.

Quantity	**Value**	**Unit**
Thermal conductivity	25	W/m K
Resistivity	0.55	Ohm.mm²/m
Melting temperature	1450-1510	°C
Density	7.7	gm/cm³

4.5 Tool Electrode

Pure copper, Cu-Cr-Zr hot rolled, CNB copper, NSS and B2 were selected as electrode materials. What distinguishes the metal of these electrodes is its good mechanical properties as well as high thermal and electrical conductivity. Electrode diameter was 16mm, about 100mm long and its polarity was negative. Electrodes and their microscopic images can be seen from Figure Appendix B. 2 to Figure Appendix B. 7. The chemical compositions of electrodes are given in Tables 4.3-4.6. Table 4.7 exhibits the crucial physical properties for EDM processing of the five electrodes. The cross-section (face) of the electrodes were polished on silicon carbide paper with grit sizes 150, 240, 320, 400, 600 and 800 before each experiment. The electrodes are weighed before conducting each experiment and cleaned, dried and weighed after carrying out each experiment.

Table 4. 3 Chemical composition (wt %) of copper Cu-Cr-Zr electrode

Element	**Cu**	**Cr**	**Zr**	**Others**
Weight (%)	Base	1,00	0.10	.0.20

Table 4. 4 Chemical composition (wt %) of copper CNB (CuCoNiBe) electrode.

Element	**Cu**	**Be**	**Co+Ni**	**Others**
Weight (%)	Base	1,00	2,00	0,50

Table 4. 5 Chemical composition of Nss (CuNi2SiCr) electrode.

Element	**Si**	**Mn**	**Cr**	**Ni**	**Fe**	**Pb**	**Cu**
Weight (%)	0,65	0,10	0,35	2,5	0,15	0,02	Balance

Table 4. 6 Chemical composition of B2 (CuBe2).

Element	**Ni**	**Be**	**Co**	**Fe**	**Cu**
Weight (%)	0,30	1,95	0,30	0,20	Balance

Table 4. 7 Physical properties of the electrodes.

	Density (g/cm^3)	Electrical conductivity (MS/m)	Thermal conductivity (W/mK)	Melting temperature range (°C)
Cu		100	386-397	1084
CuCrZr	8.9	≥ 44	167-320	1070
CNB	8.75	≥ 38	200-230	1027
B2	8,3	≥ 16	120-170	870
NSS	8,81	≥ 23	190-240	1020

4.6 CONDUCTING THE EXPERIMENTS

Taguchi design of experiments was applied to perform experiments by varying the process parameters of electrode material, peak current, pulse on-time and pulse off-

time and subsequently to predict sets of parametric combinations of optimal parameters for optimum quality characteristics. The process performance was measured in terms of MRR, TWR, Ra, OC, WLT and SCD. For the investigation of DIN 1.2767 tool steel, the process parameter levels shown in Table 4.8 were used for experiments. Materials and some equipment were used are cleared in Appendix B.

Table 4. 8 Process parameters and their levels.

Process parameters	**Parameter notation**	**Levels**				
		Level 1	**Level 2**	**Level 3**	**Level 4**	**Level 5**
Electrode type	E	Cu	Cu-Cr-Zr	CNB	NSS	B2
Ip	A	6	12	25		
T_{on}	B	50	200	200		
T_{off}	C	50	200	800		

Experiments are carried out according to the following steps:

- Clean and dry the electrode and workpiece and weigh them.
- Adjusting the machine to the levels of the process parameters, according to design for experiments, as shown in Table Appendix A.1.
- Install the electrode and the occupied one and adjust them.
- Run the machine for 60 minutes.
- Clean and dry the electrode and workpiece and weigh them.
- Take measurements and make calculations.

4.7 MEASURMENTS AND CALCULATIONS.

Measurements are taken and calculations are made as follows:

- Material Removal Rate (MRR)

MRR is calculated as in equation (4.2).

$$\text{MRR (mm}^3\text{/min)} = \frac{(Initial\ weight\ of\ workpiece - Final\ weight\ of\ workpiece) * 1000}{Time\ of\ machinig(60minutes) * \rho\ (\frac{gm}{cm^3})} \quad (4.2)$$

Where ρ is the workpiece density = 7.7 gm/cm³

- Tool Wear Ratio (TWR)

TWR is calculated as in equation (4.3).

$$\text{TWR (mm}^3\text{/min)} = \frac{(Initial\ weight\ of\ electrode - Final\ weight\ of\ electrode) * 1000}{Time\ of\ machinig(60minutes) * \rho\ (\frac{gm}{cm^3})} \quad (4.3)$$

Where ρ is the electrode density.

- Surface Roughness.

The surface roughness formed by EDM is in the form of small hemispherical craters with no distinct pattern or lay to effect measurement and can be measured in any direction. Many roughness parameters are used, including the arithmetic mean value of roughness (Ra), Mean Roughness Depth (Rz), and the mean square root value (Rq). In this work, the Ra is utilized to express surface roughness, and it is determined using equation (4.4) [75].

$$\text{Ra} = \int_o^l \frac{|y|}{l} dx \quad (4.4)$$

In this equation, Ra = average (or arithmetic mean) of roughness, l= sampling length (4mm), $y =$ the vertical deviation from nominal surface.

Three distinct measurements for each roughness parameter (Ra, Rz, Rq) were taken at different locations for each sample using Mitutoyo digital surface roughness tester as

mentioned in Table Appendix and C and shown in Figure 4.3. and the average surface roughness was calculated.

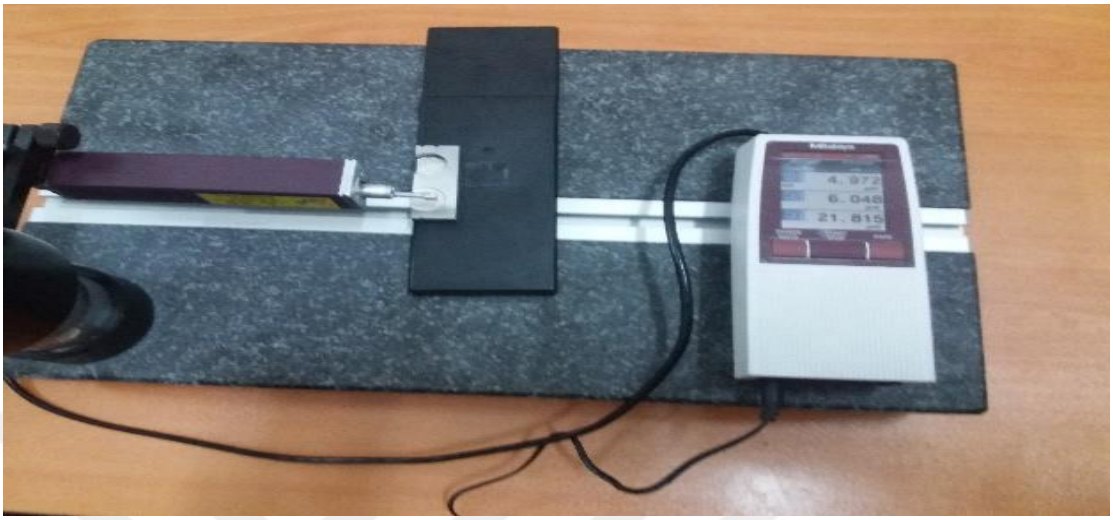

Figure 4. 3 Measuring Surface Roughness.

- Overcut (OC)

The diameter of the hole is measured by an optical microscope connected to a computer as shown in the Figure 4.4 and Figure Appendix D, then the Overcut is calculated as in Equation (4.5)

$$OC = \frac{Dh - De}{2} \tag{4.5}$$

Where *Dh* is the hole diameter and *De* is the electrode diameter before machining.

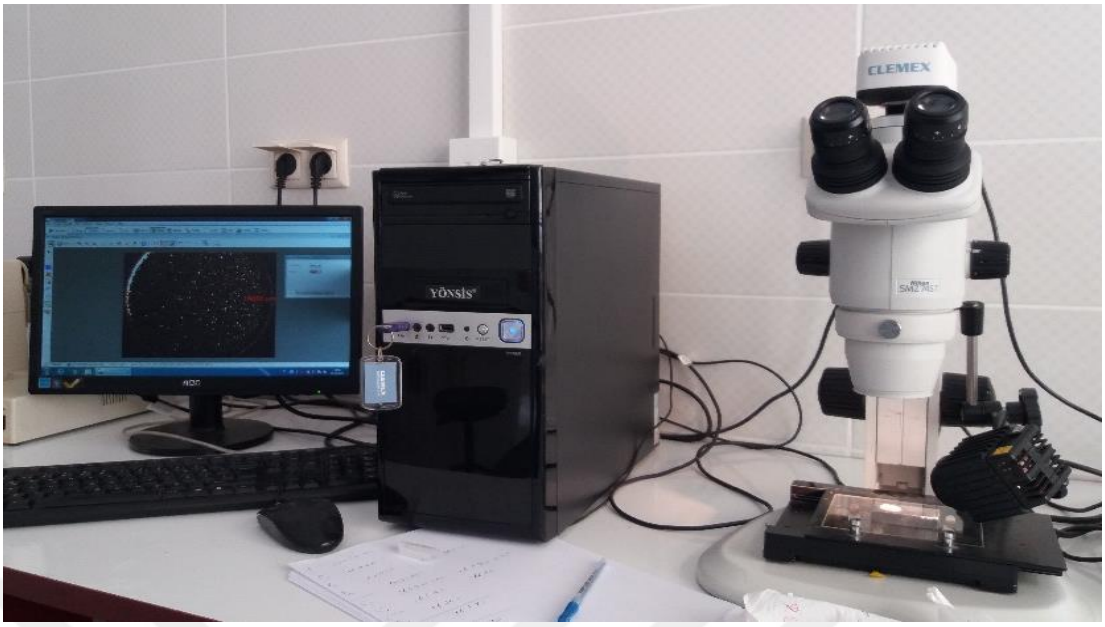

Figure 4. 4 Measuring the Overcut.

- White layer Thickness (WLT)

The samples are cut in small size and polished on silicon carbide paper with grit sizes 60,150, 240, 320, 400, 600, 800, 1000, 1200 and 2000, then polished with Water-based Monocrystalline Diamond Suspension 1micron with the addition of Water-based Diamond Lubricant, next the sample is placed in an etching solution of Nitric acid at a concentration of 5% for 20 seconds after that it is washed with distilled water and alcohol, dried and thus ready to be tested with a Scanning Electron Microscopy (SEM), as can be seen in Figure Appendix E. Using scanning electron microscopy (SEM), images are taken with a magnification factor of 250 to 1500, showing the features of the white layer. Using the ImageJ software program, measurements of the white layer area and the length of the micrograph are measured and the thickness of the white layer is obtained as in Equation (4.6)

$$\text{WLT } (\mu\text{m}) = \frac{White\ layer\ area}{length\ of\ the\ micrograph} \tag{4.6}$$

- Surface Crack Density (SCD)

Using scanning electron microscopy (SEM), images of the sample surface are taken and then using the software the length of all the cracks as well as the image area are

measured, as shown in Figure Appendix B.14 and Appendix F. The surface crack density is calculated as in Equation (4.7).

$$\text{SCD } (\mu m/\ \mu m^2) = \frac{total\ length\ of\ cracks}{area\ of\ the\ micrograph} \tag{4.7}$$

PART 5

RESULTS AND DISCUSSION

This chapter presents the results obtained from the experiments, as well as the effect of the process parameters on the responses and the analysis of variance (ANOVA) with the help of software Minitab 17.

5.1 EXPERIMENTAL RESULTS

Experiments were conducted to study the effect of four parameters (Electrode material, Ip, T_{on} and T_{off}) electrode materials at five levels and the other parameters at three levels. After preparing the workpieces and electrodes, conducting experiments, taking measurements and calculations, the results were obtained as given in Table 5.1. The table shows that the number of experiments is 45 every 9 experiments for a specific electrode. The same parameters are used for each electrode. Also, the performance measures MRR, TWR, Ra, OC, WLT, and SCD are listed in the table. Among the objectives of the study are to obtain process parameters that achieve the highest metal removal rate and low values of electrode wear rate, surface roughness, white layer thickness and surface crack density. Looking at the table, in general, it is noted that when operating with process parameters Ip (25A), T_{on} (200µs) T_{off} (50µs), it achieves the goal with a high metal removal rate as well as a low surface crack density. As for the rest of the responses, the results are not satisfactory. Also, high metal removal rates and low values of electrode wear rate and surface crack density can be obtained, but the surface roughness, overcut and thickness of the white layer will be large. Likewise, for all performance measures, where it is possible to determine the best process parameters that achieve the ideal values for one, two or three performance measures, but this will have negative results on the other performance measures. This is one of the reasons for the difficulty of bartering between the performance measures and finding the parameters of the process that achieve the target of EDM machining.

Table 5. 1 Experimental results.

Sq.	Electrode	Ip	T_{on}	T_{off}	MRR	TWR	Ra	OC	WLT	SCD
1	E1	6	50	50	1.400	0.04	4.026	0.170	6.6	0.0031
2	E1	6	200	200	0.810	0.02	4.071	0.260	13.8	0.0261
3	E1	6	800	800	0.230	0.02	2.069	0.260	21.0	0.0225
4	E1	12	50	200	1.910	0.25	5.380	0.045	4.9	0.0007
5	E1	12	200	800	1.970	0.27	4.989	0.320	7.7	0.0021
6	E1	12	800	50	2.930	0.02	2.210	0.290	19.0	0.0024
7	E1	25	50	800	3.120	1.74	5.921	0.130	7.3	0.0000
8	E1	25	200	50	28.070	0.48	9.404	0.165	22.3	0.0014
9	E1	25	800	200	19.160	0.08	9.455	0.330	19.7	0.0000
10	E2	6	50	50	1.570	0.02	4.099	0.140	5.7	0.0033
11	E2	6	200	200	0.970	0.00	3.822	0.150	12.5	0.0197
12	E2	6	800	800	0.210	0.02	2.290	0.170	14.5	0.0283
13	E2	12	50	200	2.060	0.19	4.681	0.100	5.7	0.0000
14	E2	12	200	800	2.400	0.00	8.128	0.250	13.0	0.0021
15	E2	12	800	50	2.420	0.02	5.375	0.210	15.2	0.0146
16	E2	25	50	800	3.400	1.24	6.092	0.260	9.7	0.0000
17	E2	25	200	50	25.750	0.18	11.454	0.370	16.1	0.0000
18	E2	25	800	200	17.610	0.03	9.687	0.270	29.0	0.0059
19	E3	6	50	50	2.780	0.19	4.198	0.320	6.5	0.0016
20	E3	6	200	200	1.590	0.02	3.165	0.280	9.1	0.0174
21	E3	6	800	800	0.440	0.00	1.997	0.250	16.4	0.0247
22	E3	12	50	200	4.440	0.80	7.497	0.110	7.8	0.0000
23	E3	12	200	800	7.270	0.14	10.006	0.140	14.9	0.0077
24	E3	12	800	50	3.970	0.02	2.847	0.110	12.4	0.0000
25	E3	25	50	800	3.500	0.26	6.424	0.100	16.3	0.0000
26	E3	25	200	50	22.990	2.43	10.334	0.210	7.7	0.0000
27	E3	25	800	200	24.600	0.11	10.600	0.170	24.9	0.0031
28	E4	6	50	50	3.590	0.25	5.791	0.250	7.6	0.0037

29	E4	6	200	200	2.160	0.19	4.025	0.180	9.2	0.0304
30	E4	6	800	800	0.06	0.02	2.723	0.110	7.9	0.0206
31	E4	12	50	200	4.65	1.63	5.244	0.070	6.2	0.0000
32	E4	12	200	800	7.2	0.19	8.694	0.140	11.0	0.0000
33	E4	12	800	50	4.01	0.02	4.132	0.070	18.3	0.0240
34	E4	25	50	800	2.860	1.68	6.095	0.085	30.0	0.0000
35	E4	25	200	50	22.72	2.19	10.224	0.245	15.3	0.0000
36	E4	25	800	200	25.24	0.15	10.608	0.190	18.4	0.0079
37	E5	6	50	50	3.715	0.63	3.846	0.060	7.2	0.0249
38	E5	6	200	200	2.433	0.02	2.801	0.060	9.6	0.0113
39	E5	6	800	800	0.650	0.02	1.618	0.010	15.6	0.0040
40	E5	12	50	200	0.800	0.66	4.745	0.010	7.2	0.0000
41	E5	12	200	800	4.080	0.40	7.557	0.020	12.3	0.0000
42	E5	12	800	50	4.416	0.03	2.422	0.050	24.6	0.0273
43	E5	25	50	800	1.510	0.97	5.785	0.110	19.0	0.0000
44	E5	25	200	50	22.815	2.42	9.199	0.350	11.9	0.0135
45	E5	25	800	200	20.500	0.36	10.888	0.270	11.9	0.0037

5.2 ANALYSIS AND DISCUSSION OF RESULTS

5.2.1 Effect of Process Parameter on MRR

One of the most important indicators for measuring the efficiency of EDM machining is the material removal rate (MRR). The experiments aim to obtain optimal machining conditions that achieve high removal rates. However, there are other important responses that need to be taken into consideration, such as surface quality, tool wear ratio and the overcut. Table 5.2 illustrates MRR by the five electrodes, where E1, E2, E3, E4 and E5 refer to the electrodes Cu-Cr-Zr, Cu, CNB, NSS and B2 respectively.

From Table 5.2 and Fig. 5.1, which show the values of MRR using the five different electrodes, it is noticed that the effect of the type of electrode material as well as the process parameters on the rate of metal removal. The lowest MRR for all electrodes

were when machining with the process parameters Ip (6A), T_{on} (800µ) T_{off} (800µ). The highest values of MRR were for the electrodes E1and E2 when machining with the process parameters Ip (25A), Ton (200µs) T_{off} (50µs) and the electrodes E3, E4 and E5 achieved the highest MRR for the process parameters Ip (25A), T_{on} (800µ) T_{off} (200µ). Also, it is observed that the high MRR were at high Ip, medium and high T_{on}. And short and medium T_{off}. In addition, Fig.5.1 shows that the curve trend for the removal rates is nearly the similar for all electrodes.

Table 5. 2 Comparison of electrodes performance for MRR.

Run	**Ip**	**T_{on}**	**T_{off}**	**(E1) MRR mm^3/min**	**(E2) MRR mm^3/min**	**(E3) MRR mm^3/min**	**(E4) MRR mm^3/min**	**(E5) MRR mm^3/min**
1	6	50	50	1.40	1.57	2.78	3.59	2.01
2	6	200	200	0.81	0.97	1.59	2.16	1.97
3	6	800	800	0.23	0.21	0.44	0.60	0.65
4	12	50	200	1.91	2.06	4.44	4.65	0.80
5	12	200	800	1.97	2.40	7.27	7.2	4.08
6	12	800	50	2.93	2.42	3.97	4.01	4.35
7	25	50	800	3.12	3.40	3.50	2.86	0.65
8	25	200	50	28.07	25.75	22.99	22.72	18.14
9	25	800	200	19.16	17.61	24.60	25.24	20.50

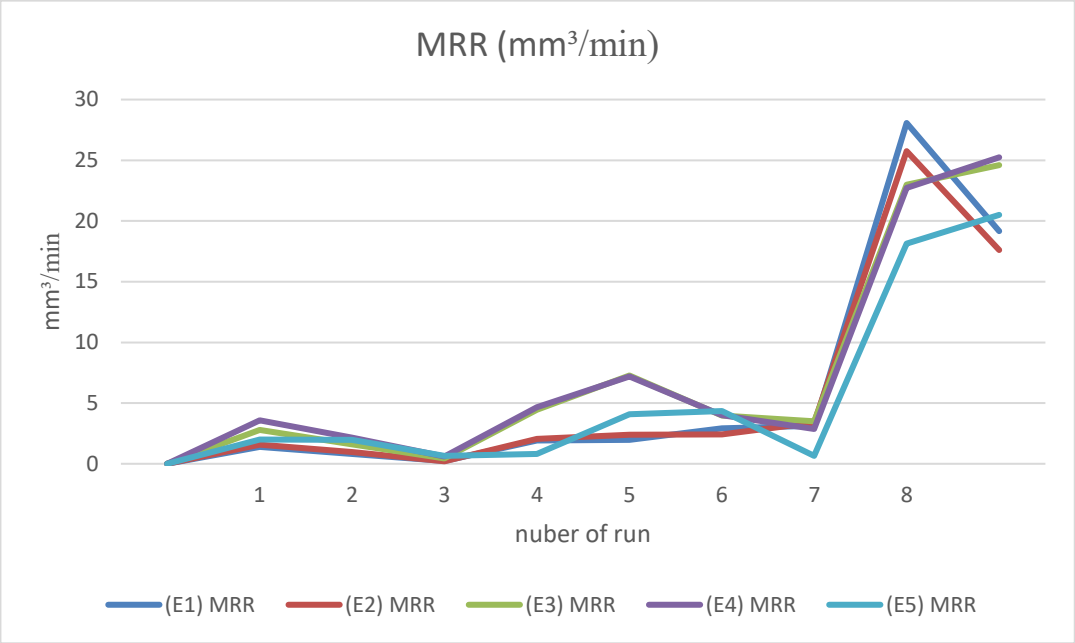

Figure 5. 1 Comparison of electrodes performance for MRR.

The main effect Plot for means explains the effect of each parameter on the response. As shown in Figure 5.2, if the line for a particular parameter has the highest inclination that implies the parameters have the most significant effect on the response. Table 5.3 illustrates the average of the response characteristic (means) for each level of each parameter. The table contains rank based on Delta statistics, which compare the relative magnitude of effects. The Delta statistic is the absolute difference between the highest and the lowest average for each parameter [88]. The highest value of Delta indicates this parameter has the highest effect on the response. The rank was assigned based on Delta values; rank 1 to the highest Delta value, rank 2 to the next highest, and so on. Figure 5.2 and Table 5.3 show that Ip is the most significant parameter, followed by T_{on}, T_{off} and the least electrode material. This sequence is desirable to follow and focus on the most influential variables to improve the removal rate. MRR is directly proportional to Ip and inversely proportional to T_{off}. The discharge energy is proportional to the peak current, as the rise of the current results in the highest temperature, and thus more MRR is achieved [60].

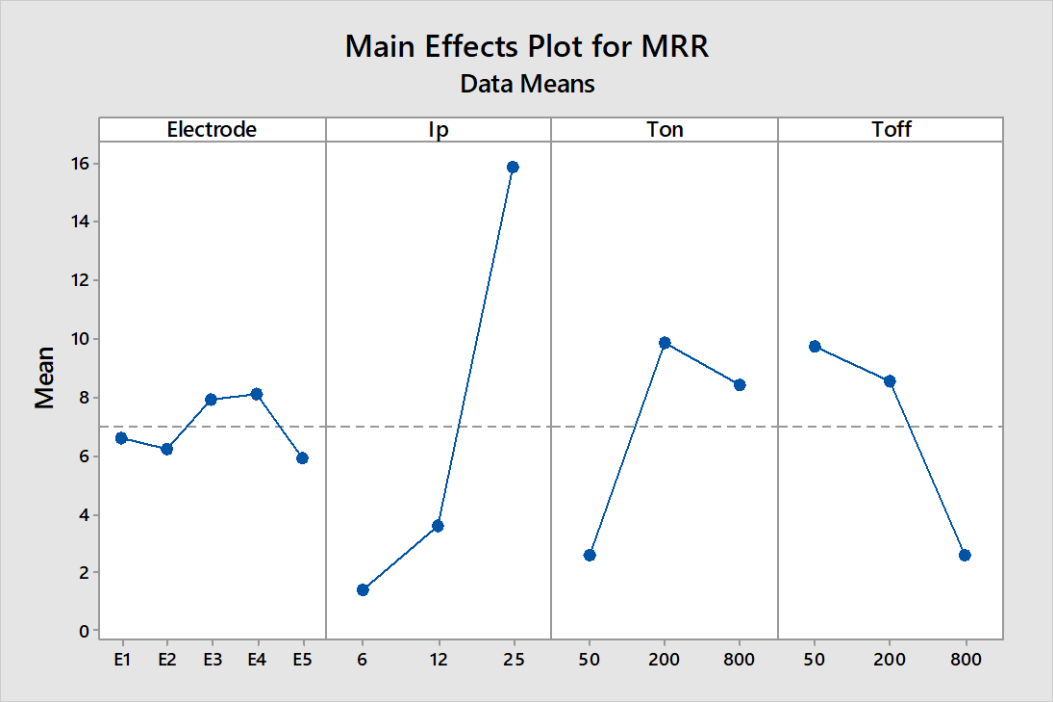

Figure 5. 2 Main effects plot for MRR.

Table 5. 3 Response for MRR.

+ Level	Electrode	Ip	T_{on}	T_{off}
1	6.622	1.399	2.583	**9.780**
2	6.266	3.631	**9.873**	8.565
3	7.953	**15.887**	8.461	2.572
4	**8.114**			
5	5.906			
Delta	2.209	14.489	7.290	7.208
Rank	4	1	2	3

At longer T_{off} time, the MRR is low; this is because the discharge energy is applied for a lesser time. MRR rises with an increase of T_{on} until the second level then decreased. This is due to the excessive T_{on}, which leads to the expansion of the electric plasma channel, hinders the energy transfer and consequently reduces MRR and Ra [28]. Although the electrode material type does not have much impact on the removal rate, the NSS electrode had the highest effect on MRR followed by NCB while Cu-Cr-Zr, Cu and B2 electrodes gave close results. The optimal combination parameters for MRR was E4A3B2C1. In order to study the significance of the process parameters towards MRR, analysis of variance (ANOVA) was employed. Table 5.4 shows the results of ANOVA for MRR. It was found that at a 5% level of significance ($\alpha = 5\%$) and confidence level of 95%, Ip, T_{on} and T_{off} are significant process parameters for MRR, Ip has the highest contribution for MRR, by 55.18% followed by T_{on} 13.55% and T_{off} 13.50%. Whereas electrode material and the interactions (Electrode*Ip, Electrode* T_{on} and Electrode* T_{off}) were non-significant since their P-values > 0.05. The contribution of electrode material 1.09%, Electrode*Ip 0.8%, Electrode*T_{on} 0.4% and Electrode* T_{off} 0.71%.

Table 5. 4 Analysis of Variance for MRR.

Source	DF	Seq SS	Adj SS	Adj MS	F	P	Contribution
Electrode	4	36.24	36.24	9.061	0.19	0.940	1.09%
Ip	2	1825.65	1825.65	912.823	18.84	0.000	55.18%
T_{on}	2	448.47	448.47	224.237	4.63	0.038	13.55%
T_{off}	2	446.72	446.72	223.361	4.61	0.038	13.50%
Electrode *Ip	8	28.21	28.21	3.526	0.07	0.999	0.8%
Electrode * T_{on}	8	14.40	14.40	1.800	0.04	1.000	0.4%
Electrode * T_{off}	8	23.68	23.68	2.961	0.06	1.000	0.71%
Error	10	484.58	484.58	48.458			
Total	44	3307.96					

Interaction effect (combined effect) occurs when the effect of one factor depends on the value of another factor [87]. The interaction effects of parameters for MRR is illustrated in Figure 5.3, with each plot showing the interaction between two process parameters. On the interaction plots, if the lines are parallel, there is no interaction between the parameters. This implies that the effect of one process parameter does not depend upon another process parameter levels. On the other hand, if the lines have different slopes, an interaction exists between the parameters. It is clear that there is slight interaction between the electrode materials and the process parameters for MRR and from Table 5.4 these interactions (Electrode*Ip, Electrode*T_{on} and Electrode* T_{off}) were non-significant and their contribution effects were very low. Also, Figure 5.3 clearly shows the interaction between T_{on} and T_{off} as the intersections of the lines are observed indicating a strong interaction between them. As for the interaction between Ip and T_{on} and Ip and T_{off}, it is considered weak, as it is noticed that the lines parallel at some levels and intersect at other levels.

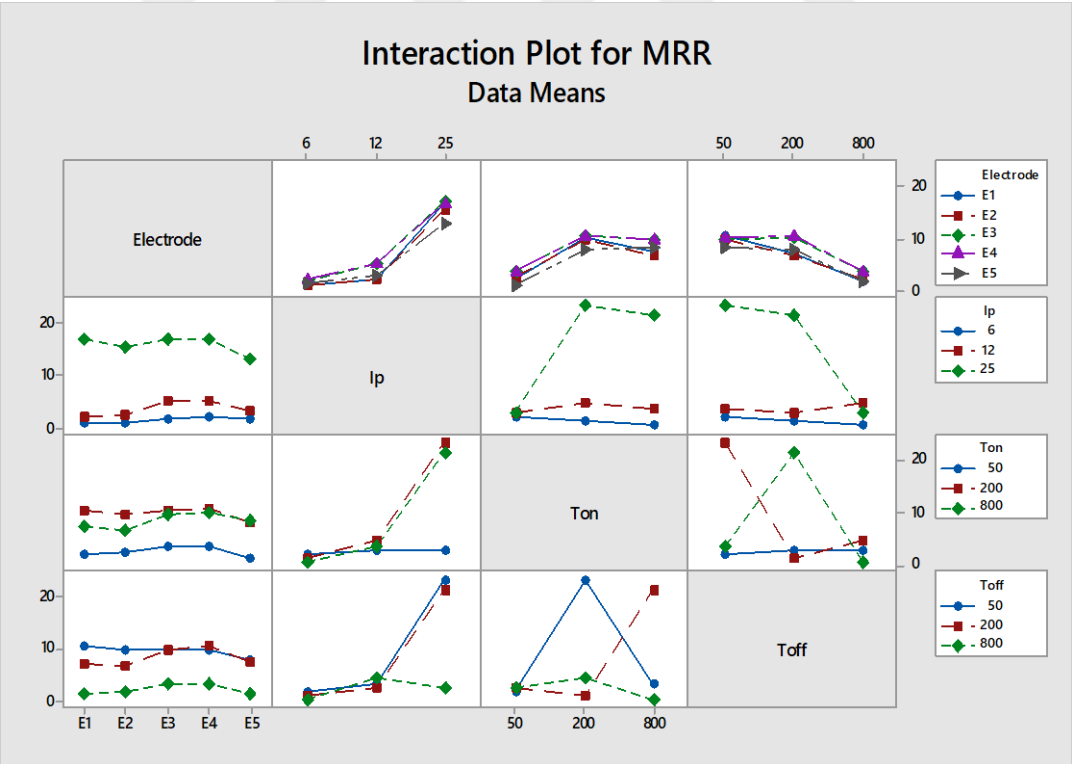

Figure 5. 3 Interaction effect plot for MRR.

5.2.2 Effect of Process Parameter on TWR

In EDM, a large number of sparks strike both tool and workpiece material, each contributing to the removal of material from both, where tiny craters are created. The presence of these small craters on the tool results in the gradual erosion of the electrode. This erosion is a function of technological parameters associated with EDM. The current study includes investigating the effect of process parameters on TWR.

Table 5.5 illustrates the values of the tool wear ratio for the five electrodes. From Table 5.5 and Figure 5.4 it is clear that the minimum value of TWR at runs 2, 3 and 6. As for the high values of E1and E2 for TWR were at runs number 7 and for E3, E4 and E5 maximum TWR was at run number 8. Where a high level of Ip and T_{on} at a medium or low level.

Table 5. 5 Comparison of electrodes performance for TWR.

Run	**Ip**	**T_{on}**	**T_{off}**	**(E1) TWR mm^3/min**	**(E2) TWR mm^3/min**	**(E3) TWR mm^3/min**	**(E4) TWR mm^3/min**	**(E5) TWR mm^3/min**
1	6	50	50	0.04	0.02	0.19	0.25	0.63
2	6	200	200	0.02	00	0.02	0.19	0.02
3	6	800	800	0.02	0.02	0.00	0.02	0.02
4	12	50	200	0.25	0.19	0.80	1.03	0.66
5	12	200	800	0.27	0.00	0.14	0.19	0.40
6	12	800	50	0.02	0.02	0.02	0.02	0.04
7	25	50	800	1.74	1.24	0.26	1.68	1.14
8	25	200	50	0.48	0.18	2.43	2.19	2.42
9	25	800	200	0.08	0.03	0.11	0.15	0.36

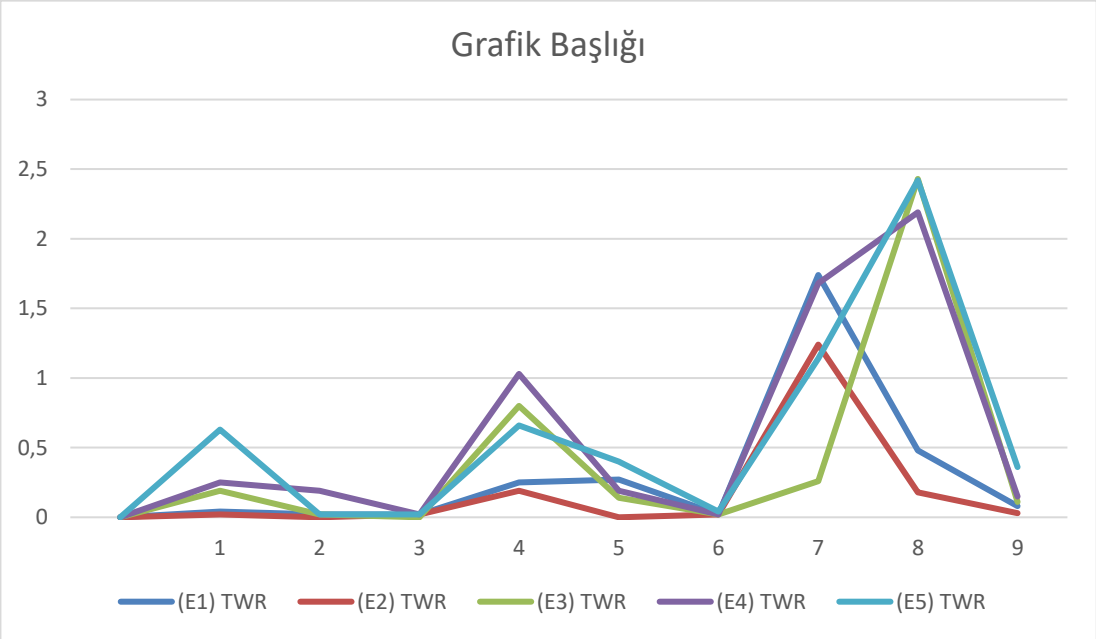

Figure 5. 4 Comparison of electrodes performance for TWR.

The effect of process parameters is shown in Figure 5.5. and Table 5.6, the results showed that the Ip is the most influencing factor on TWR, followed by T_{on}, then electrode material and the influence of T_{off} was negligible. TWR is directly proportional to Ip. TWR is inversely proportional to T_{on}. This is because of the deposition of carbon resulting from the burning of the dielectric on the electrode at a high temperature for a longer T_{on}. The deposited carbon forms a protective layer that reduces TWR [42]. As for the electrode type, the Cu is less wearing than the other electrodes. The optimal combination of process parameters for TWR is $E_2A_1B_3C_2$. To confirm the optimal combination result, an experiment was performed and the TWR was approximately zero. Furthermore, using parametric combination $E_2A_1B_3C_3$ low TWR can be obtained. In previous studies, it was mentioned that electrode wear is affected by the type of electrode material [27,40,43,67] and that the most important and most influential variables are Ip followed by T_{on} [27,61,89], as for T_{off}, its effect is non-significant [90]. To obtain a low TWR, Ip and T_{off} should be set at a medium level and the T_{on} at a high level and focus on the most profound effect parameters.

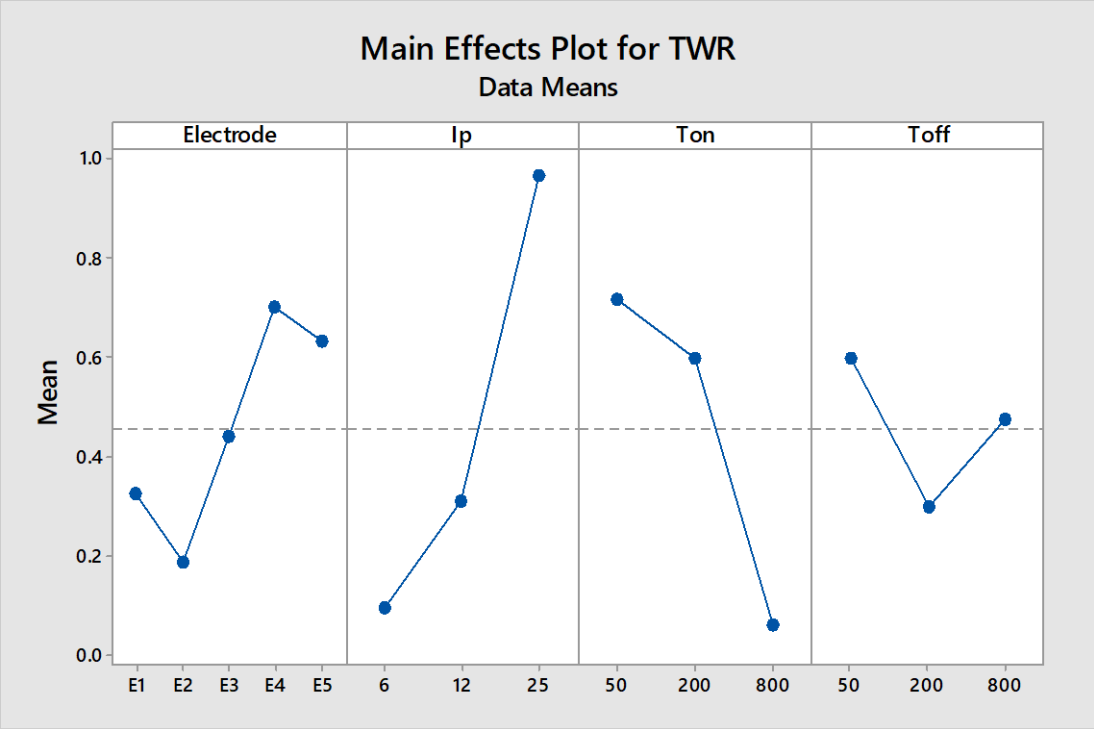

Figure 5. 5 The main plot of process parameters on TWR.

Table 5. 6 Response for TWR.

+ Level	Electrode	Ip	T_{on}	T_{off}
1	0.32444	**0.09733**	0.71467	0.59667
2	**0.18889**	0.31000	0.59667	**0.30067**
3	0.44111	0.96600	**0.06200**	0.47600
4	0.70222			
5	0.632222			
Delta	0.51333	0.86867	0.65267	0.29600
Rank	3	1	2	4

ANOVA analysis was used to determine the significance and the contribution of the process parameters affecting TWR. Table 4.7 shows the results of ANOVA for TWR. It is clear that Ip significantly affected TWR and has the highest contribution for TWR, by 29.32%, whereas T_{on}, T_{off}, electrode material and the interactions (Electrode*Ip, Electrode*T_{on} and Electrode* T_{off}) were non-significant since P-value > 0.05 and the contribution of T_{on} 17.30%, electrode material 7.74%, T_{off} 3.16%, Electrode*Ip 2.71%, Electrode*T_{on} 7.25% and Electrode* T_{off} 8.93%.

Table 5. 7 Analysis of Variance for TWR.

Source	DF	Seq SS	Adj SS	Adj MS	F	P	Contribution
Electrode	4	1.6249	1.6249	0.40622	0.82	0.540	7.74%
Ip	2	6.1507	6.1507	3.07536	6.22	0.018	29.32%
T_{on}	2	3.6288	3.6288	1.81442	3.67	0.064	17.30%
T_{off}	2	0.6646	0.6646	0.33230	0.67	0.532	3.16%
Electrode*Ip	8	0.5691	0.5691	0.07114	0.14	0.994	2.71%
Electrode* T_{on}	8	1.5217	1.5217	0.19022	0.38	0.905	7.25%
Electrode* T_{off}	8	1.8743	1.8743	0.23428	0.47	0.849	8.93%
Residual Error	7	4.9414	4.9414	0.49414			
Total	44	20.9756					

The combined effects (interaction) of input parameters on TWR is shown in Table 5.7and Figure 5.6. There is a slight interaction between the electrode material and Ip and T_{on} and a moderate interaction between electrode material and T_{off} for TWR. This is evidenced by the lack of parallel between the lines and the presence in intersections

plots between the electrode material and T_{off} (Electrode* T_{off}). As for the other interactions between the parameters (Ip* T_{on}, Ip* T_{on}, and T_{on} * T_{off}) where it is noted from the figure that there is no parallelism and the presence of intersections between the lines, and this indicates the presence of an interaction ranging between medium and strong.

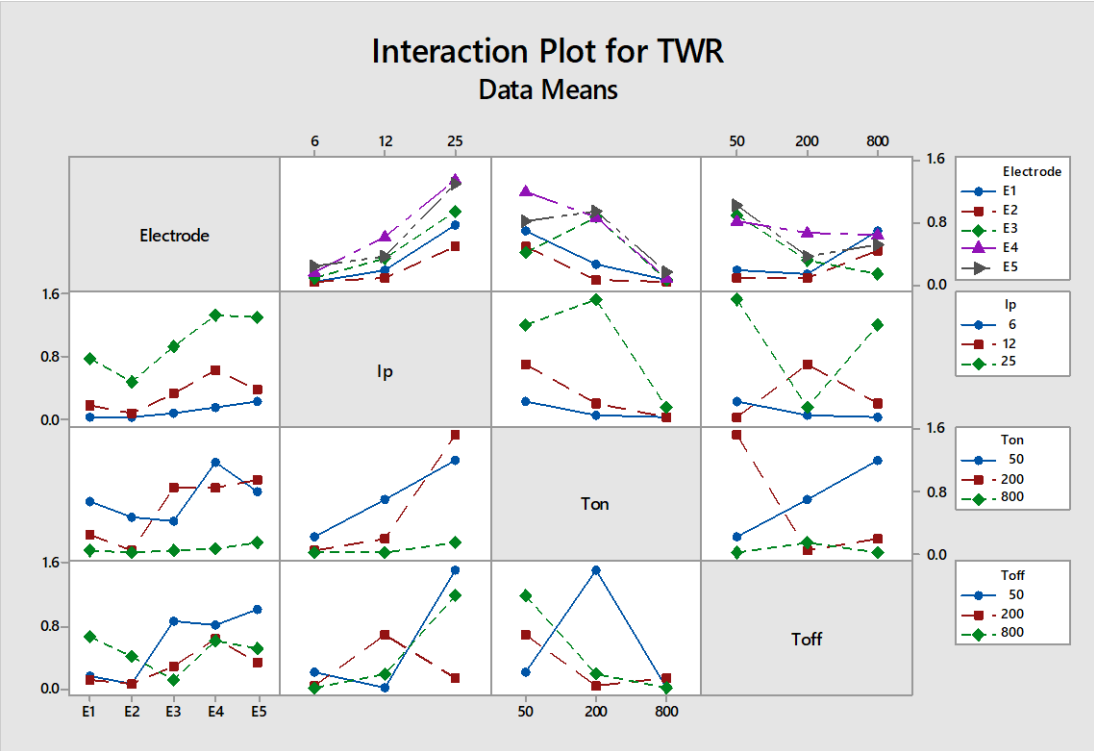

Figure 5. 6 Interaction effect plot of the process parameters on TWR.

5.2.3 Effect of Process Parameter on Ra

EDM machined surface consists of a multitude of overlapping craters. These craters are based on many machining factors such as workpiece material, electrode material, discharge current, pulse on-time, pulse off-time, dielectric fluid and flashing pressure. The individual machining spark creates individual craters on the workpiece surface. The size and the distribution of these craters affect Ra. In the present study for each sample three measurements were taken at different locations on EDM machined surface, and the average surface roughness (Ra) was calculated and mentioned in Table5.8. As can be seen from Table 4.8 and Figure 5.7 the minimum surface

roughness (1.618µm) was obtained at the combination of parameters $E_5A_1B_3C_3$ and the maximum surface roughness (11.454 µm) at $E_3A_3B_2C_1$. Also, it is clear that the minimum Ra was at run number 3 for all electrodes and the maximum was at run 8 and run 9. The Figure also shows that the carves take a similar trend.

Table 5. 8 Comparison of electrodes performance for Ra.

Run	**Ip**	**T_{on}**	**T_{off}**	**(E1) Ra**	**(E2) Ra**	**(E3) Ra**	**(E4) Ra**	**(E5) Ra**
1	6	50	50	4.026	4.099	4.198	5.791	3.846
2	6	200	200	4.071	3.822	3.165	4.025	2.801
3	6	800	800	2.069	2.290	1.997	1.965	1.618
4	12	50	200	5.380	4.681	7.497	5.349	4.745
5	12	200	800	4.989	8.128	10.006	9.906	7.557
6	12	800	50	2.210	5.375	2.847	2.748	2.422
7	25	50	800	5.921	6.092	6.424	6.095	5.785
8	25	200	50	9.404	11.454	10.334	10.549	9.199
9	25	800	200	9.455	9.687	10.600	10.556	10.888

The main effects plot and the response for Ra are explained in Figure 5.8 and Table 5.7. Ip has the highest effect on Ra and plays a significant role to achieve minimal Ra, followed by Ton then electrode material while T_{off} was the lowest. The surface roughness decreases as the Ip increases. As T_{on} and T_{off} increase from level 1 to level 2, Ra increases, then decreases.

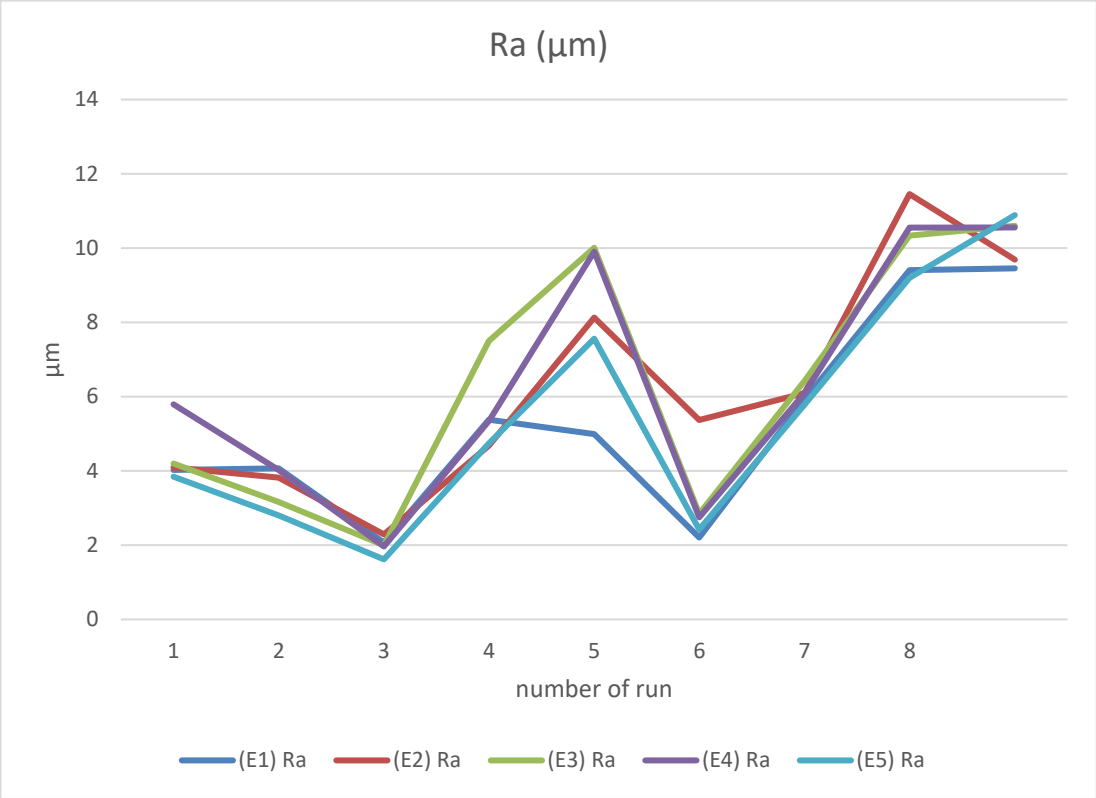

Figure 5. 7 Comparison of electrodes performance for Ra.

The optimal combination parameters for R_a is $E_1A_1B_3C_3$. However, according to previous studies, the effect of process parameters on the surface roughness; for example, Keskin explained that the type of electrode material affects both the surface roughness and the surface crack density (SCD) [35]. Chandramouli & Eswaraiah observed that T_{on} and Ip have a significant effect on both MRR and R_a while T_{off} has a lower effect than Ip and T_{on} [14]. Also, Gupta, Pandey, & Sen explained that with the excessive length of T_{on}, the electric plasma channel expands, which reduces MRR and R_a [91]. Ponappa mentioned that Ip more influential parameter in affecting MRR, EWR and R_a [92]. The minimal surface roughness can be achieved by setting the machine parameters to low pulse energy [67].

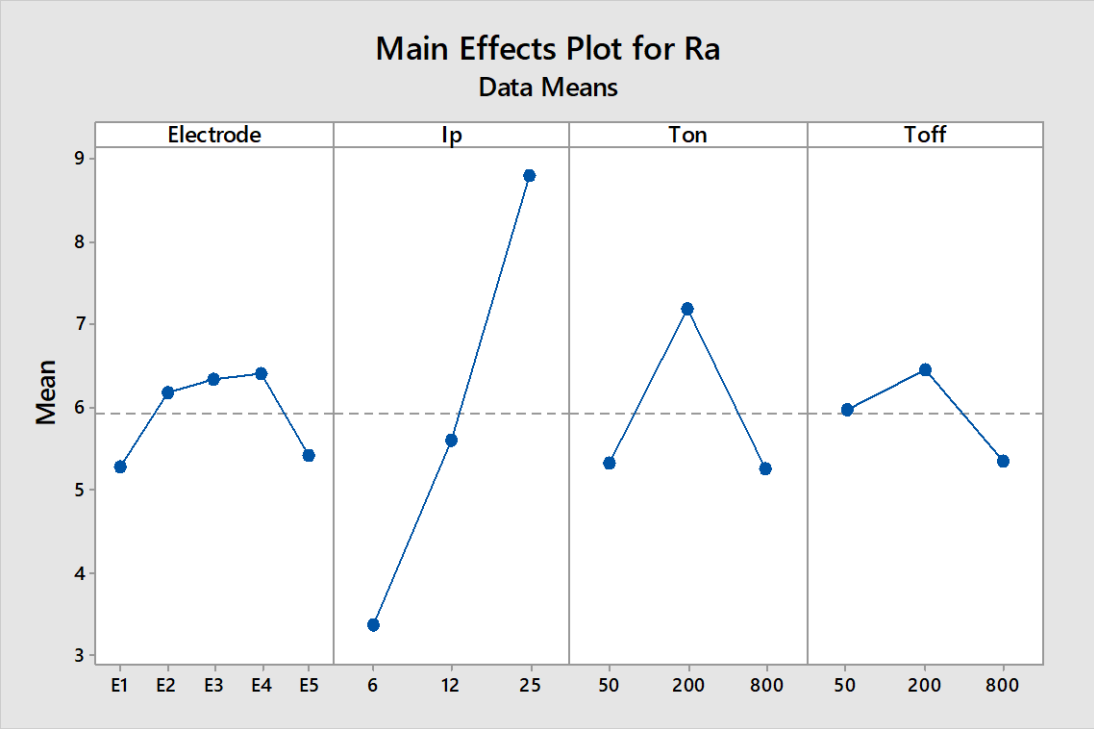

Figure 5. 8 Main effects plot of the process parameters on Ra.

Table 5. 9 Response for means of Ra.

+ Level	Electrode	Ip	T_{on}	T_{off}
1	**5.281**	**3.369**	5.329	5.971
2	6.181	5.601	7.192	6.452
3	6.341	8.811	**5.261**	**5.329**
4	6.405			
5	5.429			
Delta	1.124	5.442	1.930	1.092
Rank	**3**	**1**	**2**	**4**

Table 5.10 shows the results of ANOVA for Ra. It is clear that only Ip significantly affected on Ra because of P-value < 0.05 and the other parameters and interaction were non-significant. Ip has the highest contribution for Ra, by 59.09% followed by T_{on} with contribution 9.47%. The effect of electrode material, T_{off} and the interactions (Electrode*Ip, Electrode*T_{on} and Electrode* T_{off}) were negligible and the contribution of electrode material 2.79%, T_{off} 2.36%, Electrode*Ip 1.99%, Electrode*T_{on} 1.13% and Electrode* T_{off} 1.76%.

Table 5. 10 Analysis of Variance for Ra.

Source	DF	Seq SS	Adj SS	Adj MS	F	P	Contribution
Electrode	4	10.161	10.161	2.542	0.31	0.864	2.79%
Ip	2	224.507	224.507	112.253	13.74	0.001	59.09%
T_{on}	2	36.002	36.002	18.001	2.20	0.161	9.47%
T_{off}	2	8.993	8.993	4.496	0.55	0.593	2.36%
Electrode*Ip	8	7.566	7.566	0.946	0.12	0.997	1.99%
Electrode* T_{on}	8	4.298	4.298	0.537	0.07	1.000	1.13%
Electrode* T_{off}	8	6.688	6.688	0.836	0.10	0.998	1.76%
Residual Error	10	81.690	81.690	8.169			
Total	44	379.912					

Figure 5.9 illustrates interaction plots for various two-parameter interactions between electrode material and Ip, T_{on} and T_{off}. In the interaction plot, if the lines are parallel, the interaction effect does not exist. The strength of the degree of interaction is distinguished by the degree of non-parallelism between the lines. From Figure 5.9 and Table 5.10 it is observed that a slight interaction effect between the electrode material

and other parameters, and these interactions are non-significant and they have a low effect on Ra. Also it can be seen in the figure that there is important interaction effect are produced (Ip* T_{on}, Ip* T_{off}, T_{on} * T_{off}) because in the matrix second row, third and fourth columns, third row, second and fourth columns and fourth row, second and third columns are the places where the lines are intersecting each other.

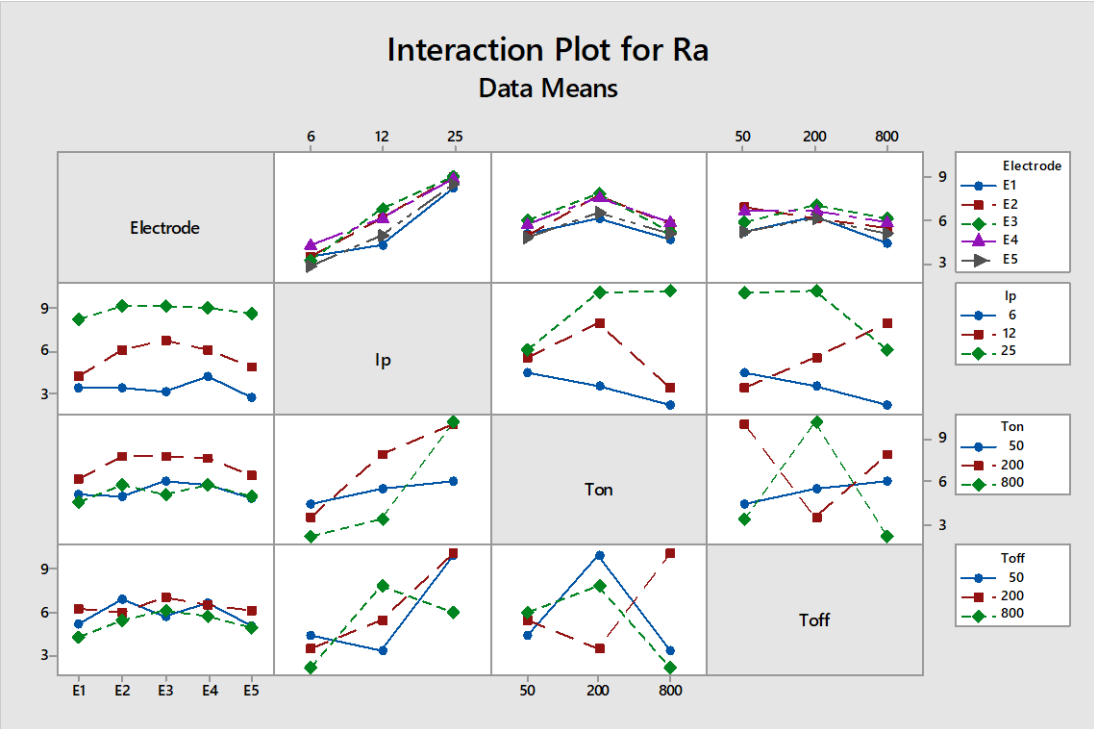

Figure 5. 9 Interaction effect plot of the process parameters on Ra.

5.2.4 Effect of Process Parameter on OC

Overcut is the amount of gap between the workpiece and the tool electrode. The accuracy attained in EDM depends largely upon the initial accuracy of the electrode, electrode wear ratio and control of the overcut. Overcut based on a number of parameters. In the current study, the effect of process parameters on OC has been studied. As can be seen from Table 5.9 and Fig. 5.10 which show the 45 results for the

Overcut using the five electrodes, the minimum Overcut (0.01mm) was obtained at runs 3 and 4 by means of E5 and the maximum overcut (0.37mm) at run number 8

using E2. The figure also shows the great variation in the trend of the curves, except for the similarity in the performance of the electrodes E3 and E4. This variation explains the significance of the electrode material effect on OC. It was also observed that the fourth experiment gave a low value of OC to all electrodes. Figures 5.11-5.15 of microscopic images depicting the hole diameter where the minimum Overcut values were obtained for each electrode.

Table 5. 11 Comparison of electrodes performance for OC.

Run	**Ip**	**T_{on}**	**T_{off}**	**(E1) OC**	**(E2) OC**	**(E3) OC**	**(E4) OC**	**(E5) OC**
1	6	50	50	0.17	0.14	0.32	0.25	0.06
2	6	200	200	0.26	0.15	0.28	0.18	0.06
3	6	800	800	0.26	0.17	0.25	0.11	0.01
4	12	50	200	0.045	0.10	0.11	0.07	0.01
5	12	200	800	0.32	0.25	0.14	0.14	0.02
6	12	800	50	0.29	0.21	0.11	0.07	0.05
7	25	50	800	0.13	0.26	0.10	0.085	0.11
8	25	200	50	0.165	**0.37**	0.21	0.245	0.35
9	25	800	200	0.33	0.27	0.17	0.19	0.27

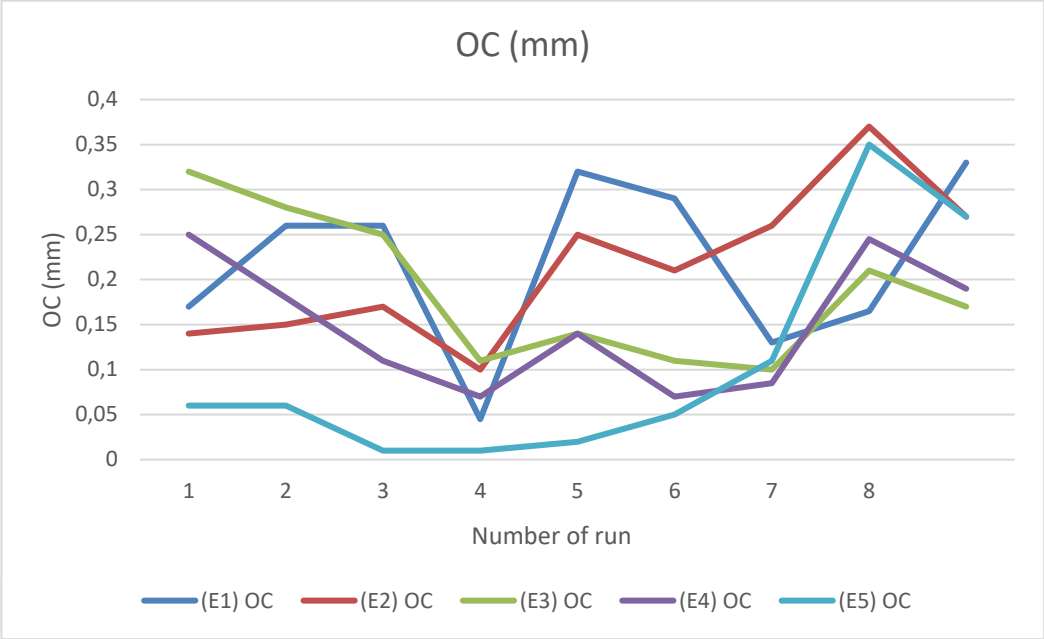

Figure 5. 10 Comparison of electrodes performance for OC.

Figure 5. 12Microscopic image of machined hole, minimum OC at process parameters E1A2B1C2.

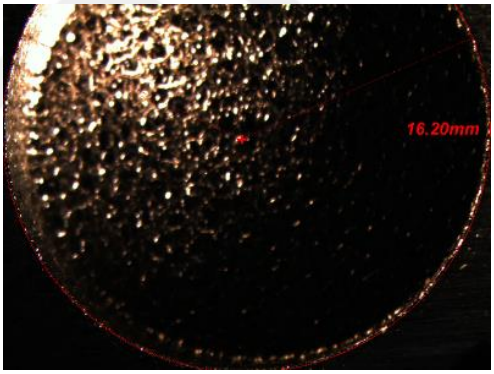

Figure 5. 11 Microscopic image of machined hole, minimum OC at process parameters E2A2B1C2

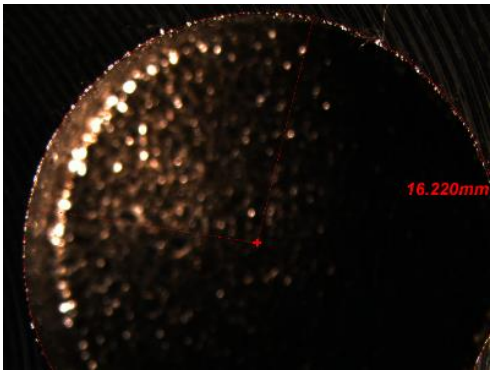

Figure 5. 13 Microscopic image of machined hole, minimum OC at process parameters E3A2B1C2.

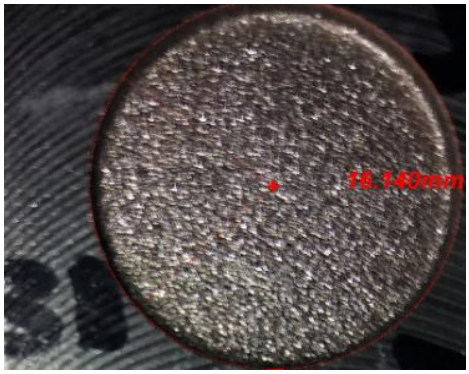

Figure 5. 13 Microscopic image of machined hole, minimum OC at process parameters E4A2B1C2.

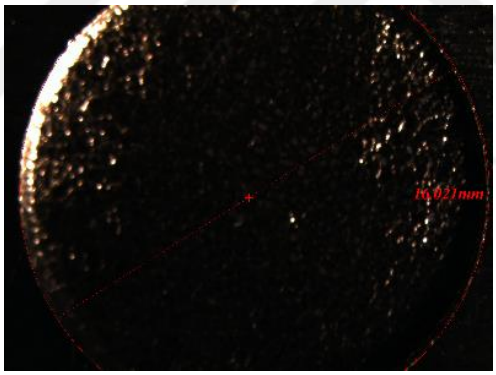

Figure 5. 14 Microscopic image of machined hole, minimum OC at process parameters E5A2B1C2.

Figure 5.16 illustrates the main effect plot for OC. The optimal OC attained at machining parameters E5A2B1C3, can be determined by minimum values of the means. A confirmation test was performed and the OC was (0.08mm). From Figure 5.16 and Table 5.10, it is clear that electrode material type is the most affected process parameter and plays as the main factor for minimizing OC followed by Ip then T_{on} and the least was T_{off}. Minimum OC results from the use of electrode E5, as this is likely due to their electrical properties, as they have lower electrical conductivity, which

results in less sparking energy [42]. Minimum OC occurs for a middle level of Ip. A similar trend was noticed by Muthukumar [89]. The results of the experiments conducted by Dhakry et al and S. Kumar show that OC is affected by the type of electrode material and that in some electrodes with increasing current the OC decreases and then increases [9], [42]. In this case, OC increases initially, when T_{on} increases from (50 µs) to (200 µs), while tends to decrease, when T_{on} increases from (200 µs) to (800 µs). As for T_{off}, OC inversely proportional to $T_{off.}$ It is also clear that the lowest OC can be achieved by using electrode E5, followed by electrode E4, discharge current 12 A then 6A, pulse on-time 50 µs followed by 800 µs and pulse off-time 800 µs then 200 µs.

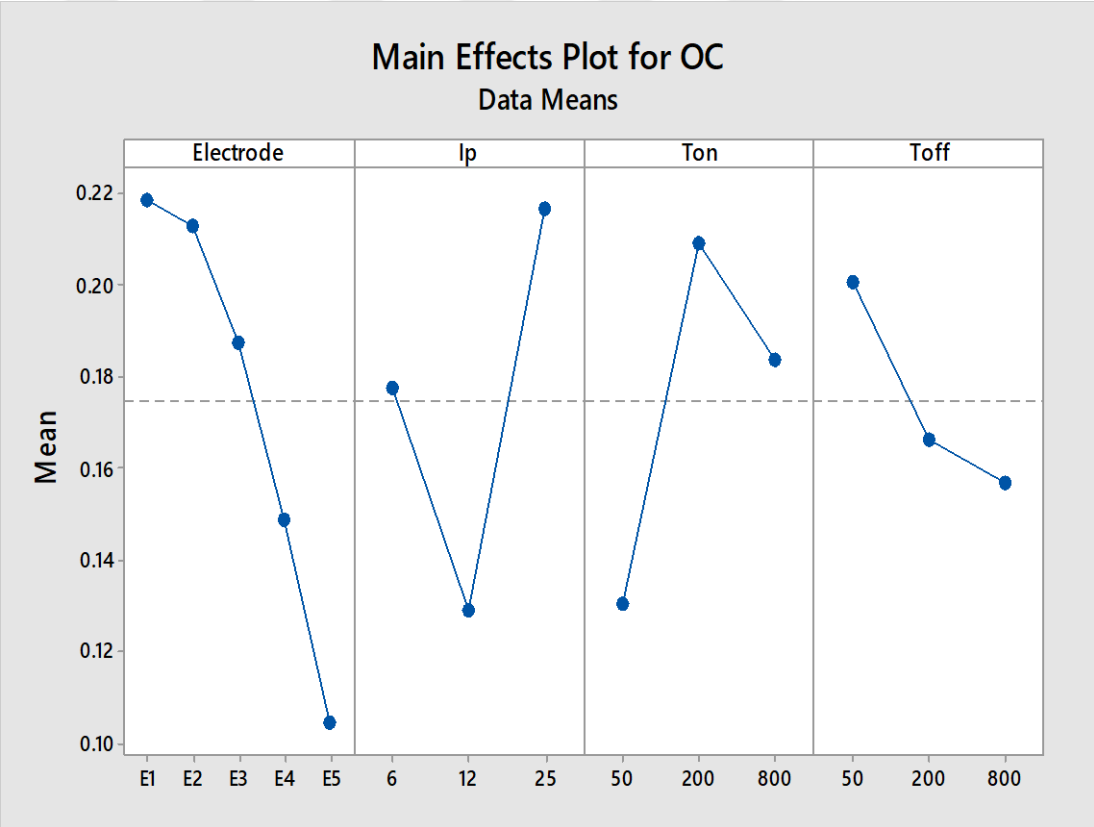

Figure 5. 15 Main effects plot of the process parameters on OC.

Table 5. 12 Response for OC.

Level	Electrode	Ip	T_{on}	T_{off}
1	0.2189	0.1780	**0.1307**	0.2007
2	0.2133	**0.1290**	0.2093	0.1663
3	0.1878	0.2170	0.1840	**0.1570**
4	0.1489			
5	**0.1044**			
Delta	0.1144	0.0880	0.0787	0.0437
Rank	1	2	3	4

In order to study the significance of the process parameters towards OC, analysis of variance (ANOVA) was employed. Table 4.13 shows the results of ANOVA for OC at 5% level of significance ($\alpha = 5\%$). It was found that electrode material, Ip, T_{on} and Electrode*Ip are significant process parameters for OC, electrode material has a contribution for OC, by 19.50%, the interaction (Electrode*Ip) 28.79%, Ip 13.71% and T_{on} 11.41%. whereas T_{off} and the interactions Electrode*T_{on} and Electrode* T_{off} were non-significant since P-value > 0.05 the contribution of T_{off} 3.37%, Electrode*T_{on} 8.32% and Electrode* T_{off} 5.42%.

Table 5. 13 Analysis of Variance of OC.

Source	DF	Seq SS	Adj SS	Adj MS	F	P	Contribution
Electrode	4	0.08296	0.08296	0.020741	5.33	0.015	19.50%
Ip	2	0.05833	0.05833	0.029165	7.50	0.010	13.71%
T_{on}	2	0.04857	0.04857	0.007932	6.22	0.018	11.41%
T_{off}	2	0.01586	0.01586	0.015314	2.04	0.181	3.37%
Electrode*Ip	8	0.12251	0.12251	0.004427	3.94	0.023	28.79%
Electrode* T_{on}	8	0.03542	0.03542	0.002882	1.14	0.416	8.32%
Electrode* T_{off}	8	0.02306	0.02306	0.003891	0.74	0.658	5.42%
Residual Error	10	0.03891	0.03891				
Total	44	0.42542					

The graph of interaction between any two parameters indicates that the effect of one parameter on the response at different levels of another parameter is not the same. It is noticed from Figure 5.17 that there is a strong interaction evidenced by the presence of intersections of the lines between Electrode and Ip and a moderate interaction between Ip and T_{off}. As for the rest of the interactions, they are considered fairly small due to the presence of quasi-parallelism between the lines of some levels. Also, Table 5.13 clearly indicates that Electrode*Ip a significant but Electrode* T_{on} and Electrode* T_{off} are non-significant.

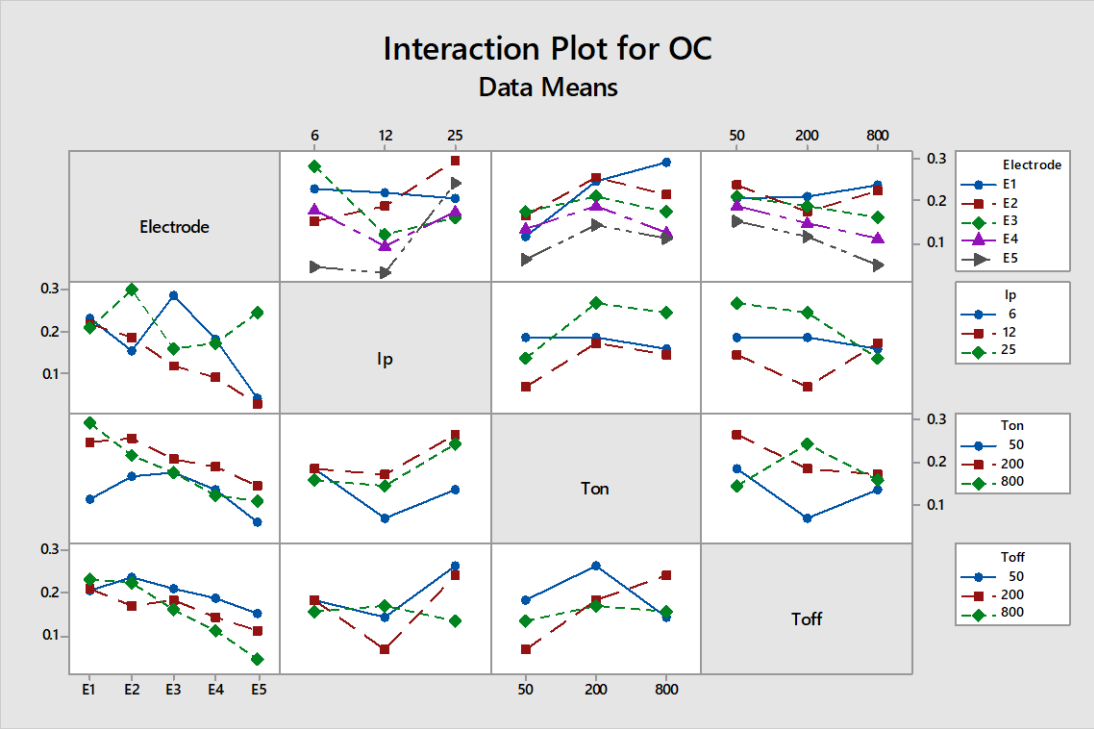

Figure 5. 16 Interaction effect plot of the process parameters on OC.

5.2.5 Effect of Process Parameter on WLT

This study also aims to find out the effect of process parameters on the thickness of the white layer as well as the set of parameters that achieve the lowest WLT. Scanning Electron Microscopy (SEM) was used to show changes to the surface integrity and ImageJ software to measure the thickness of the white layers. As can be seen from Table 5.11 and Fig. 5.18, the minimum WLT (4.9 µm) was obtained with the combination of parameters E1A2B1C2 as shown by the SEM micrograph of Fig. 5.19 and the maximum WLT (30 µm) was obtained at E4A3B1C3 as shown by the SEM micrograph Fig. 5.20. In addition, it is evident from Figure 5.18 that when the first five experiments the trend of the curves is almost the same for all the electrodes, then a big difference occurs in the trend of some of the curves. The difference in WLT illustrates the effect of the type of electrode material on the thickness of the white layer, and this is in accordance with the observations of Sahu and Dewangan [73], [93]. Also, it is noticed that the low values of WLT are when experiments 1 and 4 for all electrodes. The micrograph in Figure 5.21 to 5.24 show the minimum thickness of the white layer

when using electrodes E2, E3, E4 and E5 where the machining parameters were A2B1C2 for electrodes E2, E4 and E5 and the machining parameters using E3 was A1B1C1.

Table 5. 14 Comparison of electrodes performance for WLT.

Run	**Ip**	**T_{on}**	**T_{off}**	**E1**	**E2**	**E3**	**E4**	**E5**
1	6	50	50	6.6	5.7	6.5	7.6	7.2
2	6	200	200	13.8	12.5	9.1	9.2	9.6
3	6	800	800	21	14.5	16.4	7.9	15.6
4	12	50	200	**4.9**	5.7	7.8	6.2	7.2
5	12	200	800	7.7	13	14.9	11.0	12.3
6	12	800	50	19	15.2	12.4	18.3	24.6
7	25	50	800	7.3	9.7	16.3	30	19.0
8	25	200	50	22.3	16.1	7.7	15.3	11.9
9	25	800	200	19.7	29	24.9	18.4	11.9

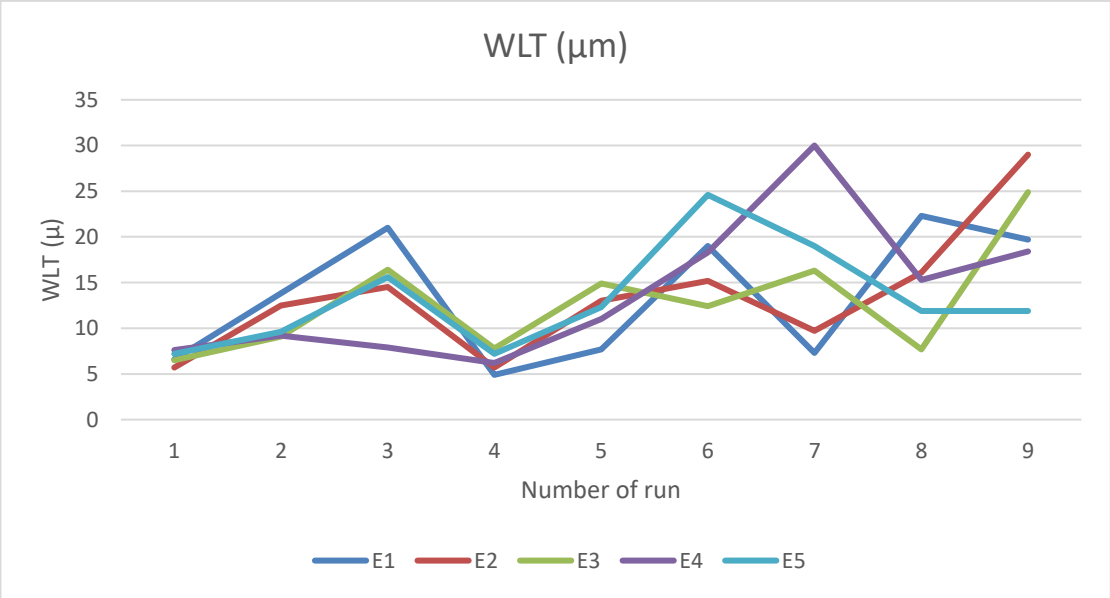

Figure 5. 17 Comparison of electrodes performance for WLT.

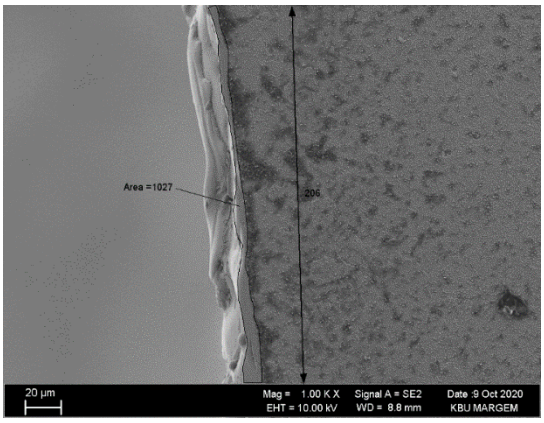

Figure 5. 18 SEM Micrograph, Min. WLT, EDM parameters; E1A2B1C2

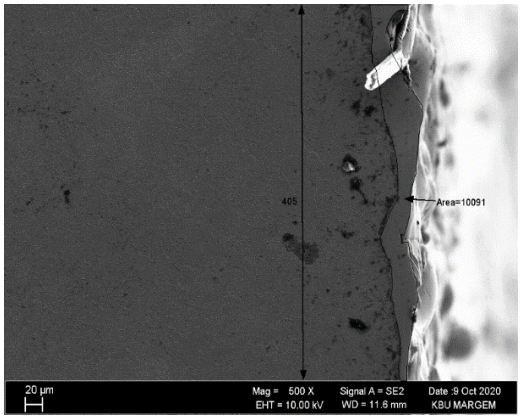

Figure 5. 19 SEM Micrograph, Max. WLT, EDM parameters; E3A3B3C1

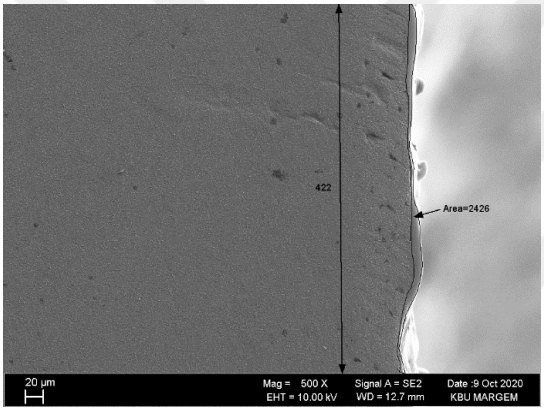

Figure 5. 20 SEM Micrograph, Min. WLT, EDM parameters; E2A2B1C2

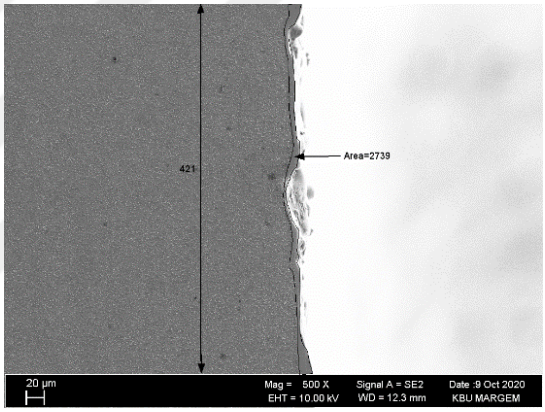

Figure 5. 21 SEM Micrograph, Min. WLT, EDM parameters; E3A1B1C1

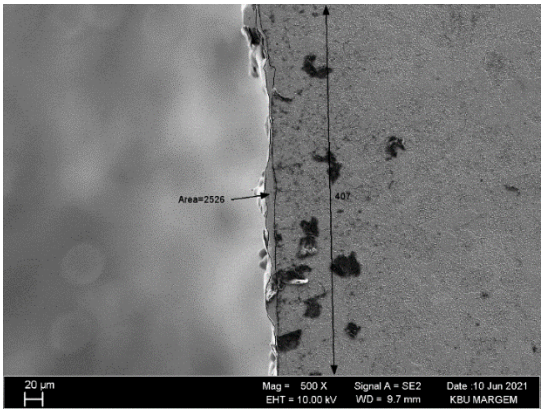

Figure 5. 22 SEM Micrograph, Min. WLT, EDM parameters; E4A2B1C2

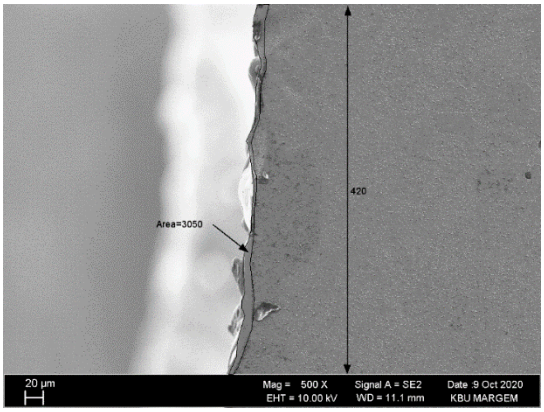

Figure 5. 23 SEM Micrograph, Min. WLT, EDM parameters; E5A2B1C2

In the case of WLT, the minimum WLT is preferable. Figure 5.25 illustrates the main effect plot for means of WLT. The optimal WLT was achieved at process parameters E3A1B1C2. To confirm the result, an experiment was conducted and the thickness of the white layer was found (6.2 µm) as shown in Figure 5.26. In addition, E1, E2 and E5 gave good results (thin WLT), while E4 was the electrode that produced the largest thickness of the white layer. The WLT value is minimum if the value of Ip, T_{on} at lower levels and T_{off} at the second level. Table 5.12 illustrates the response of WLT. Delta value of the electrode was low which implies the effect of electrode material on WLT is low. From Figure 5.25 and Table 5.12, it is clear that T_{on} is the most effecting process parameter and plays as the main factor for minimizing WLT followed by Ip then T_{off} and the least electrode material. Additionally, it is observed that WLT is directly proportional to Ip and T_{on}. Zhang, Kumar and Dewangan noticed that the WLT directly proportional to Ip and T_{on} [73], [93], [94].

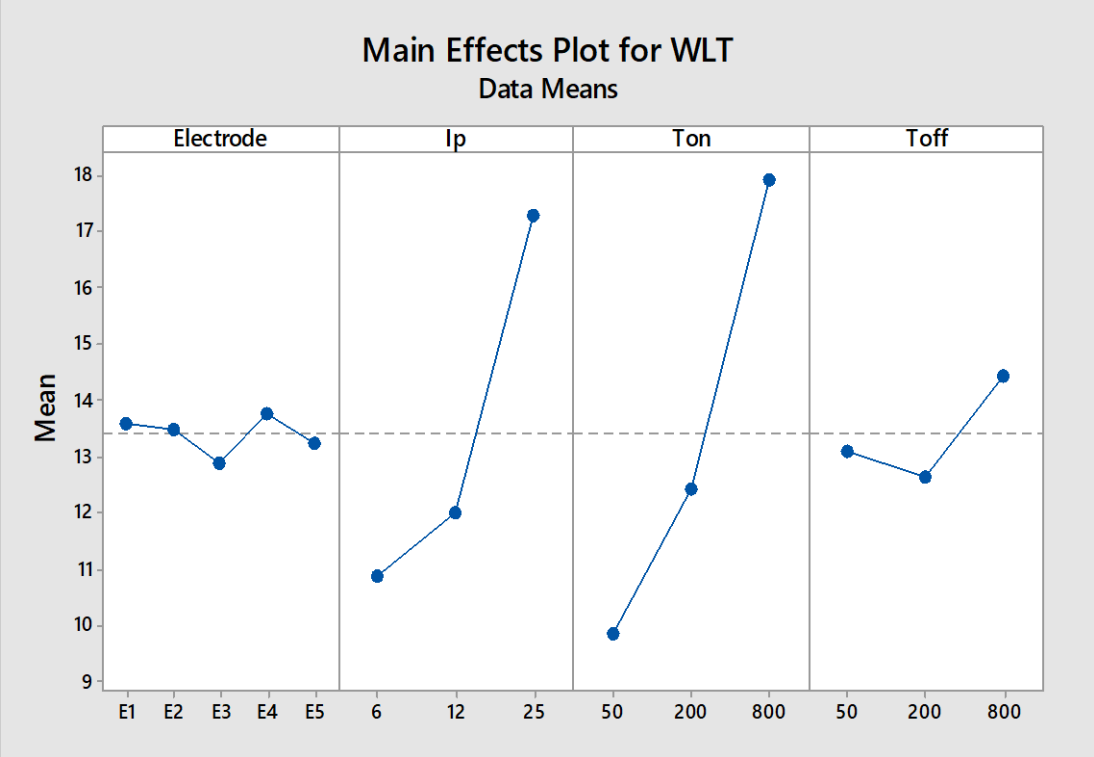

Figure 5. 24 Main effects plot of the process parameters on WLT.

Table 5. 15 Response for Means of WLT.

+ Level	Electrode	Ip	T_{on}	T_{off}
1	13.589	**10.880**	**9.847**	13.093
2	13.489	12.013	12.427	**12.660**
3	**12.889**	17.300	17.920	14.440
4	13.767			
5	13.256			
Delta	0.878	6.420	8.073	1.780
Rank	4	2	1	3

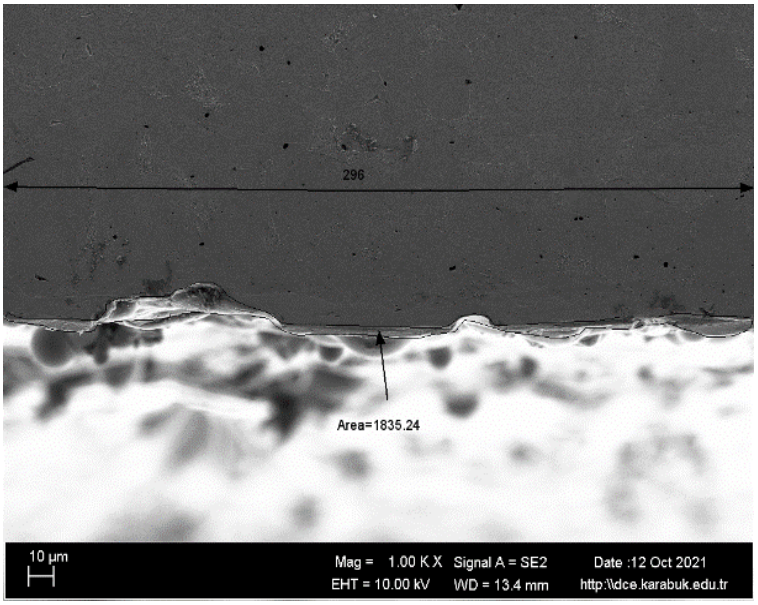

Figure 5. 25 SEM Micrograph, EDM parameters; E3A1B1C2.

Table 5. 16 Analysis of Variance of WLT.

Source	DF	Seq SS	Adj SS	Adj MS	F	P	Contribution
Electrode	4	4.14	4.14	1.035	0.03	0.998	0.23%
Ip	2	352.25	352.25	176.124	5.37	0.026	19.63%
T_{on}	2	510.06	510.06	25.030	7.77	0.009	28.43%
T_{off}	2	25.85	25.85	12.924	0.39	0.684	1.44%
Electrode*Ip	8	154.83	154.83	19.353	0.59	0.767	8.63%
Electrode* T_{on}	8	215.82	215.82	26.978	0.82	0.601	12.03%
Electrode* T_{off}	8	202.59	202.59	25.323	0.77	0.636	11.29%
Residual Error	10	328.02	328.02	32.803			
Total	44	1793.55					

Table 5.16 shows the results of ANOVA of WLT. It is clear that only T_{on} and Ip are the significant factors at a 95% confidence level for WLT. This table indicates that T_{on} is the most important factor because it has the highest percentage of contribution followed by Ip, Electrode* T_{on}, Electrode* T_{off}, Electrode*Ip, T_{off} and electrode material with percentage contributions 28.43%, 19.63%, 12.03%, 11.29% ,8.63%, 1.44% and 0.23% respectively. It is also noted that the interactions between the electrode and other parameters were not significant at the level of significance 5%, but the contribution of their effect was moderate.

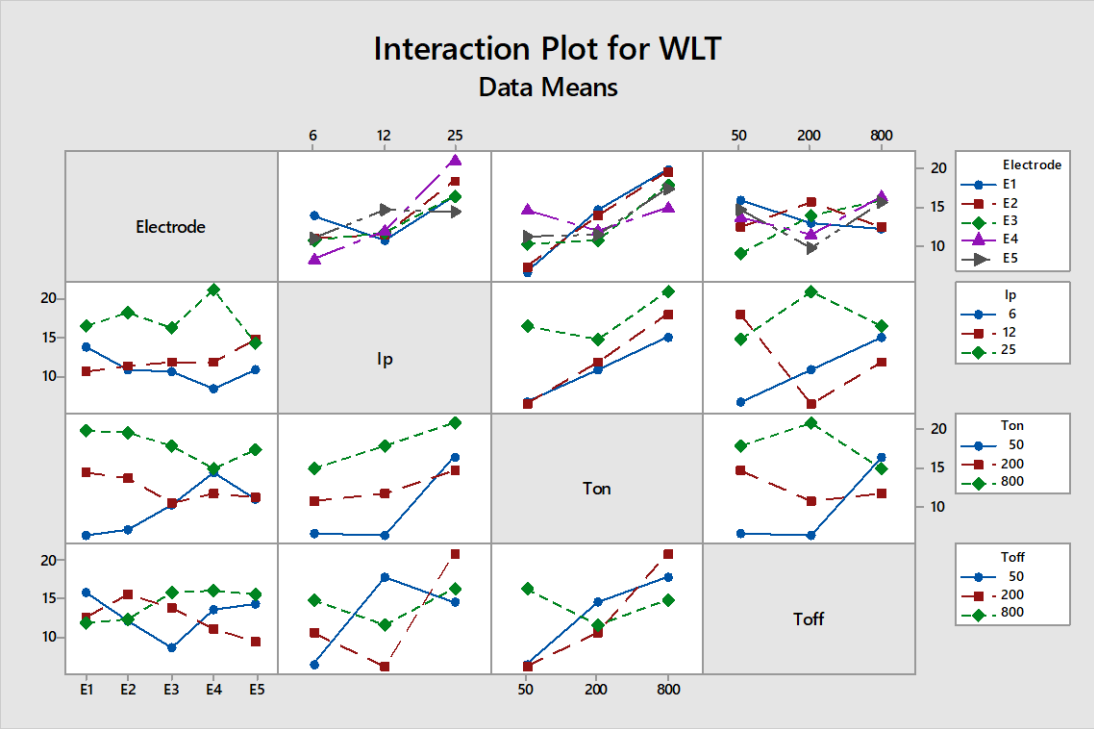

Figure 5. 26 Interaction effect plot of the process parameters on WLT.

Figure 5.27 illustrates interaction plots for various two-parameters interactions. Parallel lines show no interaction in an interaction plot. The higher the slope difference between the lines, the greater the degree of interaction. From Figure 5.19 and Table 5.16 it is observed that there are moderate interactions between Electrode*Ip, Electrode* T_{on}, Electrode* T_{off}. It is also clear from the figure 5.19 that there is a moderate interaction between T_{on} and T_{off} because the lines are not parallel. As for the interactions between the other parameters, although it is noted that there is no parallelism and the existence of intersection between the lines, but it is also noted that there is a quasi-parallelism between the lines for the same interactions, and this indicates a weak interaction between the parameters for the WLT.

5.2.6 Effect of Process Parameter on SCD

When machining with EDM, the metal surface is exposed to high heat and rapid cooling many times, which causes significant changes in surface morphology [82]. Among the disadvantages of EDM is the cracking of the workpiece surface. The

density of the cracks depends on several factors. Among the objectives of this study is to identify the effect of operating parameters on surface crack density (SCD), as well as to achieve the optimum set of process parameters for obtaining minimum SCD.

Table 5. 17 Comparison of electrodes performance for SCD.

Run	Ip	T_{on}	T_{off}	E1 (µm/µm²)	E2 (µm/µm²)	E3 (µm/µm²)	E4 (µm/µm²)	E5 (µm/µm²)
1	6	50	50	0.0031	0.0033	0.0016	0.0037	0.0024
2	6	200	200	0.0261	0.0197	0.0174	0.0304	0.0113
3	6	800	800	0.0225	0.0283	0.0247	0.0206	0.0040
4	12	50	200	0.0007	**0.0000**	**0.0000**	**0.0000**	**0.0000**
5	12	200	800	0.0021	0.0021	0.0077	0.0010	**0.0000**
6	12	800	50	0.0024	0.0146	**0.0000**	0.0224	0.0273
7	25	50	800	**0.0000**	**0.0000**	**0.0000**	**0.0000**	**0.0000**
8	25	200	50	0.0014	**0.0000**	**0.0000**	**0.0000**	0.0135
9	25	800	200	**0.0000**	0.0059	0.0031	0.0079	0.0037

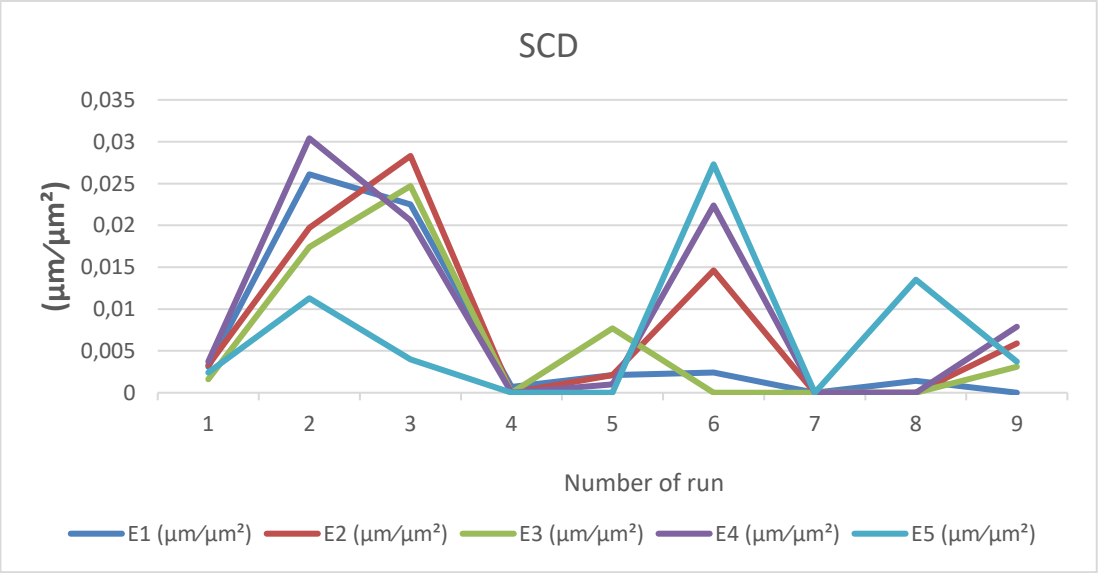

Figure 5. 27 Comparison of electrodes performance for SCD.

Figure 5.28 shows that the curve patterns of electrodes E1, E2, E3 and E4 are almost the same, while a different trend was shown in some experiments of electrode E5. Table 5.13 and Figure 5.27 clearly indicate that no cracks (SCD = Zero) were found on the surface for certain experiments (15 of 45 experiment). The values of SCD were at a minimum in experiments number 4 and 7 for all electrodes, and the noticeable observation is that T_{on} was at a low level which implies it is possible to achieve low SCD at low T_{on}. As for the highest crack density when using electrodes E1and E4 when process parameters A1B2C2, utilizing E2 and E3 the maximum SCD was at machining parameters A1B3C3 and maximum SCD for E5 was at parametric combination A2B3C1. For example, the SEM micrograph image in Figure 5.28 shows the absence of cracks when using the process parameters E4A3B1C3 and from Figure 5.29 the SEM micrograph image shows the density of surface cracks where it was at the highest value when using electrode 4 and process parameters E4A1B2C2.

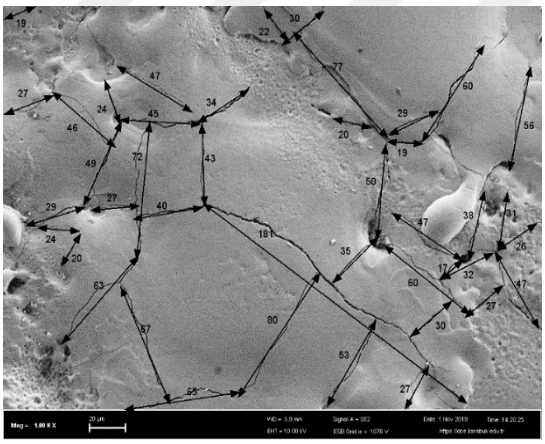

Figure 5. 29 SEM Micrograph, high SCD, EDM parameters; E4A1B2C2

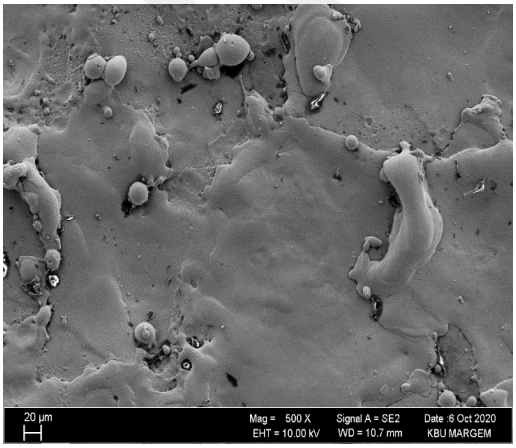

Figure 5.28 SEM Micrograph, no cracks, EDM parameters; E4A3B1C3

The optimum values of process parameters for lower SCD were attained by using main effects plot of means (Figure 5.30) and response table (Table 5.14) – namely, E3, Ip 25A, T_{on} (50µs) and T_{off} (50µs). A confirmation experiment was performed and a SEM micrograph was taken as Figure 5.31 showing that there were no cracks when machining with the optimal combination of process parameters. The second best

performance, which is considered close to the optimal performance can be obtained by E1, Ip 25 A, T_{on} (50µs) and T_{off} (50µs). Ip has the largest effect on SCD, followed by T_{on} then electrode material and the last was T_{off}. However, with increasing Ip, the SCD decreases dramatically. This phenomenon is in agreement with the study by Bhattacharyya et al [44]. SCD was directly proportional to T_{on} [71]. The minimum SCD attained at high Ip and short T_{on}. While increasing T_{off} from the first to the second level, the SCD increases significantly, and when T_{off} increases from the second to the third level, SCD decreases. The values of SCD reported by Bhattacharyya et al. [44] were minimum at Ip and T_{on} in the range 18–22A and 20–100µs respectively.

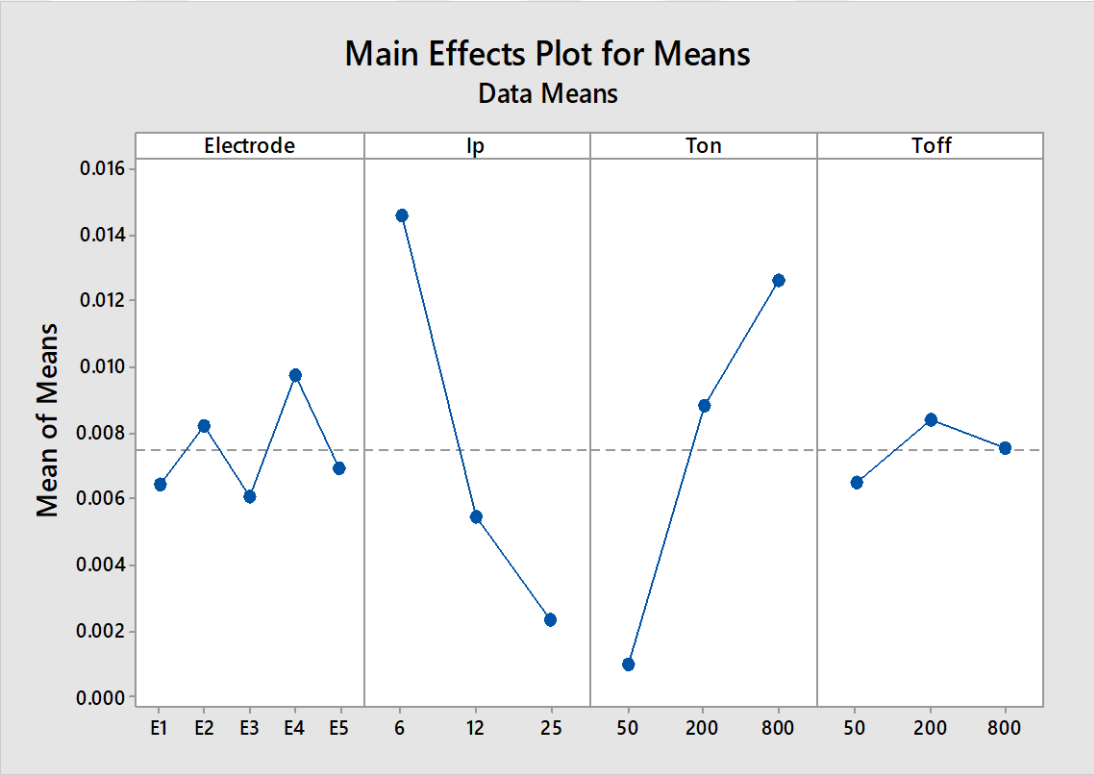

Figure 5. 30Main effects plot of the process parameters on SCD.

Table 5. 18 Response for means of SCD.

+ Level	Electrode	Ip	T_{on}	T_{off}
1	0.006478	0.014607	**0.000987**	**0.006487**
2	0.008211	0.005460	0.008847	0.008413
3	**0.006056**	**0.002367**	0.01260	0.007533
4	0.009733			
5	0.006911			
Delta	0.003678	0.012240	0.011613	0.001927
Rank	3	1	2	4

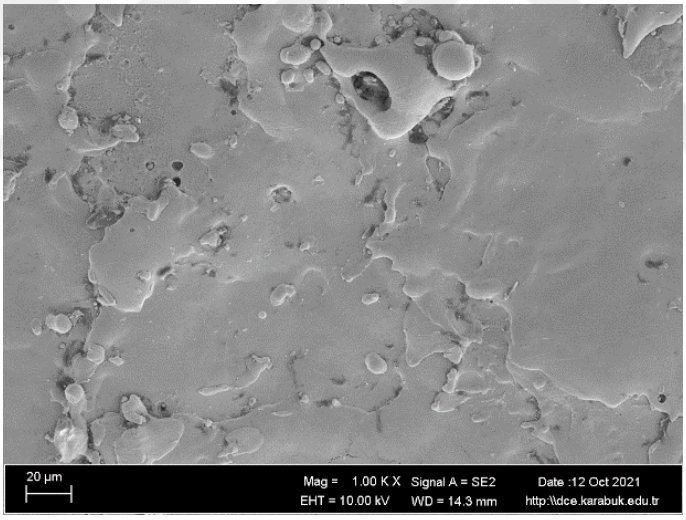

Figure 5. 31 SEM Micrograph, EDM parameters; E3A3B1C1.

Table 5.19 shows the results of ANOVA for SCD. It is observed that at a 5% level of significance the P-value of Ip and T_{on} were less than 0.05 which means they are significantly affect SCD and their contributions 28.77% and 24.96%. The electrode material and T_{off} the interactions (Electrode*Ip, Electrode * T_{on} and Electrode* T_{off}) were non-significant and their contributions' 1.91%, 0.66%, 9.66%, 3.41% and 13.24% respectively.

Table 5. 19 Analysis of Variance for SCD.

Source	DF	Seq SS	Adj SS	Adj MS	F	P	Contribution
Electrode	4	0.000081	0.000081	0.000020	0.28	0.887	1.91%
Ip	2	0.001215	0.001215	0.000608	8.28	0.008	28.77%
T_{on}	2	0.001054	0.001054	0.000527	7.18	0.012	24.96%
T_{off}	2	0.000028	0.000028	0.000014	0.19	0.830	0.66%
Electrode * Ip	8	0.000408	0.000408	0.000051	0.69	0.691	9.66%
Electrode * T_{on}	8	0.000144	0.000144	0.000018	0.25	0.971	3.41%
Electrode * T_{off}	8	0.000559	0.000559	0.000070	0.95	0.518	13.24%
Residual Error	10	0.000734	0.000734				
Total	29	0.004222					

Fig. 5.32 indicates interaction plots for SCD. It is noticed from the figure that there are parallel lines as well as intersecting lines, the intersection between the lines indicates the strength of the interaction between parameters, while the parallel lines indicate the absence of interaction. There are parallel and intersecting lines this implies a slight interaction effect between parameters. Electrode material and Ip and T_{on}, Table 5.19 shows the contribution of the interactions (Electrode*Ip 9.66% and Electrode*T_{off} 13.24%), which clears the influence of interactions effect on SCD.

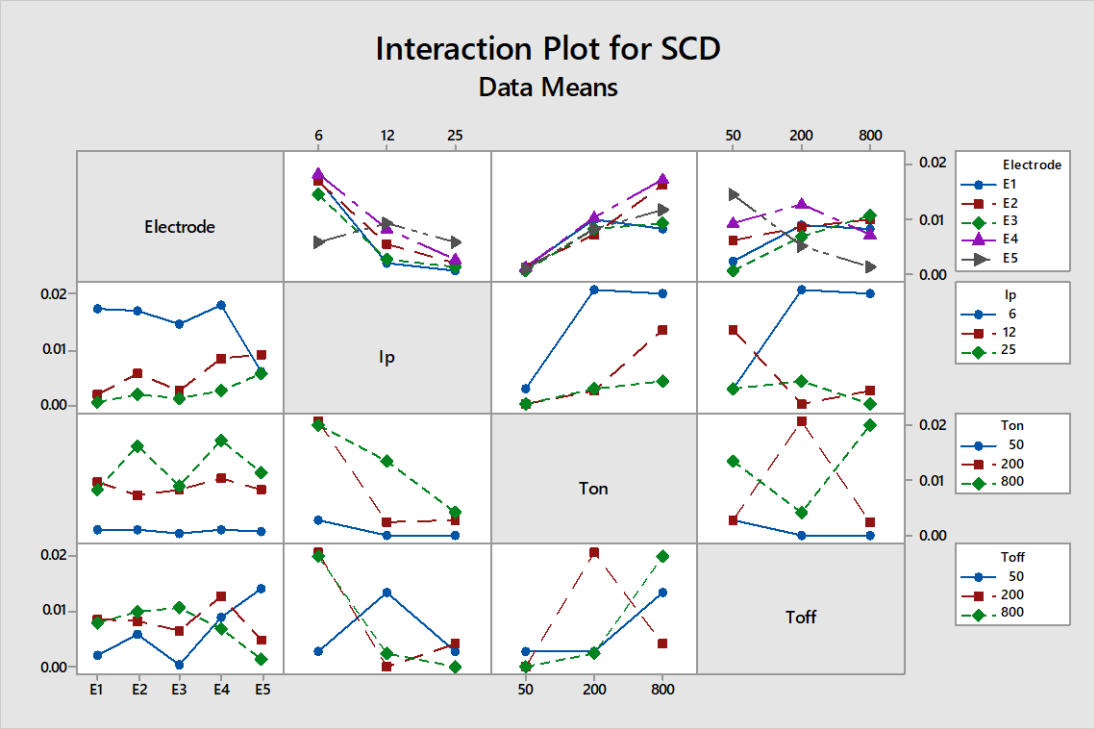

Figure 5. 32 Interaction effect plot of the process parameters on SCD.

5.3 SUMMARY

From the results that have been shown in this part, which explain the effect of the process parameters on the responses and the extent of their relationship to each other, it is summarized as follows:

1- The rank of influence of process parameters on the responses:

   Table 5.20 shows the importance of the influence of process parameters on the performance characteristics as they ranked in response of means tables. It is noted that the two most influential parameters are Ip and T_{on}. As for T_{off} and Electrode material, they are the least influential on the responses except in the case of OC, where Electrode material was the most significant parameter. Focusing on the process parameters with the highest effect on the response helps to achieve the best results when EDM of DIN 1.2767 tool steel.

Table 5. 20 The effect of parameters on the Responses.

	Electrode	**Ip**	**T_{on}**	**T_{off}**
MRR	4	1	2	3
TWR	3	1	2	4
Ra	3	1	2	4
OC	1	2	3	4
WLT	4	2	1	3
SCD	3	1	2	4

2- Contribution of process parameters and interactions on the responses

The Contribution of process parameters and interactions on the responses are summarized in Table 5.21 and indicated in Figure 4.32. It is observed that Ip has the highest contribution in average 34.38% followed by T_{on} 17.52% and the average of contributions of other parameters are low. But they have a significant effect on some responses, such as the effect of tool electrode on OC and the interaction between electrode material and discharge current for OC.

Table 5. 21 Contribution of process parameters and interactions on the Responses.

	MRR	**TWR**	**Ra**	**OC**	**WLT**	**SCD**	**Average**
Electrode	1.09%	7.74%	2.79%	19.50%	0.23%	1.91%	5.54%
Ip	55.18%	29.32%	59.09%	13.71%	19.63%	28.77%	34.38%
T_{on}	13.55%	17.30%	9.47%	11.41%	28.43%	24.96%	17.52%
T_{off}	13.50%	3.16%	2.36%	3.37%	1.44%	0.66%	4.08%

Electrode*Ip	0.8%	2.71%	1.99%	28.79%	8.63%	9.66%	8.76%
Electrode* T_{on}	0.4%	7.25%	1.13%	8.32%	12.03%	3.41%	5.42%
Electrode*T_{off}	0.71%	8.93%	1.76%	5.42%	11.29%	13.24%	6.89

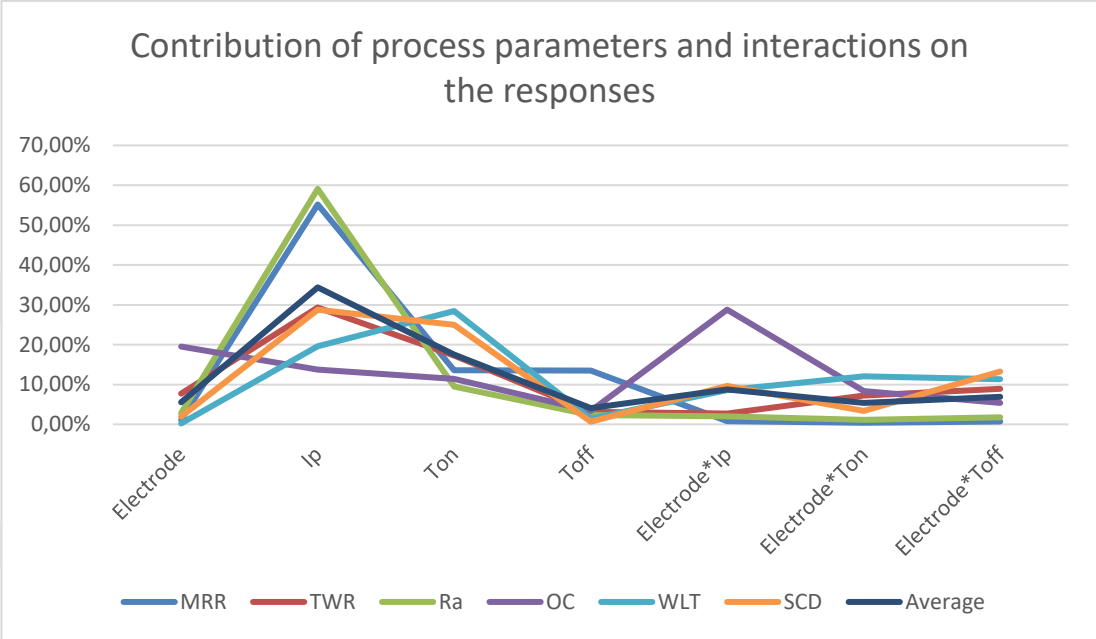

Figure 5. 33 The contribution effect of the process parameters.

3- Effect of electrode material on the performance measures.

From table 4.22, it can be seen that E4 and E3 electrodes achieve the highest MRR. Minimum TWR can be obtained by using E2 and E1. optimal surface finish (low Ra) can be attained by using E1 and E5 electrodes. The lowest OC was achieved using E5 followed by E4. And the smallest WLT can be produced by utilizing E3 and E5. E3 attained the lowest SCD then E1. Also, it is noticed that E1 was the best electrode to attain minimum Ra and the second to attain minimum TWR and SCD and for maximum MRR is was the third but to achieve minimum WLT it was the fourth and for minimum OC it was the least. Using E2 can be produced Optimal TWR and moderate WLT and Ra whereas the results of the other responses (MRR, OC and SCD) were not satisfied. E3

produced the lowest WLT and SCD and the second to attain high MRR and moderate for TWR and OC whereas the fourth effect electrode for minimum Ra. E4 was the first to achieve maximum MRR and the second for minimum OC but for the other responses, it was the last. Optimal OC and low Ra and WLT can be obtained by using E5 but it was medium for SCD, the fourth for optimal TWR and the worst to produce high MRR. In general, E3 can be considered the best electrode to achieve optimal responses.

Table 5. 22 the rank of the effect of electrode material on the responses.

	E1	**E2**	**E3**	**E4**	**E5**
MRR	3	4	2	**1**	5
TWR	2	**1**	3	5	4
Ra	1	3	4	5	**2**
OC	5	4	3	2	**1**
WLT	4	3	**1**	5	2
SCD	**2**	4	1	5	3

4- The optimal process parameters setting.

The optimal EDM performance can be determined by utilizing the setting parameters as mentioned in Table 5.23.

Table 5. 23 The optimal levels of process parameters for responses.

	Electrode	**Ip**	**T_{on}**	**T_{off}**
MRR	E4	A3	B2	C1
TWR	E2	A1	B3	C2
Ra	E1	A1	B3	C3

OC	E5	A2	B1	C3
WLT	E3	A1	B1	C2
SCD	E3	A3	B1	C1

PART 6

CONCLUSION AND RECOMMENDATIONS

This study has investigated the effects of EDM process parameters on the machining performance of Din 1.2767 tool steel workpieces using five types of copper alloy as tool electrode. ANOVA were used for data analysis. The process parameters include electrode material, peak current (IP), pulse on time (T_{on}) and pulse off time (T_{off}) and the machining performance measures include material removal rate (MRR), tool wear rate (TWR), surface roughness (Ra), overcut (OC), white layer thickness (WLT) and surface crack density (SCD). This study reached conclusions and recommendations that may contribute to increasing and improving the performance of electric discharge machining (EDM).

6.1 CONCLUSION

The study reached some conclusions that contribute to increasing productivity, improving machinability and quality of DIN 1.2767 tool steel products using electric discharge machining, the most important of which are:

- The most influential and contributing process parameters were Ip and T_{on} on all responses except for OC where the major role in the effect was the type of electrode material.
- Machining at some levels of parameters can achieve optimal performance for some responses as follows:

a) Machining with high Ip produces high MRR, TWR, OC and Ra and low SCD.
b) Machining with high T_{on} produces low TWR and Ra, moderate MRR and high OC, WLT and SCD.
c) Machining with high T_{off} produces low MRR, Ra and OC, moderate TWR and WLT and high SCD.

- The parametric combination for optimal responses were achieved as follows:
  - High MRR at NSS electrode Ip (25A), T_{on} (200µs) and T_{off} (50µs).
  - Low TWR at Cu electrode Ip (6A), T_{on} (800µs) and T_{off} (200µs).
  - Low Ra at CuCrZr electrode Ip (6A), T_{on} (800µs) and T_{off} (800µs).
  - Low OC at B2 electrode Ip (12A), T_{on} (50µs) and T_{off} (800µs).
  - Low WLT at CNB electrode Ip (6A), T_{on} (50µs) and T_{off} (200µs).
  - Low SCD at CNB electrode Ip (25A), T_{on} (50µs) and T_{off} (50µs).
- The effect of electrode material type on performance is quite close as it was found that the best MRR can be achieved using Nss electrode then CNB, Minimum TWR can be obtained by using Cu electrode next CuCrZr, Optimal surface finish can be attained by using CuCrZr electrode followed by B2, the lowest OC can be achieved using B2 electrode then NSS, the smallest WLT can be produced by utilizing CNB electrode and B2 and the lowest SCD can be attained by CNB electrode followed by CuCrZr electrode.
- The effect of Ip on the performance measures.

  MRR, TWR, Ra and WLT increase with increase Ip. Whereas for OC, with increasing Ip, OC decreases and then increases. SCD inversely proportional to Ip.
- The effect of T_{on} on the performance measures.

  TWR decrease with the increase T_{on}. Whereas WLT and SCD increase with increase of T_{on}. While MRR, Ra and OC increase with an increase of T_{on} then decreased.
- The effect of T_{off} on the performance measures.

  MRR and OC are inversely proportional to T_{off}. TWR and WLT slightly decrease due to the increase of T_{off} then increase. Ra and SCD increase with an increase of T_{off} then decreased.
- The interaction effect.

  There are interactions of different degrees between most of the process parameters for the responses, and this explains the complex relationships that the process parameters are related to and the strength of their influence on the responses.

6.2 RECOMMENDATIONS

It is recommended that future study should work on the following:

- The effect of other levels of process parameters.
- Using other type electrode materials such as graphite, aluminium and brass.
- The effect of the electrode shape and size.
- The effect of flushing mode and pressure.
- Using other type of dielectric or powders mixing with different concentrations or dry EDM.
- Studying other responses such as recast layer hardness and residual stress.
- Compare the effect of process parameters and the same level on another type of tool steel.
- Applying Grey Relation analysis or other methods for multi-response optimization.

REFERENCES

1. Ho K. H. and Newman S.T., "State of the art electrical discharge machining (EDM)," ***Int. J. Mach. Tools Manuf***., vol. 43, no. 13, pp. 1287–1300, 2003, doi: 10.1016/S0890-6955(03)00162-7.

2. Amorim F.L. and Weingaertner W.L., "The behavior of graphite and copper electrodes on the finish die-sinking electrical discharge machining (EDM) of AISI P20 tool steel," ***J. Brazilian Soc. Mech. Sci. Eng.,*** vol. 29, no. 4, pp. 366–371, 2007, doi: 10.1590/S1678-58782007000400004.

3. Muthuramalingam T. and Mohan B., "A review on influence of electrical process parameters in EDM process," ***Arch. Civ. Mech. Eng.***, vol. 15, no. 1, pp. 87–94, 2015, doi: 10.1016/j.acme.2014.02.009.

4. Yankee H., *Manufacturing Processes*. USA: Prentice-Hall, 1979.
5. Ramabalan S. and J. J., "Die Sinking Edm Process Parameters: a Review," ***Int. J. Eng. Robot. Res***., vol. 4, no. 1, 2015.

6. Venkatesh B., Naveen P., Maurya B., and Shanthi Priya D., "Experimental Investigation of Edm Using Electrode Materials Copper, Brass and Chromium Copper for Alloy Steels," ***Int. J. Adv. Eng. Res. Dev.***, vol. 2, no. 04, pp. 1–12, 2015, doi: 10.21090/ijaerd.02041.

7. Gostimirovic M., Kovac P., Sekulic M., and Skoric B., "Influence of discharge energy on machining characteristics in EDM," ***J. Mech. Sci. Technol***., vol. 26, no. 1, pp. 173–179, 2012, doi: 10.1007/s12206-011-0922-x.

8. Kumar V. and Kumar P., "Improving Material Removal Rate and Optimizing Variousmachining Parameters in EDM," ***Int. J. Eng. Sci.***, vol. 06, no. 06, pp. 64–68, 2017, doi: 10.9790/1813-0606016468.

9. Dhakry N. S., Bangar P. A., and Bhadauria G, "Analysis of process parametersin electro-discharge machining of Tungsten carbideby using taguchi," ***Int. J. Eng. Res. Appl***., vol. 4, no. 2, pp. 661–669, 2014.

10. Patil K.K. and Jadhav V.D., "Study of Machining Parameters in EDM," ***Int. J. Res. Appl. Sci. Eng. Technol***., vol. 4, no. I, pp. 72–78, 2016.

11. Pradhan M.K., "Optimisation of surface integrity model using response surface methodology for EDMed AISI D2 tool steel," ***J. Mater. Process. Technol***., November 2017, 2012, doi: 10.1504/IJMMS.2012.049967.

12. Khan A.A., Ali M. Y., and Haque M. M., "A study of electrode shape

configuration on the performance of die sinking EDM," ***Int. J. Mech. Mater. Eng.***, vol. 4, no. 1, pp. 19–23, 2009.

13. Jaharah A. G., Liang C. G., Wahid S. Z., Ab Rahman M. N., and Che Hassan, C. H. "Performance of copper electrode in electical discharge machining (EDM) of AISI H13 harden steel," ***Int. J. Mech. Mater. Eng.***, vol. 3, no. 1, pp. 25–29, 2008.

14. Chandramouli S. and Eswaraiah K., "Experimental investigation of EDM process parameters in machining of 17-4 PH Steel using taguchi method," ***Mater. Today Proc.,*** vol. 5, no. 2, pp. 5058–5067, 2018, doi: 10.1016/j.matpr.2017.12.084.

15. Bose K. and Mahapatra K., "Parametric study of die sinking EDM process on AISI H13 tool steel using statistical techniques," ***Adv. Prod. Eng. Manag***., vol. 9, no. 4, pp. 168–180, 2014, doi: 10.14743/apem2014.4.185.

16. Mishra B. P. and Routara B. C., "An experimental investigation and optimisation of performance characteristics in EDM of EN-24 alloy steel using Taguchi Method and Grey Relational Analysis," ***Mater. Today Proc***., vol. 4, no. 8, pp. 7438–7447, 2017, doi: 10.1016/j.matpr.2017.07.075.

17. Nikalje A. M., Kumar A., and Srinadh K. V. S., "Influence of parameters and optimization of EDM performance measures on MDN 300 steel using Taguchi method," ***Int. J. Adv. Manuf. Technol***., vol. 69, no. 1–4, pp. 41–49, 2013, doi: 10.1007/s00170-013-5008-8.

18. Sanjeev S., Rajdeep S., and Sandeep J., "Study the Effect of Machining Parameters in Electric Discharge Machining of EN 31 Die Steel," ***Int. J. Eng. Res***., vol. V4, no. 11, pp. 145–148, 2015, doi: 10.17577/ijertv4is110031.

19. Kiyak M. and Çakir O., "Examination of machining parameters on surface roughness in EDM of tool steel," ***J. Mater. Process. Technol.***, vol. 191, no. 1–3, pp. 141–144, 2007, doi: 10.1016/j.jmatprotec.2007.03.008.

20. Shabgard M., Faraji H., Khosrozadeh B., Amini K., and Seyedzavvar M., "Experimental investigation into the EDM process of γ-TiAl," ***Turkish J. Eng. Environ. Sci***., vol. 38, no. 2, pp. 231–239, 2014, doi: 10.3906/muh-1404-15.

21. Sihore A. and Somkuwar V., "Optimization of Process Parameter of Die Sinking EDM for machining of SS316H using Taguchi L9 Approach," ***J. Mater. Process. Technol,*** vol. 7, no. I, pp. 110–121, 2019.

22. Straka Ľ. and Hašová S., "Optimization of material removal rate and tool wear rate of Cu electrode in die-sinking EDM of tool steel," ***Int. J. Adv. Manuf. Technol.,*** vol. 97, no. 5–8, pp. 2647–2654, 2018, doi: 10.1007/s00170-018-2150-3.

23. Yadava , Dixit A. C., and jitendra K., "Optimization of EDM Parameter of

High Carbon-High Chromium Steel (AISI D3) by using Brass Electrode," ***Int. J. Eng. Trends Technol.***, vol. 34, no. 3, pp. 126–130, 2016, doi: 10.14445/22315381/ijett-v34p225.

24. Hadad M., Bui L. Q. and Nguyen C. T., "Experimental investigation of the effects of tool initial surface roughness on the electrical discharge machining (EDM) performance," ***Int. J. Adv. Manuf. Technol.,*** vol. 95, no. 5–8, pp. 2093–2104, 2018, doi: 10.1007/s00170-017-1399-2.

25. Raman K., Sathiya G. K., Saisujith K., and Mani P., "Effect of Machining Parameters in Electrical Discharge Machining of D2 Tool Steel," ***Int. J. Sci. Res.***, vol. 6, no. 7, pp. 1634–1637, 2017, doi: 10.21275/20071713.

26. Hamid F. E. A. and Lajis M. A., "High performance in EDM machining of AISI D2 hardened steel," ***Adv. Mater. Res***., vol. 500, pp. 259–265, 2012, doi: 10.4028/www.scientific.net/AMR.500.259.

27. Koteswararao B., Siva K., Kishore B., Ravi D., Kumar K. K., and Chandra P. Shekar, "Investigation of Machining Parameter in EDM of High Carbon Steel Alloy (EN31)," ***Mater. Today Proc***., vol. 4, no. 2, pp. 1375–1384, 2017, doi: 10.1016/j.matpr.2017.01.159.

28. Lee H. T., Hsu F. C., and Tai T. Y., "Study of surface integrity using the small area EDM process with a copper-tungsten electrode," ***Mater. Sci***. *Eng. A*, vol. 364, no. 1–2, pp. 346–356, 2004, doi: 10.1016/j.msea.2003.08.046.

29. Paul L. and Jose I., "Comparative study of effect of tool materials in EDM process," ***IOP Conf. Ser. Mater***. *Sci. Eng.*, vol. 396, no. 1, 2018, doi: 10.1088/1757-899X/396/1/012071.

30. Vishwakarma R., Yadav S., Kumar A., and Krishhna H., "Effect of Different Electrodes and Dielectric Fluids on Metal Removal Rate and Surface Integrity of Electric Discharge Machining : A Review," ***Int. J. Eng. Technol. Sci. Res***., vol. 4, no. 11, pp. 935–941, 2017.

31. Mahajan R., Krishna H., Singh A. K., and Ghadai R. K., "A Review on Copper and its alloys used as electrode in EDM," ***IOP Conf. Ser. Mater. Sci. Eng***., vol. 377, no. 1, 2018, doi: 10.1088/1757-899X/377/1/012183.

32. Muttamara A., "Comparison Performances of EDM on Ti6Al4V with Two Graphite Grades," ***Int. J. Chem. Eng. Appl.***, vol. 6, no. 4, pp. 250–253, 2015, doi: 10.7763/ijcea.2015.v6.490.

33. Singh S., Maheshwari S. and Pandey P. C., "Some investigations into the electric discharge machining of hardened tool steel using different electrode materials," ***J. Mater. Process. Technol***., vol. 149, no. 1–3, pp. 272–277, 2004, doi: 10.1016/j.jmatprotec.2003.11.046.

34. Puthumana R., Govindan P., "Effect of Micro Electrical Discharge Machining

Process Conditions on Tool Wear Characteristics : Results of an Analytic Study," 2016.

35. Keskin Y, Halkaci H. S., and Kizil M., "An experimental study for determination of the effects of machining parameters on surface roughness in electrical discharge machining (EDM)," ***Int. J. Adv. Manuf. Technol.***, vol. 28, no. 11–12, pp. 1118–1121, 2006, doi: 10.1007/s00170-004-2478-8.

36. Habib S., "Parameter optimization of electrical discharge machining process by using Taguchi approach," ***J. Eng. Technol. Res.***, vol. 6, no. 3, pp. 27–42, 2014, doi: 10.5897/jetr2014.0356.

37. Sultan T., "Experimental investigation of surface roughness of EN 353 on EDM with hollow tool Experimental investigation of surface roughness of EN 353 on EDM with hollow tool," no. MAY 2014, 2016, doi: 10.13140/2.1.1029.3129.

38. Krishna G., Rao M. and Rao H., "Hybrid modeling and optimization of hardness of surface produced by electric discharge machining using artificial neural networks and genetic algorithm," ***J. Eng. Appl. Sci.***, vol. 5, no. 5, pp. 72–81, 2010.

39. Salonitis K., Stournaras A., Stavropoulos P., and Chryssolouris G., "Thermal modeling of the material removal rate and surface roughness for die-sinking EDM," ***Int. J. Adv. Manuf. Technol.***, vol. 40, no. 3–4, pp. 316–323, 2009, doi: 10.1007/s00170-007-1327-y.

40. Fikri A. A., Romlie M., and Aminnudin A., "Factors Affecting the Surface Roughness in Sinking EDM Process," ***J. Mech. Eng. Sci. Technol.***, vol. 1, no. 1, pp. 9–14, 2017, doi: 10.17977/um030v1i12017p009.

41. Ahmad S. and Lajis M. A., "Electrical discharge machining (EDM) of Inconel 718 by using copper electrode at higher peak current and pulse duration," ***IOP Conf. Ser. Mater. Sci.*** *Eng.*, vol. 50, no. 1, 2013, doi: 10.1088/1757-899X/50/1/012062.

42. Kumar S., "Copper-chromium alloy as a superior electrode material for electrical discharge machining of die steels," ***Int. J. Mater. Eng. Innov.***, vol. 3, pp. 316–329, 2012, doi: 10.1504/IJMATEI.2012.049269.

43. Nallusamy S., "Analysis of MRR and TWR on OHNS die steel with different electrodes using electrical discharge machining," ***Int. J. Eng. Res. Africa***, vol. 22, pp. 112–120, 2016, doi: 10.4028/www.scientific.net/JERA.22.112.

44. Bhattacharyya B., Gangopadhyay S., and Sarkar B. R., "Modelling and analysis of EDMED job surface integrity," ***J. Mater. Process. Technol.***, vol. 189, no. 1–3, pp. 169–177, 2007, doi: 10.1016/j.jmatprotec.2007.01.018.

45. Ghanem V, Braham C., and Sidhom H., "Influence of steel type on electrical discharge machined surface integrity," ***J. Mater. Process. Technol.***, vol. 142,

no. 1, pp. 163–173, 2003, doi: 10.1016/S0924-0136(03)00572-7.

46. Boujelbene M., Bayraktar V, and Wissem T., “Influence of machining parameters on the surface integrity in small-hole electrical discharge machining,” ***Arch. Mater. Sci. Eng***., vol. 37, no. 2, pp. 110–116, 2009.

47. Çaydaş U. and Hasçalik A., “Modeling and analysis of electrode wear and white layer thickness in die-sinking EDM process through response surface methodology,” ***Int. J. Adv. Manuf. Technol***., vol. 38, no. 11–12, pp. 1148–1156, 2008, doi: 10.1007/s00170-007-1162-1.

48. Cusanelli G., Hessler-Wyser A., Bobard F., Demellayer R., Perez R., and Flükiger R., “Microstructure at submicron scale of the white layer produced by EDM technique,” ***J. Mater. Process. Technol.***, vol. 149, no. 1–3, pp. 289–295, 2004, doi: 10.1016/j.jmatprotec.2003.11.047.

49. Younis M. A., Abbas M. S., Gouda M. A., Mahmoud F. H., Abd S. A., and Abd Allah S. A., “Effect of electrode material on electrical discharge machining of tool steel surface,” ***Ain Shams Eng. J***., vol. 6, no. 3, pp. 977–986, 2015, doi: 10.1016/j.asej.2015.02.001.

50. Lee L. C., Lim L. C., and Wong V, “Towards crack minimisation of EDMed surfaces,” ***J. Mater. Process. Tech***., vol. 32, no. 1–2, pp. 45–54, 1992, doi: 10.1016/0924-0136(92)90162-L.

51. Wang C. C., Chow H. M., Yang L. D., and Te Lu C., “Recast layer removal after electrical discharge machining via Taguchi analysis: A feasibility study,” ***J. Mater. Process. Technol***., vol. 209, no. 8, pp. 4134–4140, 2009, doi: 10.1016/j.jmatprotec.2008.10.012.

52. Ekmekci B., “White layer composition, heat treatment, and crack formation in electric discharge machining process,” ***Metall. Mater. Trans. B Process Metall. Mater. Process. Sci***., vol. 40, no. 1, pp. 70–81, 2009, doi: 10.1007/s11663-008-9220-0.

53. Guu Y. H., “AFM surface imaging of AISI D2 tool steel machined by the EDM process,” ***Appl. Surf. Sci.***, vol. 242, no. 3–4, pp. 245–250, 2005, doi: 10.1016/j.apsusc.2004.08.028.

54. Lee V and Tai T. Y., “Relationship between EDM parameters and surface crack formation,” ***J. Mater. Process. Technol.***, vol. 142, no. 3, pp. 676–683, 2003, doi: 10.1016/S0924-0136(03)00688-5.

55. Lee L. C., Lim L. C., Narayanan V, and Venkatesh V. C., “Quantification of surface damage of tool steels after EDM,” ***Int. J. Mach. Tools Manuf***., vol. 28, no. 4, pp. 359–372, 1988, doi: 10.1016/0890-6955(88)90050-8.

56. Kruth I. P., Stevens I., Froyen I., and Lauwers I., “Study of the White Layer of a Surface Machined by Die-Sinking Electro-Discharge Machining,” ***CIRP Ann.***

- ***Manuf. Technol.,*** vol. 44, no. 1, pp. 169–172, 1995, doi: 10.1016/S0007-8506(07)62299-9.

57. Dewangan S., Gangopadhyay S., and Biswas C. K., "Multi-response optimization of surface integrity characteristics of EDM process using grey-fuzzy logic-based hybrid approach," ***Eng. Sci. Technol. an Int. J.***, vol. 18, no. 3, pp. 361–368, 2015, doi: 10.1016/j.jestch.2015.01.009.

58. Ekmekci B., "Residual stresses and white layer in electric discharge machining (EDM)," ***Appl. Surf. Sci.,*** vol. 253, no. 23, pp. 9234–9240, 2007, doi: 10.1016/j.apsusc.2007.05.078.

59. Yerui F., Zongfeng L., Yongfeng G., and Zongfeng L., "Experimental Investigation of EDM Parameters for TiC/Ni Cermet Machining," ***Procedia CIRP,*** vol. 42, no. Isem Xviii, pp. 18–22, 2016, doi: 10.1016/j.procir.2016.02.177.

60. Dastagiri M. and Hemantha Kumar A., "Experimental investigation of EDM parameters on stainless Steel & En41b," ***Procedia Eng.***, vol. 97, no. I, pp. 1551–1564, 2014, doi: 10.1016/j.proeng.2014.12.439.

61. Kalyon A., "Optimization of machining parameters in sinking electrical discharge machine of caldie plastic mold tool steel," ***Sādhanā,*** 2020, doi: 10.1007/s12046-020-1305-8.

62. Habib S. S., "Study of the parameters in electrical discharge machining through response surface methodology approach," ***Appl. Math. Model.***, vol. 33, no. 12, pp. 4397–4407, 2009, doi: 10.1016/j.apm.2009.03.021.

63. Gopalakannan S., Senthilvelan T., and Ranganathan S., "Statistical optimization of EDM parameters on machining of aluminum Hybrid Metal Matrix composite by applying Taguchi based Grey analysis," ***J. Sci. Ind. Res. (India).***, vol. 72, no. 6, pp. 358–365, 2013.

64. Arunkumar V, Rawoof H. S. A., and Vivek R., "Investigation on the Effect Of Process Parameters For Machining Of EN31 (Air Hardened Steel) By EDM," ***Int. J. Eng.***, vol. 2, no. 4, pp. 1111–1121, 2012.

65. Haron C. H. C., Deros M., Ginting A., and Fauziah M., "Investigation on the influence of machining parameters when machining tool steel using EDM," ***J. Mater. Process. Technol.***, vol. 116, no. 1, pp. 84–87, 2001.

66. Haron C. H. C., Ghani J. A., Burhanuddin Y., Seong Y. K., and Swee C. Y., "Copper and graphite electrodes performance in electrical-discharge machining of XW42 tool steel Copper and graphite electrodes performance in electrical-discharge machining of XW42 tool steel," no. May, pp. 2–6, 2008, doi: 10.1016/j.jmatprotec.2007.11.285.

67. Mahajan A., Sidhu S. S. and Devgan S., "Metal Removal Rate & Surface

Morphological Analysis of Electrical Discharge Machined Co-Cr Alloy," ***Emerg. Mater. Res.***, vol. 9, no. 1, pp. 1–5, Mar. 2020, doi: 10.1680/jemmr.19.00034.

68. Panda S., Mishra D., Biswal B. B. and Nanda P., "Optimization of multiple response characteristics of EDM process using taguchi-based grey relational analysis and modified PSO," ***J. Adv. Manuf. Syst.,*** vol. 14, no. 3, pp. 123–148, 2015, doi: 10.1142/S0219686715500092.

69. Kumar M., Kumar K., Kr T. and Sahoo P., "Application of Artificial bee Colony Algorithm for Optimization of MRR and Surface Roughness in EDM of EN31 tool steel," vol. 6, no. Icmpc, pp. 741–751, 2014, doi: 10.1016/j.mspro.2014.07.090.

70. Kumar B., "ScienceDirect On Electro-Discharge Machining of Inconel 718 Super Alloys : An Experimental Investigation," vol. 5, pp. 4861–4869, 2018, doi: 10.1016/j.matpr.2017.12.062.

71. Roy A. K. and Kumar K., "Effect and Optimization of Machine Process Parameters on MRR for EN19 & EN41 materials using Taguchi," ***Procedia Technol.,*** vol. 14, pp. 204–210, 2014, doi: 10.1016/j.protcy.2014.08.027.

72. Kumar P., Dewangan S. and Pandey C., "Materials Today : Proceedings Analysis of surface integrity and dimensional accuracy in EDM of P91 steels," ***Mater. Today Proc.***, no. xxxx, 2020, doi: 10.1016/j.matpr.2020.03.119.

73. Dewangan S., Biswas C. K. and Gangopadhyay S., "Materials and Manufacturing Processes Influence of Different Tool Electrode Materials on EDMed Surface Integrity of AISI P20 Tool Steel Influence of Different Tool Electrode Materials on EDMed Surface Integrity of AISI P20 Tool Steel," no. December, pp. 37–41, 2014, doi: 10.1080/10426914.2014.930892.

74. Schumacher B. M., Krampitz R. and Kruth V, "Historical phases of EDM development driven by the dual influence of 'Market Pull' and 'Science Push,'" ***Procedia CIRP***, vol. 6, pp. 5–12, 2013, doi: 10.1016/j.procir.2013.03.001.

75. Groover M. P., *FUNDAMENTALS OF MODERN MANUFACTURING. **Materials, Processes, and Systems.***, 4th ed. USA: JOHN WILEY & SONS, INC., 2010.

76. Pandy A. and Singh S., "Current research trends in variants of Electrical Discharge Machining: A review," ***Int. J. Eng. Res. Technol.***, vol. 2, no. 6, pp. 2172–2191, 2010.

77. Abbas M. N. *et al.*, "A review on current research trends in electrical discharge machining (EDM)," ***Int. J. Mach. Tools Manuf.***, vol. 47, no. 7–8, pp. 1214–1228, 2007, doi: 10.1016/j.ijmachtools.2006.08.026.

78. Sabur A., Ali M. Y., Maleque M. A. and Khan A. A., "Investigation of material

removal characteristics in EDM of nonconductive ZrO2 ceramic," ***Procedia Eng.,*** vol. 56, pp. 696–701, 2013, doi: 10.1016/j.proeng.2013.03.180.

79. Black J. and Kohser R., ***Materials and Processes In Manufacturing,*** 11th ed. USA: JOHN WILEY & SONS, INC., 2012.

80. Yadav R. N. and Yadava V., "Influence of input parameters on machining performances of slotted-electrical discharge abrasive grinding of Al/SiC/Gr metal matrix composite," ***Mater. Manuf. Process.***, vol. 28, no. 12, pp. 1361–1369, 2013, doi: 10.1080/10426914.2013.832300.

81. Raju L. and Hiremath S. S., "A State-of-the-art Review on Micro Electro-Discharge Machining," ***Procedia Technol.,*** vol. 25, no. Raerest, pp. 1281–1288, 2016, doi: 10.1016/j.protcy.2016.08.222.

82. Guitrau E. B., *The EDM handbook*. Hanser Gardner Publications, 1997.

83. A. Jamwal, U. Vates, and A. Aggarwal, "Effect of Electrical and Non Non-electrical Parameters arameters on the Performance erformance Measures of Electro Electro-Discharge Machining : achining : A Review," ***Indian J. Trend Sci. Res.*** *Dev.*, vol. 1, no. 6, pp. 926–936, 2017.

84. El-Hofy H., *Advanced machining processes Nontraditional and Hybrid Machining Processes*. USA: McGraw-Hill, 2005. doi: 10.1036/0071466940.

85. Antony J., *Design of Experiments for Engineers and Scientists*, no. October. Elsevier Science & Technology Book, 2003.

86. Khosrow Dehnad, *Quality control, robust deSign, and the Taguchi method.* California: Wadsworth & Brooks/Cole Advanced Books & Software Pacific Grove, California, 1989. doi: 10.10071978-1-4684-1472-1.

87. Bowerman B. L. and O'Connell R. T., *Business statistics in Practice*, 4th ed. USA: McGraw-Hill, 2007.

88. Krishnaiah K. and Shahabudeen P., *Applied Design of Experiments and*. New Delhi: Asoke K. Ghosh, PHI Learning Private Limited, 2012.

89. Muthukumar V., Rajesh N., Venkatasamy R., Sureshbabu A. and Senthilkumar N., "Mathematical Modeling for Radial Overcut on Electrical Discharge Machining of Incoloy 800 by Response Surface Methodology," ***Procedia Mater. Sci.,*** vol. 6, no. Icmpc, pp. 1674–1682, 2014, doi: 10.1016/j.mspro.2014.07.153.

90. Reddy V. V., Valli P. M., Kumar A. and Reddy C. S., "Influence of process parameters on characteristics of electrical discharge machining of PH17-4 stainless steel," ***J. Adv. Manuf. Syst.***, vol. 14, no. 3, pp. 189–202, 2015, doi: 10.1142/S0219686715500122.

91. Gupta S., Pandey H. and Sen S., “Experimental Investigation of Machining Parameters for Edm of ‘Za-27’ Alloy Using Taguchi Analysis,” ***Int. J. Mod. Trends Eng. Res***., vol. 3, no. 8, pp. 189–195, 2016, doi: 10.21884/ijmter.2016.3023.lz5ui.

92. Ponappa K., Sasikumar K. S. K., Sambathkumar M. and Udhayakumar M., “Multi-objective optimization of edm process parameters for machining of hybrid aluminum metal matrix composites (Al7075/TiC/B4C) using genetic algorithm,” ***Surf. Rev. Lett.,*** vol. 26, no. 10, 2019, doi: 10.1142/S0218625X19500719.

93. Kumar A., Siba S. and Mahapatra S., “Surface Characteristics of EDMed Titanium Alloy and AISI 1040 Steel Workpieces Using Rapid Tool Electrode,” ***Arab. J. Sci. Eng***., no. 0123456789, 2019, doi: 10.1007/s13369-019-04144-7.

94. Zhang Y., Liu Y., Ji R. and Cai B., “Applied Surface Science Study of the recast layer of a surface machined by sinking electrical discharge machining using water-in-oil emulsion as dielectric,” ***Appl. Surf. Sci***., vol. 257, no. 14, pp. 5989–5997, 2011, doi: 10.1016/j.apsusc.2011.01.083.

APPENDIX A.

LARGER VIEWS OF MSTs

` `

Table Appendix A. 1 Design of experiments.

Sq.	Control Variables	Electrode	Ip	Ton	Toff
1	$E_1A_1B_1C_1$	CuCrZr	6	50	50
2	$E_1A_1B_2C_2$	CuCrZr	6	200	200
3	$E_1A_1B_3C_3$	CuCrZr	6	800	800
4	$E_1A_2B_1C_2$	CuCrZr	12	50	200
5	$E_1A_2B_2C_3$	CuCrZr	12	200	800
6	$E_1A_2B_3C_1$	CuCrZr	12	800	50
7	$E_1A_3B_1C_3$	CuCrZr	25	50	800
8	$E_1A_3B_2C_1$	CuCrZr	25	200	50
9	$E_1A_3B_3C_2$	CuCrZr	25	800	200
10	$E_2A_1B_1C_1$	Cu	6	50	50
11	$E_2A_1B_2C_2$	Cu	6	200	200
12	$E_2A_1B_3C_3$	Cu	6	800	800
13	$E_2A_2B_1C_2$	Cu	12	50	200
14	$E_2A_2B_2C_3$	Cu	12	200	800
15	$E_2A_2B_3C_1$	Cu	12	800	50
16	$E_2A_3B_1C_3$	Cu	25	50	800
17	$E_2A_3B_2C_1$	Cu	25	200	50
18	$E_2A_3B_3C_2$	Cu	25	800	200
19	$E_3A_1B_1C_1$	CNB	6	50	50
20	$E_3A_1B_2C_2$	CNB	6	200	200
21	$E_3A_1B_3C_3$	CNB	6	800	800
22	$E_3A_2B_1C_2$	CNB	12	50	200
23	$E_3A_2B_2C_3$	CNB	12	200	800
24	$E_3A_2B_3C_1$	CNB	12	800	50
25	$E_3A_3B_1C_3$	CNB	25	50	800
26	$E_3A_3B_2C_1$	CNB	25	200	50
27	$E_3A_3B_3C_2$	CNB	25	800	200
28	$E_4A_1B_1C_1$	NSS	6	50	50

29	$E_4A_1B_2C_2$	NSS	6	200	200
30	$E_4A_1B_3C_3$	NSS	6	800	800
31	$E_4A_2B_1C_2$	NSS	12	50	200
32	$E_4A_2B_2C_3$	NSS	12	200	800
33	$E_4A_2B_3C_1$	NSS	12	800	50
34	$E_4A_3B_1C_3$	NSS	25	50	800
35	$E_4A_3B_2C_1$	NSS	25	200	50
36	$E_4A_3B_3C_2$	NSS	25	800	200
37	$E_5A_1B_1C_1$	B2	6	50	50
38	$E_5A_1B_2C_2$	B2	6	200	200
39	$E_5A_1B_3C_3$	B2	6	800	800
40	$E_5A_2B_1C_2$	B2	12	50	200
41	$E_5A_2B_2C_3$	B2	12	200	800
42	$E_5A_2B_3C_1$	B2	12	800	50
43	$E_5A_3B_1C_3$	B2	25	50	800
44	$E_5A_3B_2C_1$	B2	25	200	50
45	$E_5A_3B_3C_2$	B2	25	800	200

APPENDIX B

MATERIALS AND EQUIMENTS

Figure Appendix B. 1 Workpieces before experiments.

Figure Appendix B. 2 The electrodes.

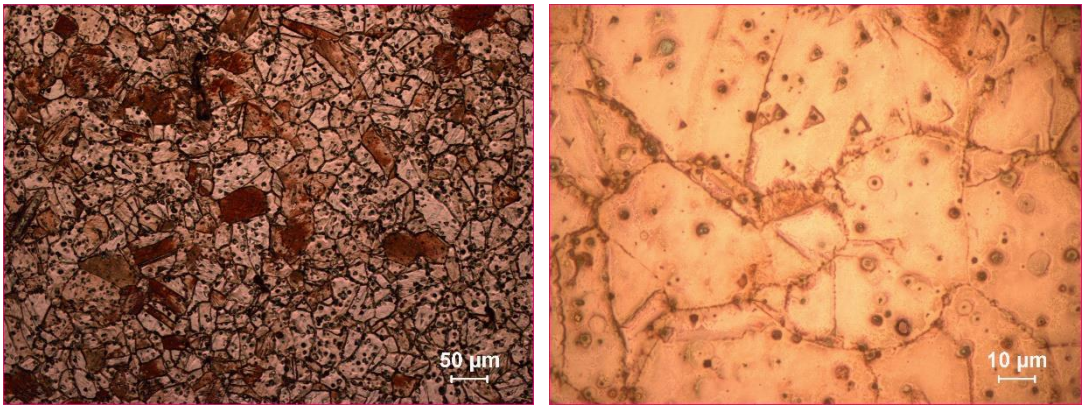

(a) (b)

Figure Appendix B. 3 Microscopic images of a CuCrZr electrode ((a) 20X, (b) 100X).

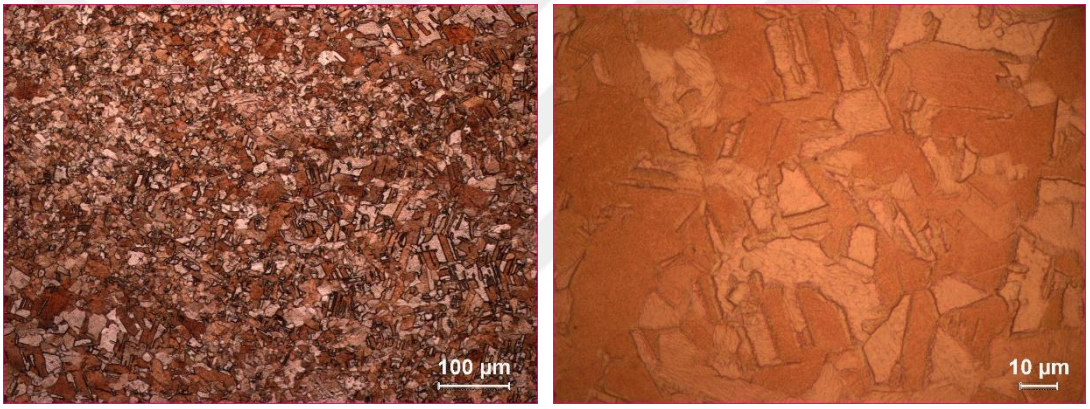

(a) (b)

Figure Appendix B. 4 Microscopic images of a Cu electrode ((a) 20X, (b) 100X).

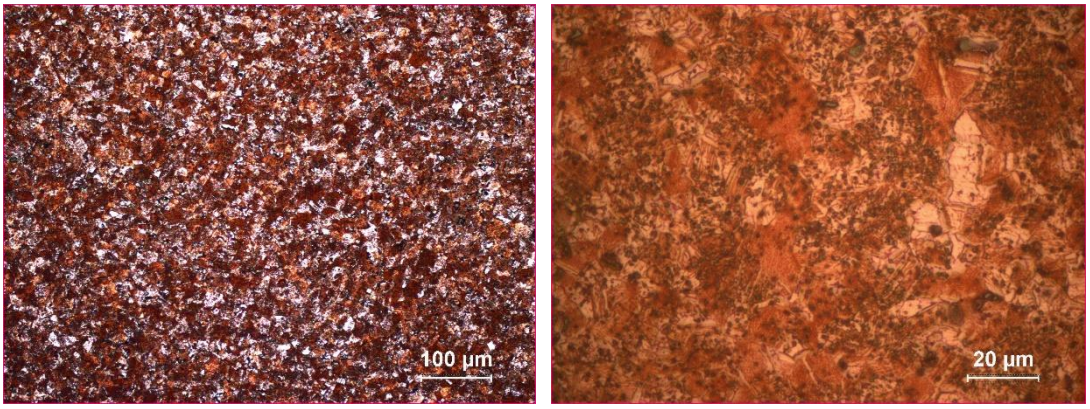

(a) (b)

Figure Appendix B. 5 Microscopic images of a CNB electrode ((a) 20X, (b) 100X).

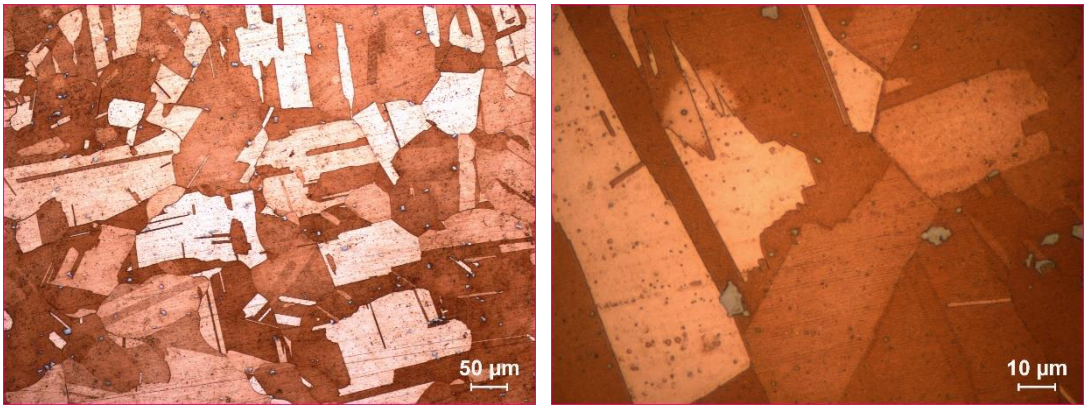

(a) (b)

Figure Appendix B. 6 Microscopic images of a NSS electrode ((a) 20X, (b) 100X).

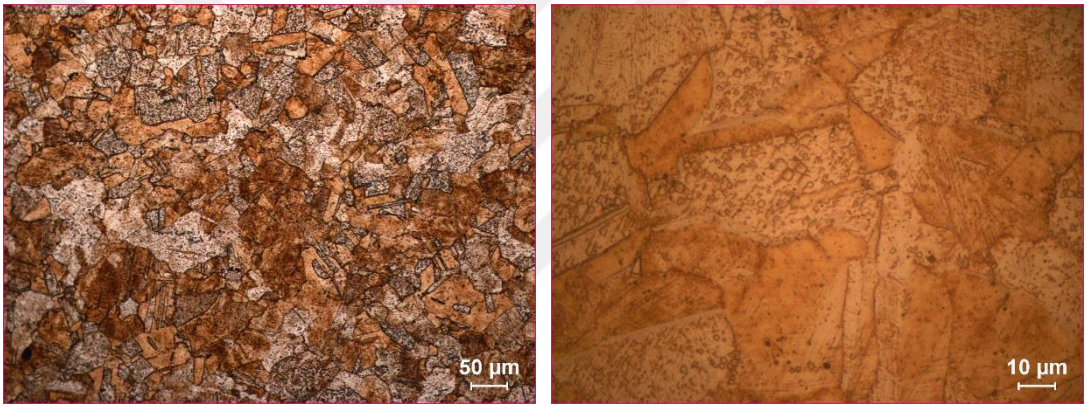

(a) (b)

Figure Appendix B. 7 Microscopic images of a B2 electrode ((a) 20X, (b) 100X).

Figure Appendix B. 8 Polishing machine.

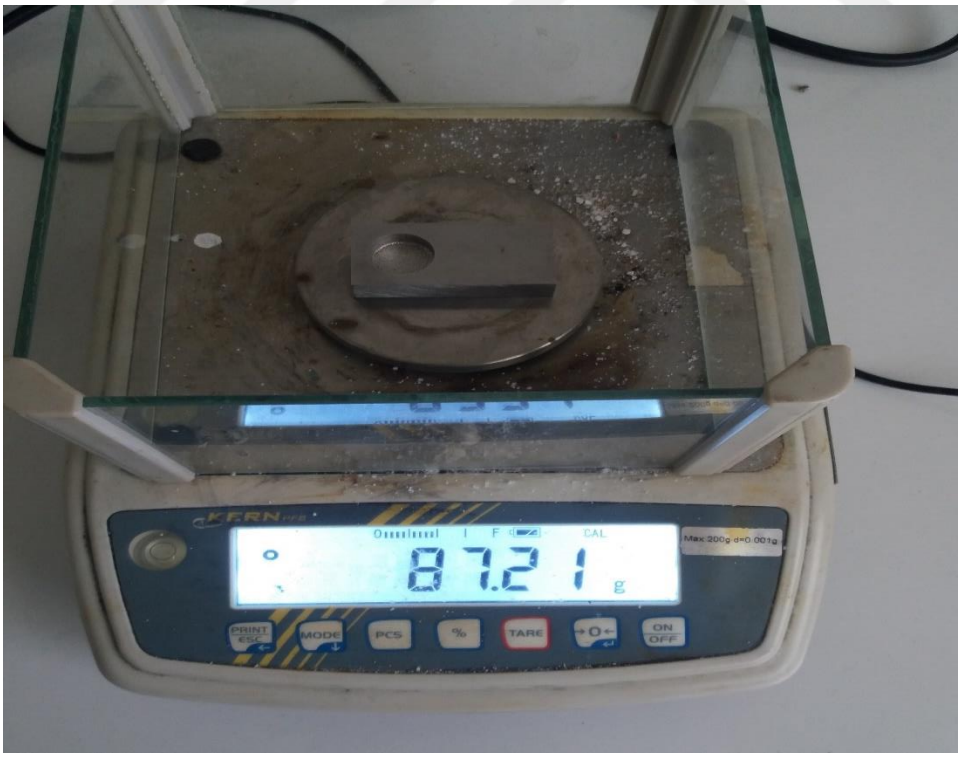

Figure Appendix B. 9 Electronic scale.

Figure Appendix B. 10 Samples and an electrode after experiment.

Figure Appendix B. 11An electrode after experiment.

Figure Appendix B. 12 Water-based Monocrystalline.

Figure Appendix B. 13 Water-based Diamond Lubricant.

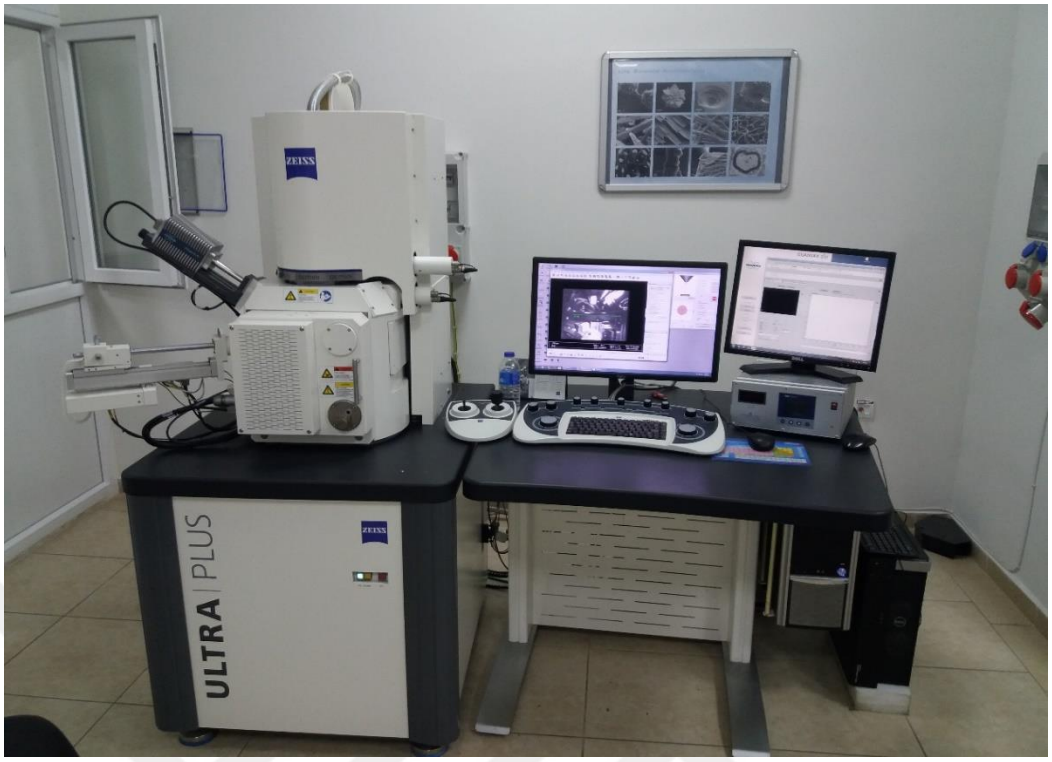

Figure Appendix B. 14 Scanning Electron Microscopy.

Figure Appendix B. 15 Samples prepared for SEM iimages.

APPENDIX C

SURFACE ROUGHNESS MEASURMENTS

Table Appendix C. 1 Measurements of workpieces surface roughness using Cu-Cr-Zr electrode.

	Ra1	Ra2	Ra3	**Ra**	Rq1	Rq2	Rq3	**Rq**	Rz1	Rz2	Rz3	**Rz**
1	3.565	4.198	4.317	**4.026**	4.335	5.040	5.282	**4.885**	19.018	19.843	22.575	**20.478**
2	4.346	4.105	3.762	**4.071**	5.379	5.187	4.749	**5.105**	22.471	23.187	20.458	**22.038**
3	2.495	2.118	1.594	**2.069**	3.217	2.594	2.058	**2.623**	13.669	10.701	9.981	**11.450**
4	5.320	5.170	5.480	**5.380**	6.595	6.700	6.728	**6.674**	28.080	28.080	26.461	**27.985**
5	5.558	4.284	5.125	**4.989**	6.920	5.455	6.268	**6.220**	29.148	25.996	25.007	**26.717**
6	2.077	2.394	2.160	**2.210**	2.649	2.931	2.688	**2.765**	12.147	11.620	11.564	**11.777**
7	5.609	6.445	5.701	**5.921**	6.859	8.280	7.193	**7.444**	28.277	34.704	31.388	**31.456**
8	9.808	9.092	9.312	**9.404**	11.155	13.899	12.369	**12.474**	38.713	50.208	44.005	**44.308**
9	9.347	9.055	9.974	**9.455**	11.266	15.340	12.215	**12.940**	39.268	49.990	43.558	**44.272**

Table Appendix C. 2 Measurements of workpieces surface roughness using Cu electrode.

	Ra1	Ra2	Ra3	**Ra**	Rq1	Rq2	Rq3	**Rq**	Rz1	Rz2	Rz3	**Rz**
1	4.114	4.346	3.837	**4.099**	4.939	5.286	4.779	**5.001**	20.823	23.919	21.143	**21.961**
2	3.658	3.850	3.960	**3.822**	4.454	4.780	4.730	**4.654**	18.237	21.085	18.877	**19.399**
3	2.752	2.208	1.910	**2.290**	3.617	2.719	2.304	**2.88**	15.542	11.952	9.695	**12.396**
4	4.817	4.256	4.972	**4.681**	5.921	4.985	6.048	**5.651**	23.156	18.727	21.815	**21.232**
5	9.608	8.088	6.690	**8.128**	11.819	9.210	8.178	**9.735**	46.482	33.596	35.771	**38.616**
6	5.290	5.216	5.621	**5.375**	6.561	6.429	6.906	**6.632**	29.170	27.463	29.333	**28.655**

7	6.198	5.571	6.509	**6.092**	7.729	7.244	8.175	**7.716**	31.887	33.735	35.831	**33.817**
8	10.699	12.331	11.332	**11.454**	13.213	10.585	13.416	**12.404**	45.506	42.584	50.531	**46.147**
9	8.937	11.876	8.224	**9.687**	14.634	14.708	13.725	**14.355**	49.761	54.590	43.672	**49.341**

Table Appendix C. 3 Measurements of workpieces surface roughness using CNB electrode.

	Ra1	Ra2	Ra3	**Ra**	Rq1	Rq2	Rq3	**Rq**	Rz1	Rz2	Rz3	**Rz**
1	4.295	4.364	4.037	**4.198**	5.024	5.398	4.972	**5.131**	21.353	24.322	21.859	**22.511**
2	2.900	3.426	3.170	**3.165**	3.678	4.230	3.836	**3.914**	15.734	18.316	16.323	**16.791**
3	2.610	1.530	1.851	**1.997**	3.456	1.860	2.383	**2.569**	15.651	7.788	10.651	**11.363**
4	7.008	8.000	7.485	**7.497**	9.029	9.385	9.330	**9.248**	43.881	36.676	46.700	**42.419**
5	9.832	8.850	11.336	**10.006**	12.214	11.271	13.197	**12.227**	52.426	54.247	54.201	**53.624**
6	3.314	2.437	2.792	**2.847**	4.119	3.061	3.684	**3.621**	17.660	13.800	20.018	**17.213**
7	6.260	7.436	5.578	**6.424**	8.206	10.093	7.372	**8.557**	46.432	63.931	37.390	**49.251**
8	11.137	9.996	9.869	**10.334**	20.579	16.787	17.864	**18.410**	84.934	69.011	72.670	**75.538**
9	11.109	10.806	9.885	**10.600**	19.337	16.743	17.954	**18.011**	64.187	71.328	73.597	**69.704**

Table Appendix C. 4 Measurements of workpieces surface roughness using NSS electrode.

	Ra1	Ra2	Ra3	**Ra**	Rq1	Rq2	Rq3	**Rq**	Rz1	Rz2	Rz3	**Rz**
1	6.743	5.835	4.796	**5.791**	8.401	7.160	5.889	**7.150**	38.814	31.909	31.519	**34.080**
2	3.877	3.674	4.524	**4.025**	4.715	4.564	5.547	**4.942**	19.984	22.346	27.353	**23.227**
3	2.306	3.072	2.793	**2.723**	2.799	4.069	3.445	**3.437**	15.771	22.879	15.826	**18.158**
4	5.342	4.981	5.724	**5.349**	6.341	6.248	7.260	**6.616**	30.368	30.901	34.566	**31.945**
5	9.112	8.552	8.418	**8.694**	12.396	13.099	10.732	**12.075**	45.749	50.677	42.399	**46.275**
6	3.907	4.044	4.445	**4.132**	5.001	4.325	3.994	**4.438**	29.658	31.225	28.788	**29.890**
7	6.119	5.814	6.352	**6.095**	7.334	6.857	6.339	**6.843**	35.011	37.224	34.951	**35.728**
8	10.798		9.963	**10.224**	14.860	10.063	13.507	**12.810**	53.128	40.160	52.280	**48.522**
9	11.002	10.716	10.106	**10.608**	11.607	14.811	11.958	**12.792**	45.109	55.930	45.088	**48.088**

Table Appendix C. 5 Measurements of workpieces surface roughness using B2 electrode.

	Ra1	Ra2	Ra3	**Ra**	Rq1	Rq2	Rq3	**Rq**	Rz1	Rz2	Rz3	**Rz**
1	4.191	3.390	3.957	**3.846**	6.356	5.206	6.905	**6.156**	26.262	21.477	29.003	**25.580**
2	2.768	2.521	3.114	**2.801**	5.461	6.936	6.314	**6.237**	23.720	27.104	25.389	**25.404**
3	1.549	1.205	2.100	**1.618**	2.016	1.864	2.857	**2.241**	13.331	12.089	13.335	**12.918**
4	5.230	4.449	4.556	**4.745**	6.451	7.001	5.627	**6.359**	18.346	16.754	15.002	**16.700**
5	8.012	7.198	7.461	**7.557**	7.652	6.884	8.871	**7.802**	23.648	24.348	21.887	**23.265**
6	2.464	2.153	2.709	**2.442**	3.169	4.393	4.018	**3.860**	12.155	16.631	14.357	**14.381**

7	6.205	5.928	5.222	**5.785**	8.425	8.932	9.013	**8.791**	35.705	42.659	38.683	**39.015**
8	8.992	8.478	10.127	**9.199**	13.125	10.666	10.762	**11.517**	54.833	42.776	41.289	**46.299**
9	11.303	11.103	10.258	**10.888**	12.357	11.112	11.668	**11.666**	44.315	52.001	46.964	**47.760**

RESUME

Abubaker Yousef FATATIT graduated first, elementary and high school education in this city. He started undergraduate program in Tripoli University Department of Mechanical and Industrial Engineering in 1986. Then in 2009 he started M. Sc. Education in Engineering Project Management in The Libyan Academy (Misurata Branch) and then he started to work as a lecturer (part time) at College of Industrial Technology in Misurata. Also, he has been working for Libyan Iron and Steel Company since 1996.